The effect of stack height, stack location and rooftop structures on air intake contamination

A laboratory and full-scale study

STUDIES AND RESEARCH PROJECTS

Ted Stathopoulos
Louis Lazure
Patrick Saathoff
Amit Gupta

R-392

REPORT

irsst

Established in Québec since 1980, the Institut de recherche Robert-Sauvé en santé et en sécurité du travail (IRSST) is a scientific research organization known for the quality of its work and the expertise of its personnel.

OUR RESEARCH *is working* for you!

MISSION

- To contribute, through research, to the prevention of industrial accidents and occupational diseases as well as to the rehabilitation of affected workers.
- To offer the laboratory services and expertise necessary for the activities of the public occupational health and safety prevention network.
- To disseminate knowledge, and to act as scientific benchmark and expert.

Funded by the Commission de la santé et de la sécurité du travail, the IRSST has a board of directors made up of an equal number of employer and worker representatives.

TO FIND OUT MORE...

Visit our Web site for complete up-to-date information about the IRSST. All our publications can be downloaded at no charge.
www.irsst.qc.ca

To obtain the latest information on the research carried out or funded by the IRSST, subscribe to *Prévention au travail*, the free magazine published jointly by the IRSST and the CSST.

Subscription: 1-817-221-7046

IRSST – Communications Division
505, boul. De Maisonneuve Ouest
Montréal (Québec)
H3A 3C2
Telephone: (514) 288-1551
Fax: (514) 288-7636
www.irsst.qc.ca

The effect of stack height, stack location and rooftop structures on air intake contamination

A laboratory and full-scale study

STUDIES AND RESEARCH PROJECTS

REPORT

Ted Stathopoulos[1], Louis Lazure[2], Patrick Saathoff[1] and Amit Gupta[1]

[1]Université Concordia
[2]Hygiène du travail, IRSST

Clic Research
www.irsst.qc.ca

This publication is available free of charge on the Web site.

This study was financed by the IRSST. The conclusions and recommendations are those of the authors.

Abstract

The dispersion of exhaust from a rooftop stack on a low-rise building in an urban environment has been investigated using field and wind tunnel experiments. The major goals of the study were:

1) to evaluate the influence of various parameters on plume concentration at typical locations of fresh air intakes. These parameters include stack height, exhaust momentum, upwind turbulence etc.
2) to evaluate dilution models that have recently been adopted by the American Society of Heating, Refrigerating and Air Conditioning Engineers (ASHRAE),
3) to assess the accuracy of wind tunnel modeling; and
4) to provide guidelines for reducing the risk of reingestion of stack emissions.

Tracer gas experiments were carried out on the roof of a 3-storey building in downtown Montreal. Sulfur hexafluoride (SF_6) was emitted from either a 1 m or 3 m tall stack and the tests were performed for low exhaust speed ($w_e \sim 7.5$ m s $^{-1}$) and high exhaust speed ($w_e \sim 17.5$ m s $^{-1}$).

Air samples were obtained at up to fifteen locations on the roof or wall of the emitting building. In some cases, samples were also obtained on the leeward wall of an adjacent 12-storey building when this building was located upwind of the emitting building. Five-minute samples were obtained at each location using a sampling system designed and built by IRSST. Ten samples were collected during each test and thus, the duration of each test was 50-minutes.

Wind tunnel simulations of the field tests were conducted in the boundary layer wind tunnel of Concordia University. The experiments were performed at a model scale of 1:200.

The following provides a summary of various design guidelines formulated on the basis of results obtained in the study:

Stack location: For open fetch situations, it is better to place the stack near the center of the roof. In this way, the leading edge recirculation zone is avoided, thus, maximizing plume rise. In addition, the required plume height to avoid contact with leeward wall receptors is minimized.

For the case of a taller building upwind of the emitting building, the center of the roof may not be the optimum stack location for receptors on the emitting building. Concentrations over most of the roof can be reduced by placing the stack near the leading edge. However, this stack location will result in higher concentrations on the leeward wall of the adjacent building.

Stack height: Increasing the stack height from 1 m to 3 m reduces concentrations near the stack by approximately a factor of two. Far from the stack ($x > 20$ m), the effect is negligible. A stack height of at least 5 m is required to provide significant reduction of k at such distances.

Stack exhaust speed: Increasing stack exhaust speed by a factor of 2.5 reduces concentrations near the stack by the same factor. For distant receptors ($x>20$ m), the

effect of exhaust speed depends on the M-value (the ratio of exhaust speed to wind speed). In the low M range (1.5<M<4.5), which is typical of wind speeds exceeding 5 m/s, increasing exhaust speed may not be beneficial for distant receptors because the plume rise may not be sufficient to avoid them. On the other hand, for light wind conditions, doubling the exhaust speed may cause M to be high enough so that concentrations are reduced over the entire roof.

ASHRAE (2003) vs ASHRAE (1999) model: The ASHRAE (1999) D_{min} model is less conservative than the ASHRAE (2003) D_r model and significantly better for distant samplers (S>30m).

For the **typical design situation** of low M cases (2.5<M<3.5), the ASHRAE (2003) D_r model appears to be overly conservative, especially for distant samplers – it underestimates dilution by a factor of 10 for receptors located more than 30 m from the stack. For high M cases (M~10), i.e. low wind speed, the D_r model is unconservative for samplers near the stack.

Placement of fresh air intakes: The case of an emitting low building in the wake of a taller building was particularly investigated. For wind coming from the direction of the taller building:

- intakes should not be placed on leeward wall of upwind building.
- intakes on emitting building should be placed on its leeward wall if possible.

In addition to the design guidelines above, the following conclusions stem from this study.

- Wind tunnel predictions of concentration were often within 10-20% and generally within a factor of 2 of the field values.

- Some discrepancies between wind tunnel and field data occurred for the emitting building in the wake of a taller building. This may have been due to low turbulence intensity and/or the absence of large-scale turbulence in the wind tunnel for some configurations.

    - concentrations on leeward wall of tall building were consistently too large in wind tunnel, by approximately a factor of 3 on average;
    - wind tunnel concentrations measured near the stack on emitting building were too small, especially for low M cases;
    - wind tunnel and field concentrations on emitting building roof were similar for samplers far from the stack.

- For the open fetch configurations tested, the D_{min} model [ASHRAE (1999)] more accurately predicted minimum dilutions on the roof, compared to the D_r model [ASHRAE (2003)]. This demonstrates the usefulness of the two-

component dilution model in which initial dilution and distance dilution are taken into account.

The results are encouraging because they demonstrate the general adequacy of the wind tunnel data to represent real design situations and the limitations of the ASHRAE models to predict real dilutions for particular building configurations and stack locations. The design guidelines provided in this report will be very helpful to the typical ventilation design engineer to tackle a multi-faceted complicated problem, for which codes and standards are either mute or extremely general to apply to particular real conditions.

TABLE OF CONTENTS

LIST OF FIGURES

LIST OF TABLES

Table No.

LIST OF SYMBOLS

Symbol	Definition	Units
A_e	Stack area	(m^2)
B_l	Distance dilution parameter (D_{min} model)	(-)
C_{max}	Maximum concentration at receptor	(-)
C_e	Exhaust pollutant concentration	(-)
D	Dilution	(-)
D_{min}	Minimum dilution, ASHRAE (1999)	(-)
D_o	Initial dilution	(-)
D_d	Distance dilution	(-)
D_r	Predicted dilution, ASHRAE (2003)	(-)
d_s	Stack diameter	(m)
h_c	Maximum height above roof level of upwind roof edge flow recirculation zone	(m)
h_r	Plume rise	(m)
h_s	Effective stack height	(m)
h_{top}	Height of critical recirculation zone	(m)
h_{small}	Maximum plume height required to avoid critical receptor	(m)
h	Effective plume height	(m)
k	Normalized concentration	(-)
L	Along-wind dimension of BE Building	(m)
M	Exhaust momentum ratio (w_e/U_H)	(-)
Q_{SF6}	Sulfur Hexafluoride flow rate	(m^3 s^{-1})

Re_b	Building Reynolds number	(-)
Re_s	Stack Reynolds number	(-)
SL	Stack location	(-)
t_{avg}	Averaging time	(min)
T.I.	Turbulence intensity	(%)
U_H	Wind velocity at building height	(m s^{-1})
W_b	Nominal building dimension	(m)
w_e	Exhaust velocity	(m s^{-1})
x	Distance from windward edge of BE Building	(m)
S	Stretch-string distance from stack to receptor	(m)
Greek		
δ	Boundary-layer height	(m)
β	Stack capping factor	(-)
ν	Kinematic viscosity	(m^2 s^{-1})
σ_o	Intial plume spread standard deviation	(m)
σ_y	Horizontal plume spread standard deviation	(m)
σ_z	Vertical plume spread standard deviation	(m)
σ_θ	Standard deviation of wind direction fluctuations	(degrees)
θ	Wind direction	(degrees)
σ_u	Standard deviation of wind velocity in along-wind direction	(m s^{-1})
α	Power Law exponent	(0.30)

Chapter 1

Introduction

One of the major causes of poor indoor air quality at some facilities is the sporadic occurrence of exhaust reingestion at fresh air intakes. University, hospital and industrial laboratories as well as manufacturing facilities are particularly susceptible to this phenomenon since they emit a wide range of toxic and odorous chemicals. The effect on worker health and comfort is substantial. Unfortunately, the state-of-the-art has not been sufficiently advanced to allow building engineers to apply appropriate design criteria to avoid this problem for new construction or to help alleviate it for existing buildings. Consequently, numerous incidents of poor air quality have been recorded and documented.

The first phase of the study, commissioned by IRSST in 1996 [Stathopoulos et al. (1999)] provided a significant amount of information on the dispersion of plumes emitted from buildings in an urban environment. Experiments were performed on two buildings for a limited number of wind directions; corresponding tests were also carried out in a wind tunnel. The results indicated that the use of high velocity exhaust stacks does not guarantee adequate plume dilution at all locations on the roof, and the exhaust momentum ratio, M (i.e. the ratio of exhaust velocity to wind speed), was found to significantly influence the dilution of a tracer gas emitted from a stack. Both current ASHRAE design formulas and wind tunnel modelling may, at a given location, underpredict the maximum concentration of a contaminant.

This report describes the second phase of the study, which commenced in January 2000. The main goals of the study were:

1. Evaluation and improvement of the two most commonly-used modelling tools (empirical design formulas [e.g. ASHRAE] and wind tunnel simulation) for the assessment of concentration of rooftop stack exhaust at various locations,

and

2. Development of design guidelines to assist engineers in the proper selection of location, geometry and functional characteristics of rooftop stacks for various cases by revising the current models when appropriate.

The study included both field tests and wind tunnel experiments. A series of field tracer gas experiments were carried out on a 3-storey building in Montreal using a portable fan as the emission source. The influence of the following factors on short-range plume dispersion were investigated :

1. location of the stack relative to regions of flow separation;
2. stack height;
3. M-value
4. atmospheric turbulence (associated with roughness of upwind terrain);
5. rooftop structures,
6. a taller upwind adjacent building;

In the field study, sulfur hexafluoride, SF_6, was emitted from a variable speed fan located on the roof. Experiments were carried out for two exhaust speeds (7.5 m/s , 17.5 m/s) and two stack heights (1 m, 3 m). Tracer gas concentrations were obtained at 15 locations using the

air sampling methodology developed in the first phase of the study.

Four stack locations were chosen for the study. Field tests performed with the stack at locations 1 and 2 provided data for cases with high upstream turbulence. Stacks 3 and 4 were used for tests with a tall upwind building. Stack 4 was also used for an open fetch case with typical suburban roughness.

A parametric study was carried out in the wind tunnel to provide more detailed information regarding the influence of stack height and M on plume dispersion.

.

Chapter 2

Literature Review

Current standards for building ventilation systems recommend that rooftop stacks be designed such that their emissions do not contaminate fresh air intakes of the emitting building or nearby buildings. This may require extending the height of the stack, h_s, or increasing its exit velocity, w_e. The effects of h_s and w_e on concentration distributions on building surfaces have been investigated using wind tunnel or water channel simulations. In most of these studies, plume dispersion was evaluated for a single isolated building model.

Schulman and Scire (1991) carried out a wind tunnel study to investigate the influence of stack height and exit velocity on the dispersion of emissions from a rooftop stack. The experiments were performed with an isolated low-rise building with a stack in the center of the roof. Figure 2.1 shows the influence of stack height on normalized dimensional concentration, $C^*=CU_H/Q_m$, where C is the receptor concentration, U_H is wind speed at building height and Q_m is the mass flow rate of tracer gas. The results are given for a typical exhaust velocity, expressed in terms of the exhaust momentum ratio, $M=w_e/U_H$. In this case, M=3, which is generally associated with moderately strong winds. The results show that increasing h_s from 0 to 4.6 m causes C* to reduce by a factor of 100 near the stack. However, at the leeward edge of the building, the increase in stack height produces only a marginal benefit. The 4.6 m stack has a C* reduction factor of 4.

Figure 2.2 shows the effect of M on C* for a short stack (h_s = 1.5m). The data show that near the stack, C* can be reduced by a factor of 100 by increasing M from 1.5 to 5. Near the leeward edge of the building the effect of M is reduced; C* is reduced by a factor of 10 as M is increased from 1.5 to 5.

The potential for reducing indoor pollutant concentrations using hidden (wall) fresh air intakes was investigated in a wind tunnel study carried out by Petersen and LeCompte (2002). The study provided a method for predicting concentrations at hidden intakes based on standard dispersion models (ASHRAE, Gaussian). However, since the results were obtained with an isolated building model, further tests are required to determine the applicability of the method for cases when other buildings are nearby.

Meroney et al. (1999) evaluated dispersion and flow patterns around various building shapes using wind tunnel experiments. Flow visualization experiments demonstrated that flow recirculation zones are intermittent and consequently, the direction of flow at a rooftop location may change frequently from upwind to downwind. The authors suggest that the inaccuracy of CFD dispersion predictions is due, in part, to the absence of intermittency in the computer model.

Wilson et al. (1998) investigated the effect of h_s and w_e on the dispersion of building exhaust in a series of water channel experiments. In addition to an isolated low-rise building, tests were also performed for cases in which an adjacent building was upwind or downwind of the emitting building.

Results obtained with a taller upwind building showed that the leeward wall of the upwind building may experience low dilution values (high concentrations), depending on stack location, stack height and exhaust velocity. Figure 2.3 shows measurements of minimum dilution on the leeward wall of the adjacent building due to exhaust from a 2.1 m stack near the leading edge of the emitting building. The dilution values are expressed in normalized form: $D_{min}Q_e/U_HH^2$, where Q_e is the exhaust volume flow rate and H is the height of the emitting building.

The results indicate that, for all M, the lowest dilution values occur near the top of the leeward wall. Dilution increases significantly with increasing M; an increase in M from 1.5 to 8 causes normalized dilution to increase by approximately a factor of 10. On the roof of the emitting building, dilution did not vary significantly with distance from the stack. The average dilution on the roof was approximately equal to the minimum dilution measured on the wall of the adjacent building.

The study found that stacks should not be located near building edges and fresh air intakes should not be placed on the leeward wall of a building if emissions from a lower downwind building are toxic or odorous. Furthermore, a lower adjacent building upwind of the emitting building tends to **increase** dilution on the emitting building roof, whereas in the case of a higher upwind building, increasing exhaust velocity is more beneficial than increasing stack height.

Fluid modeling studies have demonstrated the benefits of high exit velocities and increasing stack height in reducing pollutant concentrations at critical receptors. However, field studies have shown that even with high exit velocities and moderately high stacks, pollutant concentrations may be unacceptably high at particular locations [Wilson and Lamb (1994), Georgakis et al. (1995) Saathoff et al. (2002)]. Several factors may account for the occasional poor performance of rooftop stacks. These factors include the location of the stack relative to regions of flow separation and flow re-attachment, the presence of rooftop irregularities such as penthouses and high upstream turbulence.

It is important to validate the results of fundamental fluid modeling studies with full-scale data. Although most flow features (e.g. wake size, reattachment lengths etc.) under neutral atmospheric conditions can be accurately simulated in wind tunnels and water channels, it is necessary to determine the limitations of fluid modeling with respect to plume dispersion.

Relatively few studies have compared wind tunnel concentration data with field data for nearfield diffusion cases (i.e. receptors within 50 m of a stack). This is one of the most difficult fluid modeling applications, since the plume characteristics may be sensitive to a number of local factors (building wake effects, the position of the stack relative to rooftop recirculation zones or delta-wing vortices, stack Reynolds number etc.). On the other hand, for far-field applications, plume characteristics are much less sensitive to these factors.

Higson et al. (1994) conducted field tracer gas experiments with a stack at varying distances upwind of a small rotatable building and compared the results with wind tunnel data. They found that the maximum concentrations were generally overestimated in the wind tunnel tests; the minimum concentrations were underestimated. This suggests that the wind tunnel plume was narrower than the field plume due to the absence of large-scale turbulence in the wind tunnel.

Several studies by the authors have evaluated the accuracy of wind tunnel dispersion measurements [Stathopoulos et al. (2002), Saathoff et al. (2002)]. For the most part, the results indicate good agreement between wind tunnel and field data. The wind tunnel concentration values were usually within a factor of two of the field values. The accuracy of the wind tunnel generally increased as stack-receptor distance increased.

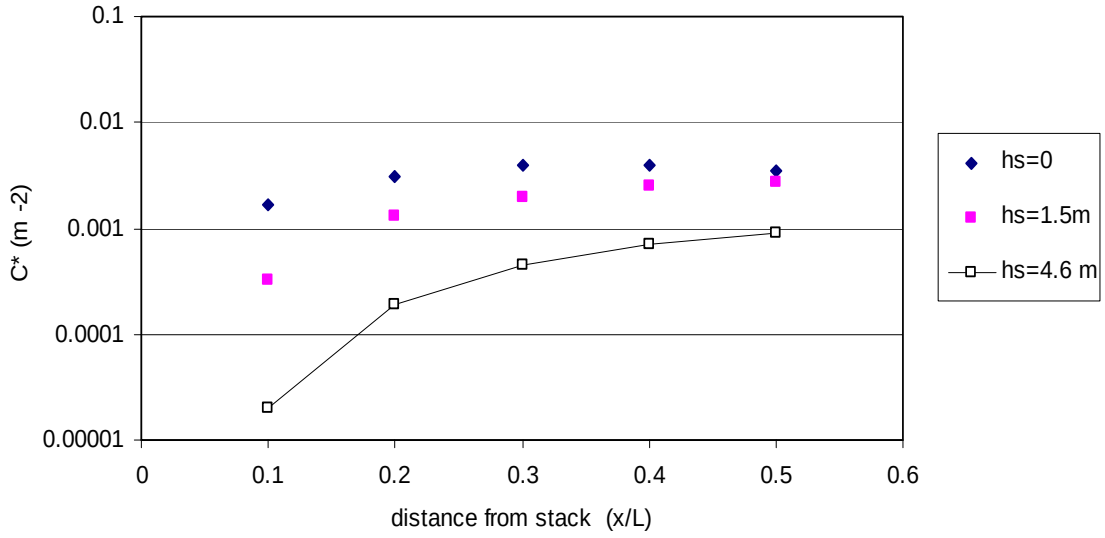

Figure 2.1 Effect of stack height on normalized concentration [from Shulman-Scire (1991)]

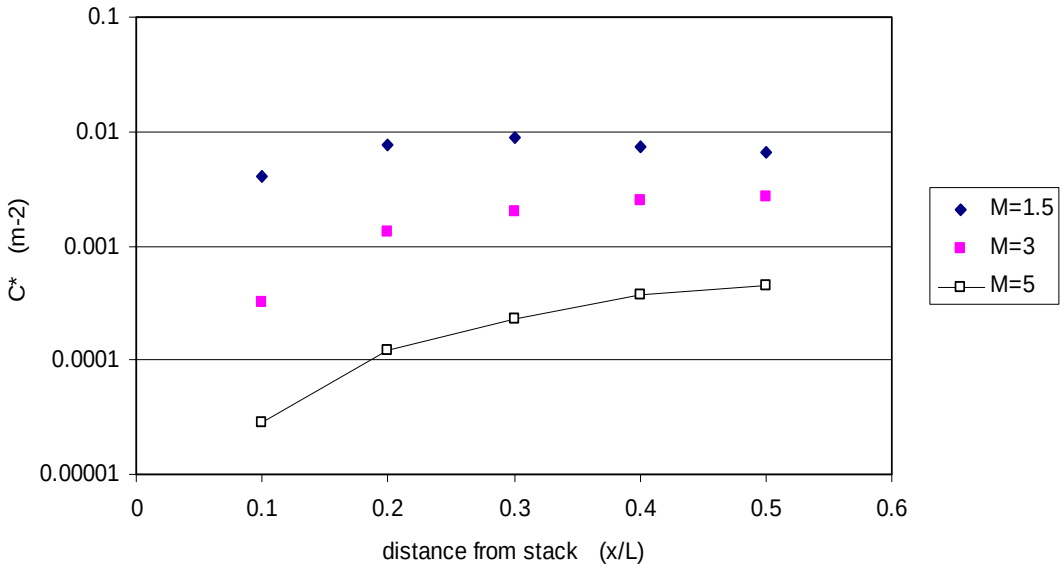

Figure 2.2 Effect of M (exhaust momentum) on normalized concentration [from Shulman-Scire
(1991)]

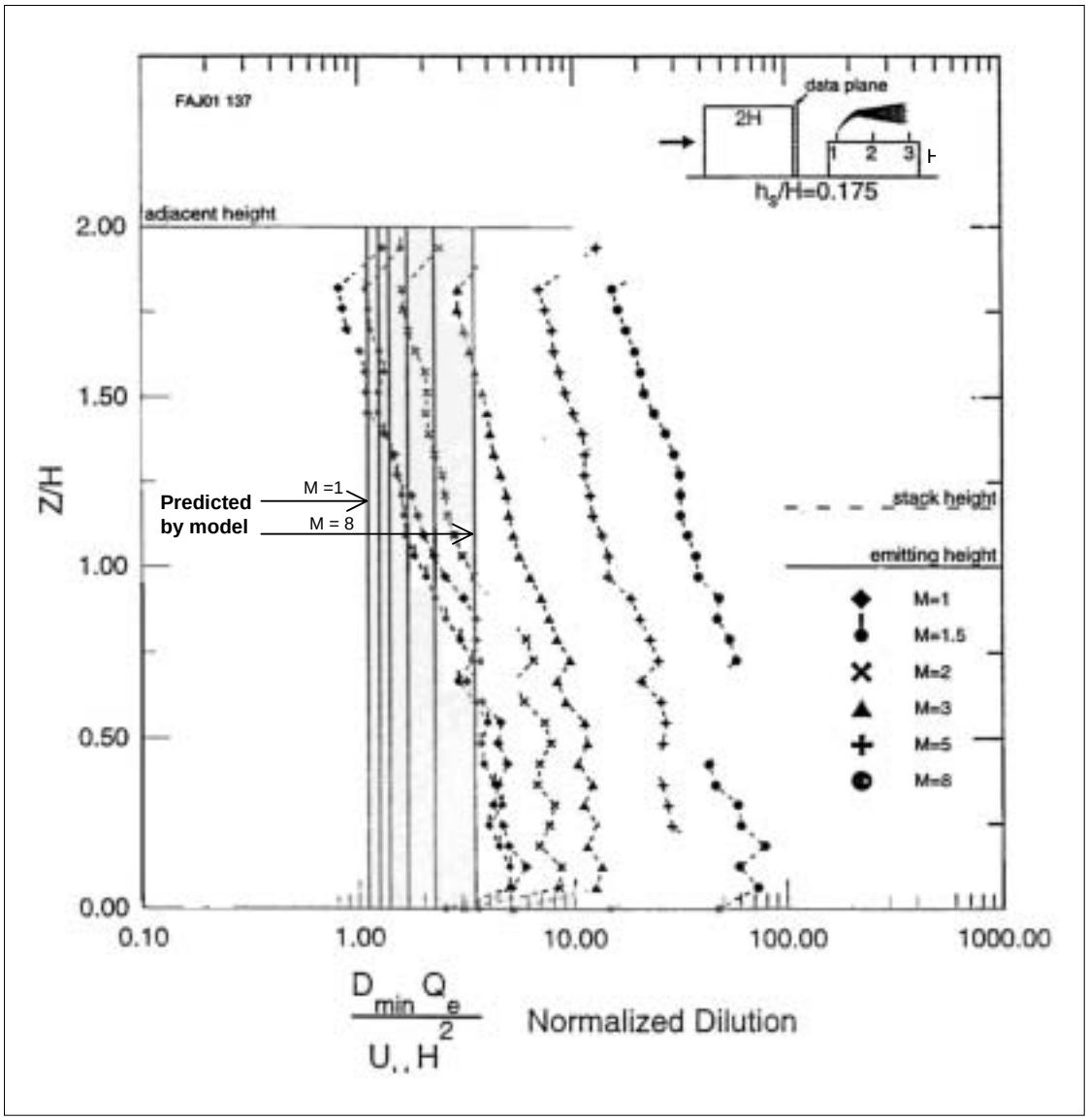

Figure 2.3 Normalized dilutions on the downwind wall of 2H high building with a downwind emitting building of height, H. Buildings separated by a gap size, H [from Wilson et al. (1998)]

Chapter 3

ASHRAE Dispersion Models

In the present study, experiments can be divided into two types:

1. the emission source exposed to the approaching flow (open fetch)
2. the emission source in the wake of a tall building.

Various models have been developed for estimating nearfield dilution of plumes emitted from rooftop stacks for open fetch situations. Two such models are recommended in ASHRAE (1999) and ASHRAE (2003) and are described below. The accuracy of these models will be evaluated in Chapter 5 using field data obtained in the present study.

For the case of a tall building upwind of an emitting building, dilution estimates are required for receptors on the adjacent building leeward wall, as well as the roof of the emitting building. To date, an acceptable dilution model for this case has not been developed [e.g. see Wilson et al. (1998)].

In addition to dilution models that provide quantitative estimates of plume dispersion, ASHRAE (2003) also provides a geometric method to predict the likelihood of a plume making contact with a critical rooftop receptor. This method, which is qualitative in nature, is described below.

3.1 The ASHRAE Geometric Design Method

ASHRAE (2003) provides a geometric stack design method for estimating the minimum stack height to avoid plume entrainment in the flow recirculation zones of a building and its rooftop structures. Dimensions of the recirculation zones are expressed in terms of the scaling length, R, which is defined as:

$$R = B_s^{0.67} B_L^{0.33} \quad (3\text{-}1)$$

where B_s is the smaller of upwind building height or width and B_L is the larger of these dimensions. The dimensions of flow re-circulation zones that form on the building and roof-top structures are:

$$H_c = 0.22R \quad (3\text{-}2)$$

$$X_c = 0.5R \quad (3\text{-}3)$$

$$L_c = 0.9R \quad (3\text{-}4)$$

$$L_r = 1.0R \quad (3\text{-}5)$$

where H_c is the maximum height of the roof recirculation zone, X_c is the distance from the leading edge to H_c, L_c is the length of the roof recirculation zone, and L_r is the length of the building wake zone. Note that the height of the wake zone is equal to the height of the structure.

Figure 3.1 shows the recirculation zones for a typical building.

The design method assumes that the boundary of the high turbulence region is defined by a line with a slope of 10:1 extending from the top of the leading edge separation bubble. The location of the plume relative to the recirculation zones is determined by taking into account plume rise due to exhaust momentum and assuming a conical plume with a slope of 5:1.

The effective height of the plume above the roof or rooftop structure is:

$$h = h_s + h_r - h_d \qquad (3\text{-}6)$$

where h_s is stack height, h_r is plume rise and h_d is the reduction in plume height due to entrainment into the stack wake during periods of strong winds. It should be noted that h_s is the height of the stack tip above the roof minus the height of rooftop obstacles (including their recirculation zones) that are in the path of the plume.

Plume rise, which is assumed to occur instantaneously, is calculated using the formula of Briggs (1984):

$$h_r = 3\beta d_e (w_e/U_H) \qquad (3\text{-}7)$$

where d_e is the stack diameter, w_e is the exhaust velocity, U_H is the wind speed at building height and β is the stack capping factor. The value of β is 1 for uncapped stacks and 0 for capped stacks. To account for the stack downwash caused by low exit velocities, when $w_e/U_H < 3.0$, Wilson et al. (1998) recommended a stack wake downwash adjustment h_d, which is defined as,

$$h_d = d_e (3.0 - \beta w_e/U_H) \qquad (3\text{-}8)$$

For $w_e/U_H > 3.0$ there is no stack downwash ($h_d = 0$).

3.2 Dilution Models for an Open Fetch

A number of semi-empirical models have been developed for predicting minimum dilution ($D_{min} = C_e/C_{max}$) of exhaust from rooftop stacks, where C_e is the exhaust concentration and C_{max} is the

concentration at a roof or wall receptor on the plume center-line. The ASHRAE Applications Handbook [ASHRAE (2003)] recommends a Gaussian dilution model that was developed using data from water channel experiments of Wilson et al. (1998). In an earlier version of the Handbook [ASHRAE (1999], minimum dilution models formulated by Wilson and Lamb (1994) and Halitsky (1963) were recommended. Of these, the Wilson and Lamb model provides a more accurate lower bound of dilution, based on wind tunnel and field case studies [Petersen and Wilson (1989), Stathopoulos et al. (2002)]. The Halitsky model has been shown to be overly conservative in most cases.

In the current study, the accuracy of the Wilson-Lamb and ASHRAE (2003) dilution models will be evaluated using data obtained in field tests conducted with an open fetch.

3.2.1 The Wilson-Lamb Model

The Wilson-Lamb model, hereafter designated as WL, is based on a previous dilution model for flush vents ($h_s = 0$) derived from wind tunnel data obtained with isolated building models [Wilson and Chui (1985, 1987), Chui and Wilson (1988)]. In this model, minimum dilution along the plume centre-line is given by:

$$D_{min} = (D_o^{0.5} + D_d^{0.5})^2 \qquad (3\text{-}9)$$

where D_o is the initial dilution at the location and D_d is the distance dilution which is produced by atmospheric and building-generated turbulence. The formulas for D_o and D_d recommended in ASHRAE (1999) are:

$$D_o = 1 + 13\beta M \qquad (3\text{-}10)$$

$$D_d = B_1 S^2 / M A_e \qquad (3\text{-}11)$$

where B_1 is the distance dilution parameter, S is the stretched string distance from stack to receptor and M is the ratio of exhaust gas velocity, w_e, to the mean wind speed at the building height, U_H. The parameter, β, is the stack capping factor and is set equal to 1.0 for uncapped stacks. The parameter, B_1, is set at a constant value with the magnitude dependent on the location of the receptors.

Dilution data obtained in a field study [Wilson and Lamb (1994)] and a wind tunnel study [Wilson and Chui (1987)] indicate that B_1 is strongly affected by the level of atmospheric turbulence in the approaching flow. The effect of upstream turbulence on the distance dilution parameter is approximated by the following formula:

$$B_1 = 0.027 + 0.0021\sigma_\theta \qquad (3\text{-}12)$$

where σ_θ is the standard deviation of wind direction fluctuations in degrees and varies between 0° and 30°. The model suggests that distance dilution has two components -- the dilution due to building-generated turbulence and that due to atmospheric turbulence. It assumes that D_d is significantly enhanced by atmospheric turbulence. For an urban environment, ASHRAE (1997) recommends a typical value of σ_θ =15°, which gives a value of 0.032 for the atmospheric component of the distance dilution parameter, B1=0.059. Thus, more than 50% of D_d is assumed to be due to upstream turbulence.

3.2.2 Gaussian Dilution Model (ASHRAE 2003)

The Gaussian dilution model recommended in ASHRAE (2003) is based on a series of experiments carried out in a water flume by Wilson et al. (1998). The model predicts **worst-case** dilution at roof-level, D_r, assuming that the plume has a Gaussian (bell-shaped) concentration profile in both the vertical and horizontal directions, as shown in Figure 3.2. It should be noted that D_r is the predicted dilution **on the plume centre-line** and thus, corresponds to D_{min} obtained using the WL model.

The roof-level dilution for a plume at height, h, at a receptor distance, X, from the stack is given as:

$$D_r = 4\frac{U_H}{w_e}\frac{\sigma_y}{d_e}\frac{\sigma_z}{d_e}\exp\left[\frac{h^2}{2\sigma_z^2}\right] \qquad (3\text{-}13)$$

where U_H is the wind speed at the building height, d_e is stack diameter, w_e is the exhaust speed and σ_y and σ_z are the plume spreads in the horizontal and vertical directions, respectively. The height of plume above the roof or rooftop structure, h, is determined using Eq. 6.

The equations for σ_y and σ_z are the equations used in the ISCST dispersion model, which was developed by the U.S. EPA [EPA (1995)], adjusted from a 60 minute averaging time to a 2 minute averaging time using the 0.2 power law applied to both vertical and crosswind spreads. The plume spread formulas are based on water channel data of Wilson et al. (1998), which are assumed to have a full-scale equivalent averaging time of 2 minutes.

The cross-wind and vertical spreads are given by the equations,

$$\frac{\sigma_y}{d_e} = 0.071\left(\frac{t_{avg}}{2.0}\right)^{0.2}\frac{X}{d_e} + \frac{\sigma_o}{d_e} \qquad (3\text{-}14)$$

$$\frac{\sigma_z}{d_e} = 0.071\frac{X}{d_e} + \frac{\sigma_o}{d_e} \qquad (3\text{-}15)$$

where t_{avg} is the concentration averaging time in minutes, and σ_o is the initial source size that accounts for stack diameter and for dilution due to jet entrainment during plume rise. The formula for σ_o/d_e is:

$$\frac{\sigma_o}{d_e} = \left[0.125\beta\frac{w_e}{U_H} + 0.911\beta\left(\frac{w_e}{U_H}\right)^2 + 0.250\right]^{.5} \qquad (3\text{-}16)$$

where β is the rain cap factor, also described previously: β=1 for no rain cap and 0 if the rain cap is present.

The Gaussian dilution model (Eq. 13) should not be used when the plume height, h, is less than the maximum height of the roof recirculation zones that are in the path of the plume. This critical height is referred to as h_{top} and is shown in Figure 3.3. For cases in which the plume height is greater than h_{top} but less than the height required to escape all critical recirculation zones (h_{valid} in Figure 3.3), the physical stack height should be set at 0 when calculating h [ASHRAE (2003)].

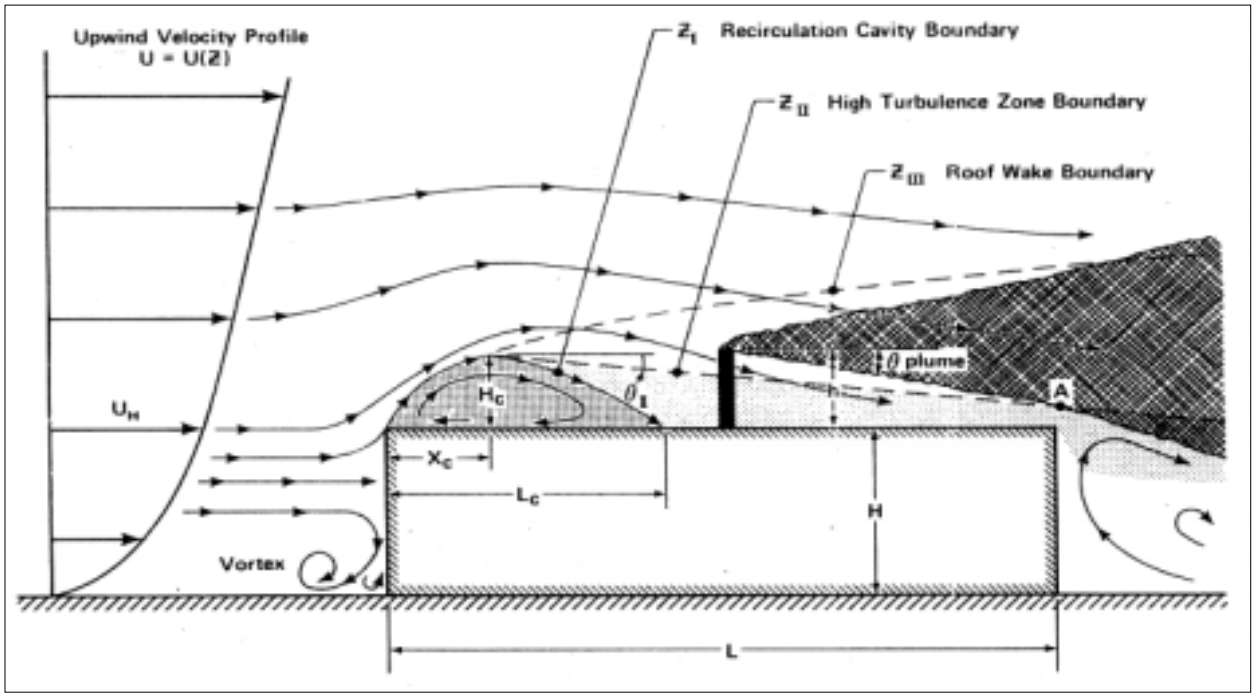

Figure 3.1 Design procedure for required stack height to avoid contamination [from Wilson (1979)]

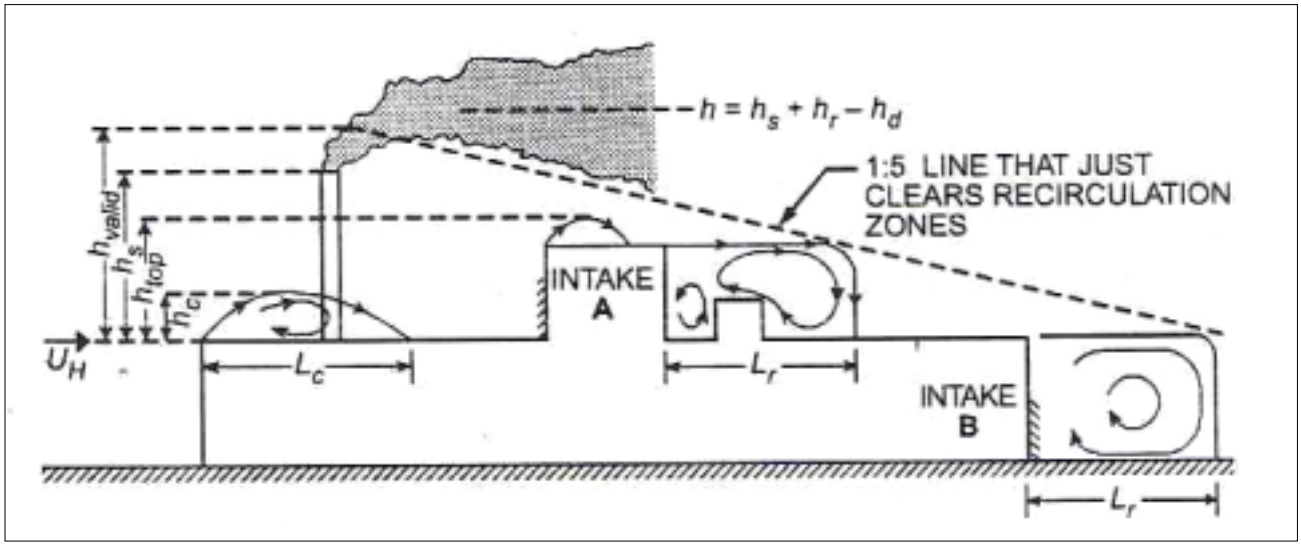

Figure 3.3 Flow recirculation regions and exhaust-to-intake stretched-string distances [from ASHRAE (2003)]

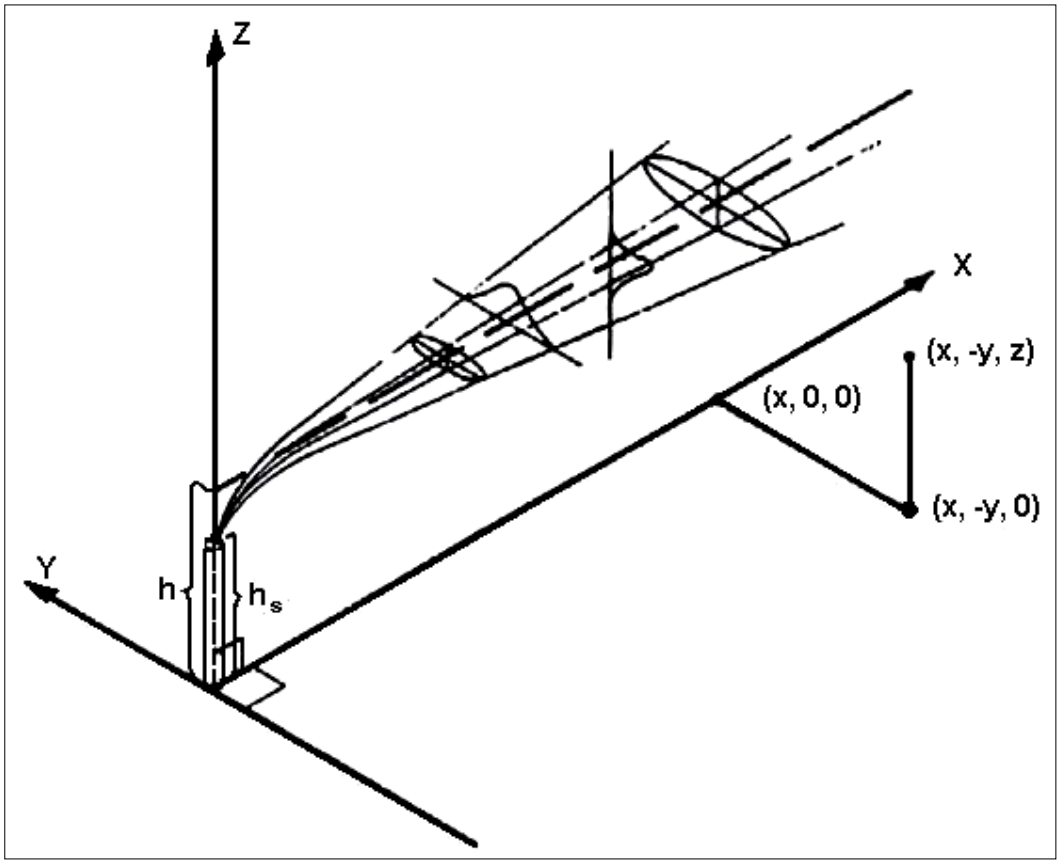

Figure 3.2 Coordinate system showing Gaussian distributions in the horizontal and vertical direction [from Turner (1994)]

Chapter 4

Experimental Procedures

4.1 Field Tests

Full-scale tracer gas experiments were performed on the roof of a 3-storey building in downtown Montreal. The BE building, shown in Figure 4.1, houses the Department of Building, Civil and Environmental Engineering of Concordia University and various commercial shops. Rows of buildings of similar height are connected to the BE building on its northeast and southeast sides.

A detailed drawing of the roof of the BE building is shown in Figure 4.2. The height of the main roof is 12.5 m. Several small structures are located on the roof and these vary in height from 2.2 m to 4 m. Four stack locations (SL1-SL4) were used in the study, as indicated in Figure 4.2.

A map of the surroundings showing locations of tall buildings is shown in Figure 4.3. The most significant nearby structure is the 12-storey Faubourg building, which is 50m in height and is located across the street on the southwest side. A number of high-rise apartment buildings are located to the west and northwest of the BE building at distances between 100 and 300 m. Not shown on the map is Mount Royal, a 233 m tall hill whose summit is located approximately 1 km northwest of the BE building. Photographs of the

surroundings for the tested wind directions (west, northwest, southwest and southeast) are shown in Figure 4.4.

The wind climate in the vicinity of the BE building is similar to that of Dorval Airport, located 20 km west of Montreal. The wind rose for Dorval Airport in Figure 4.5 shows that the predominant wind directions are west-southwest and northeast. In the city center, the frequency and magnitude of westerly winds is reduced due to the sheltering effect of Mount Royal. The wind rose shown in Figure 4.6, which clearly shows the influence of Mount Royal, was derived from data obtained on a 14-storey building on the campus of McGill University, located approximately 1 km northeast of the BE building.

Most of the field tests were carried out in moderately strong winds ($U_{Dorval} > 4$ m s^{-1}). This wind speed category generally corresponds to a neutral or slightly unstable atmosphere [Turner (1994)] and is therefore suitable for wind tunnel modelling. The decision to carry out a test on a given day was based on wind forecasts by Environment Canada (Dorval) and by the availability of personnel from IRSST and Concordia University.

For most open fetch field tests, wind data were measured on the BE building using a 3-component GILL sonic anemometer, mounted at a height of 4 m above the skylight structure, as shown in Figure 4.2. The anemometer provided mean wind speed (U_H), wind direction (θ) and standard deviations of 3-components of velocity (σ_x, σ_y and σ_z) at 1 min intervals. The subscripts x and y refer to the horizontal axes of the anemometer, rather

than the flow direction. The values of σ_x and σ_y were used to calculate σ_u and σ_v, the standard deviations of the longitudinal and lateral velocity fluctuations. The method used to determine σ_u and σ_v is described in Appendix A of Stathopoulos et al. (1999).

Note that the wind speed data have not been corrected for the difference in height between the main roof (elev. 12.5 m) and the anemometer (elev. 19 m).

In one open fetch test (Nov. 21, 2002, SL4), the sonic anemometer was not operational. For this test, a 3-cup anemometer mounted on a 3 m mast was placed on the 4 m tall rooftop structure near the south corner of the building, as shown in Figure 4.2. Wind data for all of the open fetch tests are shown in Table 4.1, except for the last test day (Nov. 21, 2002) for which turbulence intensity and wind direction data are not available due to a malfunction of the anemometer.

For tests carried out with the Faubourg building upwind of the BE building, wind data obtained on the BE building are not useful due to wake effects. During these tests, wind data were obtained with a YOUNG propeller anemometer mounted on a 5 m mast on the penthouse of the Faubourg building. This anemometer measured mean wind speed (U_{ref}), mean wind direction (θ) and the standard deviation of wind speed and wind direction (σ_u, σ_θ) at 5-minute intervals. The wind speed at the height of the BE building was derived from U_{ref} , using a power law exponent $\alpha = 0.30$. This value of α is appropriate for the built environment shown in Figure 4.7. Wind data obtained with the Faubourg anemometer are shown in Table 4.2.

Sulfur hexafluoride, SF_6, was used as the tracer gas during the field tests. Pure SF_6 was injected into the inlet of the variable-speed fan shown in Figure 4.8; the outlet concentration was measured at 1-minute intervals using a BRUEL & KJAER multi-gas analyzer. The stack had an outlet diameter (d_s) of 0.4 m and a height (h_s) that could be extended from 1 m to 3 m. Turning vanes were installed in the bend of the outlet duct to provide uniform flow at the outlet. The tests were performed using low exhaust flow ($Q \sim 1.0\ m^3s^{-1}$) and high flow ($Q \sim 2.3\ m^3s^{-1}$). Table 4.3 shows the exhaust parameters for each of the tests. Volumetric air flow rates were calculated from measurements of cross-sectional air velocities with a TSI anemometer (Model 8384).

Air samples were obtained in 1-litre Cali-5-Bond sampling bags (CALIBRATED INSTRUMENTS INC.) using 15 automatic air samplers that were designed and constructed by IRSST. During each 50-min. test, ten 5-minute samples were collected. In order to evaluate the effect of stack height or exhaust speed under similar conditions, usually two tests were performed per day. During some of the tests, wall samples were obtained at two or three locations on the Faubourg or BE buildings. The wall samplers were placed near the roof edge and had 3 m long plastic tubes attached to the standard inlet tubes. This allowed samples to be obtained along the wall approximately 2.5 m below the roof edge. Wall samples were also obtained at different heights on the Faubourg building using a pump to extract air continuously through plastic tubes. A syringe pump was connected to the tubes to obtain 5-minute samples corresponding to the bag samples obtained at the other locations.

Locations of roof samplers used in all of the field tests and in the wind tunnel study are shown in Figure 4.9. Wall sampler locations on the northeast wall of the Faubourg building and the northwest side of the BE building are also shown. Appendix A shows sampler locations for the individual field tests.

Table 4.1 Wind data obtained using anemometers on BE building

Test Date	Hour	U_{ref} (ms^{-1})	Turbulence Intensity σ_u/U_{ref}	Mean Wind Direction θ °
Oct-12-00	1	3.3	0.48	240
	2	3.0	0.47	242
Nov-15-00	1	2.8	0.48	248
	2	2.4	0.47	252
June-28-01	1	1.5	0.44	321
	2	1.6	0.45	310
Aug-29-01	1	1.9	0.40	310
	2	1.8	0.43	312
Oct-30-01	1	2.3	0.45	305
	2	2.1	0.45	316
May-15-02	1	3.0	0.48	267
Nov-21-02	1	1.5	**	160*
	2	1.7	**	160*

** missing

* measured at Dorval Airport

Table 4.2 Wind data obtained at a height of 55m on Faubourg building

Test Date	Hour	U_{ref} (ms^{-1})	Turbulence Intensity σ_u/U_{ref}	Mean Wind Direction θ °	σ_θ°	U_H * (ms^{-1})
Aug-12-02	1	5.7	0.25	223	13.1	3.7
	2	5.9	0.29	220	15.2	3.8
Aug. 26-02	1	7.2	0.30	219	16.8	4.6
	2	7.0	0.27	224	14.6	4.5
Sept.-6-02	1	4.1	0.36	213	20.4	2.6
	2	4.7	0.28	227	13.9	3.0
Oct.-1-02	1	5.7	0.32	222	15.5	3.6
	2	6.8	0.31	227	18.3	4.4

* U_H estimated using power law approximation with $\alpha = 0.30$

Table 4.3 Exhaust parameters for all field tests

Test Date	Hour	Flow Rate ($m^3\ s^{-1}$)	Exhaust Velocity w_e (ms^{-1})	Momentum ratio (M)	Stack Height h_s (m)
Oct-12-00	1	2.29	17.7	5.4	1
	2	0.95	7.4	2.5	1
Nov-15-00	1	2.29	17.7	6.3	1
	2	2.29	17.7	7.5	3
June-28-01	1	2.44	18.8	12.9	1
	2	1.05	8.1	5.1	1
Aug-29-01	1	2.3	17.8	9.4	3
	2	0.98	7.6	4.4	3
Oct-30-01	1	0.98	7.6	3.4	1
	2	0.98	7.6	3.6	3
May-15-02	1	0.98	7.6	2.5	3
Aug.-12-02	1	2.33	18.0	4.9	1
	2	1.14	8.8	2.3	1
Aug.-26-02	1	0.99	7.7	1.7	3
	2	2.29	17.7	3.9	3
Sept.-6-02	1	0.98	7.6	2.9	1
	2	0.98	7.6	2.5	3
Oct.-1-02	1	0.94	7.3	2.0	1
	2	2.12	16.4	3.7	1
Nov-21-02	1	0.99	7.7	5.6	1
	2	2.3	17.8	10.7	1

After the tests were completed, half of the sample bags (approx. 150) were transported to the IRSST lab for analysis. The remaining bags were analyzed at Concordia University. At IRSST, the analysis was carried out using a Lagus gas chromatograph (GC), which had a measurement precision of ± 3% of the reading within the dynamic range. The

Concordia analysis was performed with a Varian GC with an electron capture detector. The precision of this instrument is similar to the Lagus GC. Selected samples were analyzed using both gas chromatographs and these showed good agreement with a variability usually within 10%.

4.2 Wind tunnel experiments

Wind tunnel experiments were carried out in the boundary layer wind tunnel at Concordia University. The wind tunnel is an open-circuit facility, as shown in Figure 4.10. The working section is 1.8 m by 1.8 m and the length is 12.2 m. The roof of the tunnel was adjusted to ensure that the longitudinal static pressure gradient was negligible.

Detailed models of the BE and Faubourg buildings and their surroundings were constructed at a scale of 1:200. In the upwind direction, the surroundings were modeled out to a distance of at least 250 m; downwind buildings within 50 m were included. Photographs of the maquette are shown in Figure 4.11. The influence of Mt. Royal on the results was not simulated because of the difficulties in constructing the hill profile for a variety of wind directions. The effect of the hill may be significant for west and northwest winds. However, it is assumed that the tall buildings near the BE building will have a much greater influence than the hill on plume behavior.

Wind tunnel blockage can affect the flow field around wind tunnel models and thus may influence concentration measurements. ASCE (1999) recommends that measurements be corrected if the blockage ratio, A_m/A_o, exceeds 5%, where A_m is the projected area of the

model normal to the flow and A_o is the cross-sectional area of the wind tunnel. In the present study blockage was generally low: however the estimated maximum blockage ratio was approximately 7 %. Blockage corrections have not been applied to the wind tunnel measurements.

A certified mixture of sulfur hexafluoride and nitrogen was emitted from a 2 mm diameter brass stack. The flow out of the stack was regulated using a Matheson mass flow controller. Air samples with a duration of 1 minute were obtained at up to 20 locations simultaneously using multi-syringe samplers. The air samples were analyzed using a VARIAN gas chromatograph.

Wind velocity and turbulence data were obtained with a TSI hot wire anemometer. Mean velocity and turbulence intensity profiles for the upstream conditions (without the maquette) are shown in Figure 4.12. The mean velocity profile obtained in the present study has a power law exponent, $\alpha = 0.30$, which is representative of an urban exposure. On the other hand, turbulence intensities at each height were less than those specified by ESDU (1985) for an urban exposure.

The longitudinal integral scale (L_x) was obtained by fitting the turbulence spectrum, measured at a full-scale height of 10 m, to the Von Karman spectrum. The model value of L_x was 0.40 m, which corresponds to a full-scale value of 80 m.

The model roughness length, z_o, was 3.3 mm. At the model scale of 1:200, the equivalent full-scale roughness length is 0.66m, which is at the low end of the expected range for an urban environment (0.5 m < z_o < 1.5 m) [Wieringa (1993)].

An important parameter for modeling the dispersion of stack emissions is the exhaust momentum ratio, $M = w_e/U_H$ where, w_e is the exhaust velocity and U_H is the wind speed at the height of the BE building. The reference wind speed (U_{ref}) was measured at a full-scale height (H_{ref}) of 55 m at the location of the field anemometer. The value of U_H was estimated using the power law:

$$U_H = U_{ref}(H/H_{ref})^{\alpha}$$

Assuming α=0.30, the correction factor to obtain U_H is $(12.5/55)^{0.3} = 0.64$.

The following criteria are generally considered to be sufficient for modeling of dispersion of nonbuoyant exhaust in a neutral atmosphere:

- Similarity of wind tunnel boundary layer with the atmospheric surface layer
- Similar geometric dimensions
- Building Reynolds number ($Re_b=U_HW_b/\nu > 11,000$)
- Stack Reynolds number ($Re_s=w_ed_s/\nu > 2000$)
- Similar stack momentum ratio ($M=w_e/U_H$)

where ν is the kinematic viscosity of the air, W_b is the nominal building dimension and d_s is the stack diameter.

Tables 4.4 and 4.5 provide wind tunnel and field values of the modeling parameters for open fetch and for the Faubourg building upwind of the BE building, respectively. It should be noted that the stack Reynolds number criterion was not always satisfied. At the minimum M-value (i.e. minimum exhaust speed), the Re_s value was approximately 1700 for Faubourg wake tests and 1880 for open fetch tests. Because most of the model tests satisfied the Re_s criterion, the use of a turbulence-generating device in the model stack was not considered necessary.

The minimum model value of building Reynolds No. (Re_b) was 20,000, well above the generally accepted limit of 11,000. Meroney (2003) has noted that this criterion should be viewed with some skepticism since it was derived from a limited amount of data. Nevertheless, it is assumed that plume dispersion is independent of Re_b in the present study.

Concentration data are expressed in terms of the non-dimensional concentration coefficient, K, which is defined as:

$$K = CU_H H^2(10^{-6})/Q_{SF6}$$

where C is concentration in ppb and Q_{SF6} is the emission rate of SF_6 in m^3s^{-1}.

Appendix B shows K values obtained in individual field tests and the corresponding wind tunnel values.

Measurement Uncertainty

As stated previously, the precision of the gas chromatographs was approximately ±5%. The Young propeller anemometer located on the roof of the Faubourg building has a specified accuracy of ± 0.3 m s^{-1} for wind speed and ± 3º for wind direction. The Gill sonic anemometer used for open fetch tests (located on the BE building) has a specified accuracy of ± 3 % for wind speed and ± 3º for wind direction.

The field exhaust velocity is assumed to have a measurement uncertainty of ± 0.1 m s^{-1} (± 0.6% - 1.2%). However, the exhaust momentum ratio will have a significantly larger uncertainty (± 10%) since the anemometer was located some distance away from the stack.

Calibration curves for the VARIAN gas chromatograph and other instruments are provided in Appendix C.

Table 4.4 Experimental parameters for open fetch tests

Stack Locations 1, 2 and 4		
Parameters	Wind Tunnel[m]	Field
Z_{ref} (m)	0.6	120[e]
U_{ref} (m/s)	12.5	2.6 - 5.7[m]
U_{BE} (m/s)[a]	4.7 - 7.5	1.5 - 3.3[m]
Z_o (m)	0.66	0.5 - 1.5[c]
L_x (m)	0.4	100[e]
$\sigma_u/U_{(BE)}$	0.18 - 0.40	0.40 - 0.48[m]
Re_b	20000 - 33000	1250000 – 2750000[m]
Re_s	1880 - 9500	187000 – 472000[m]

Table 4.5 Experimental parameters for tests with Faubourg building upwind

Stack Locations 3 and 4		
Parameters	Wind Tunnel[m]	Field
Z_{ref} (m)	0.6	120[e]
U_{ref} (m/s)	12.5	5.2 – 9[e]
U_{FB} (m/s)[b]	10.5	4.1 - 7.0[m]
Z_o (m)	0.66	0.5 - 1.5[c]
L_x (m)	0.4	100[e]
$\sigma_u/U_{(FB)}$	0.12 - 0.13	0.25 - 0.36[m]
Re_b	**	**
Re_s	1700 - 6000	187000 – 472000[m]

Figure 4.1 BE building, Centre for Building Studies, Concordia University, Montreal viewed from west

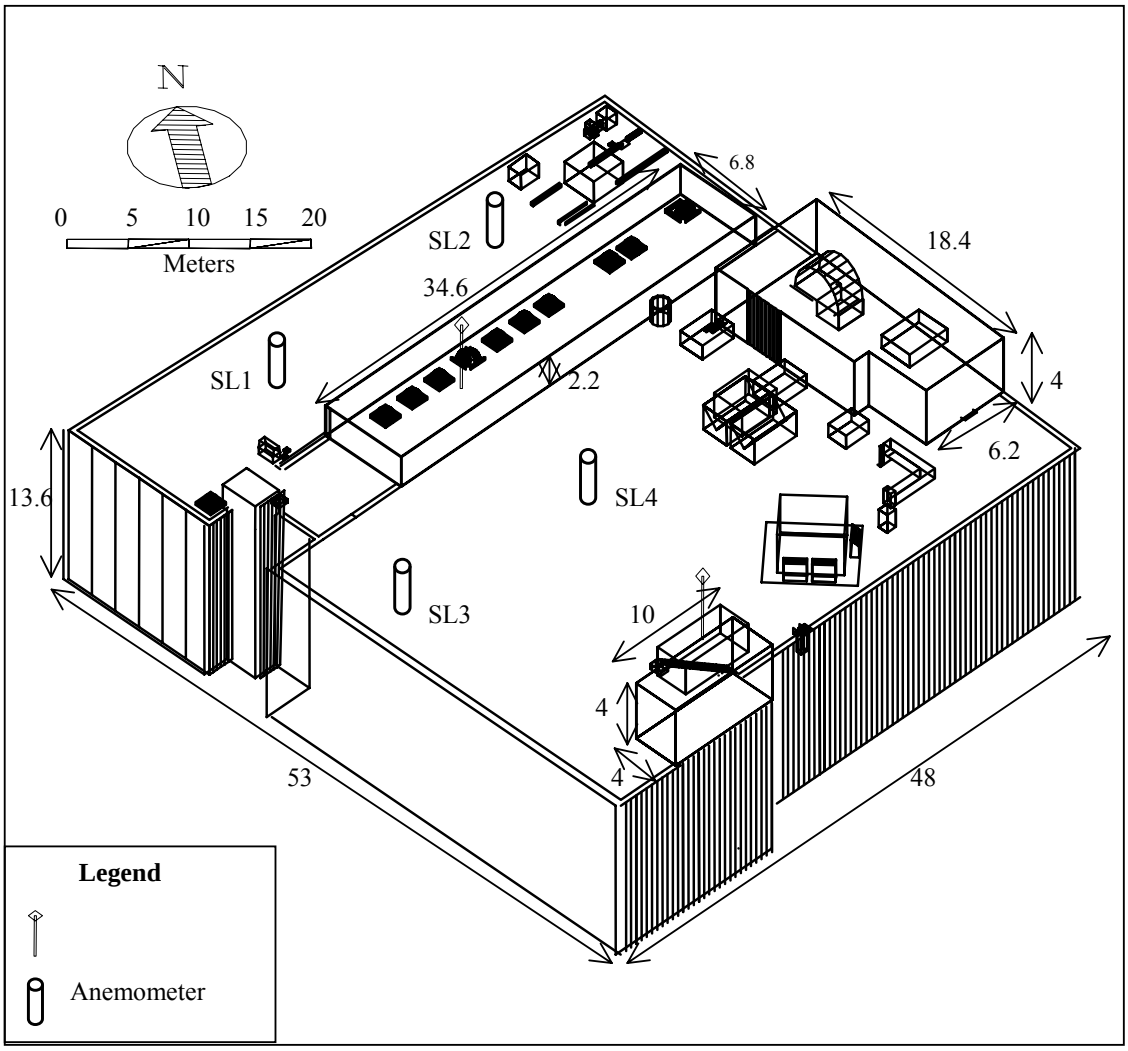

Figure 4.2 Detailed view of the BE building showing stack locations, anemometers and various rooftop structures (dimensions in m)

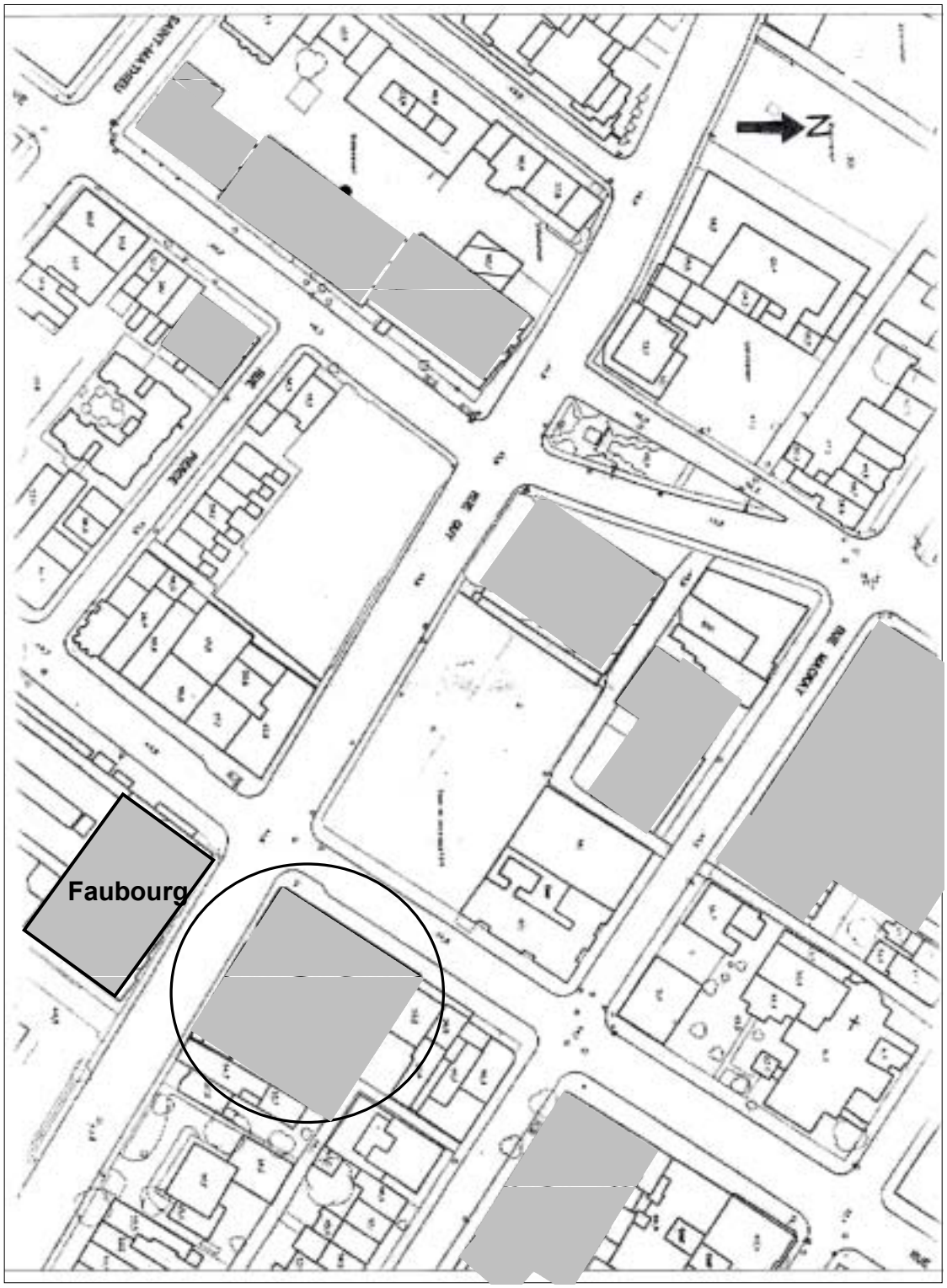

*** Scale 1:1650**

Figure 4.3 Location of BE building and surrounding buildings - shaded buildings have heights varying from 30-65m

a) West

b) Northwest

Figure 4.4 Photographs showing upwind terrain for the various field tests

c) Southwest

d) Southeast

Figure 4.4 (ctd) Photographs showing upwind terrain for the various field tests

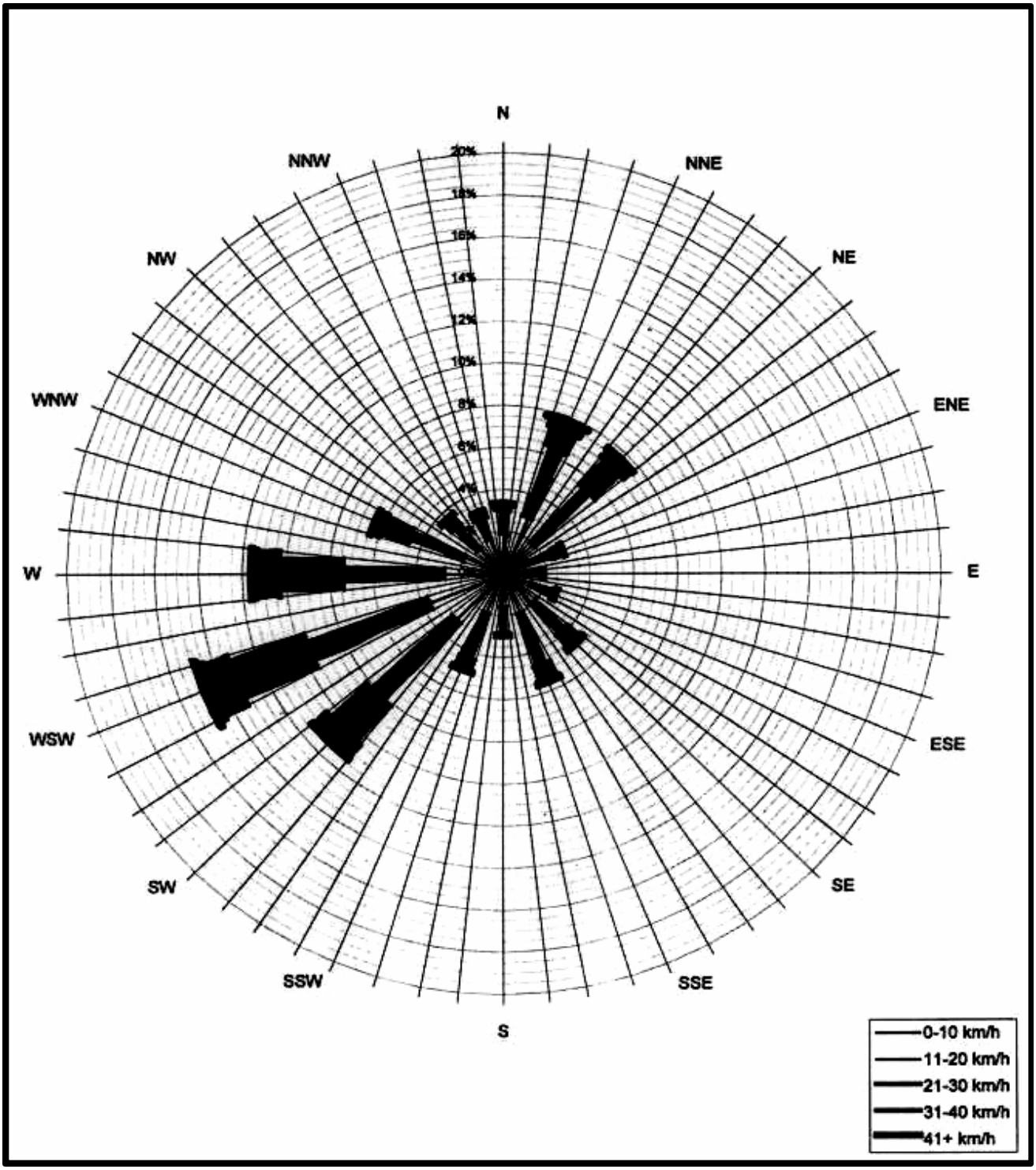

Figure 4.5 Wind frequency chart for Montreal (@ z=300m) based on Dorval airport data

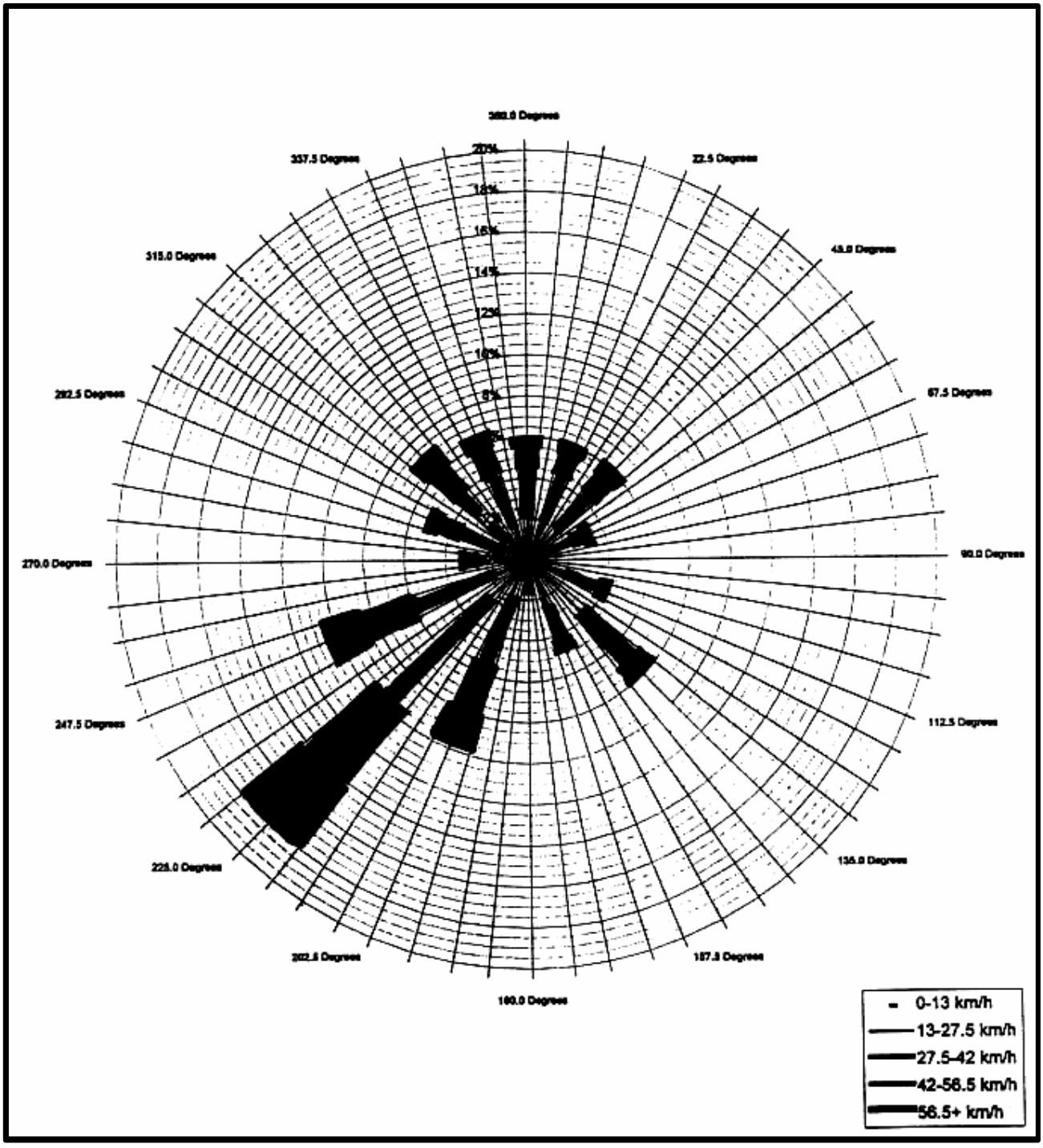

Figure 4.6 Wind frequency chart for Montreal (@ z=300m) based on McGill observatory data

Figure 4.7 Photograph showing the built-up environment around the BE building (taken from Faubourg building penthouse looking Southwest)

Figure 4.8 Photograph of the test stack used on the BE building (low stack with h_s=1m)

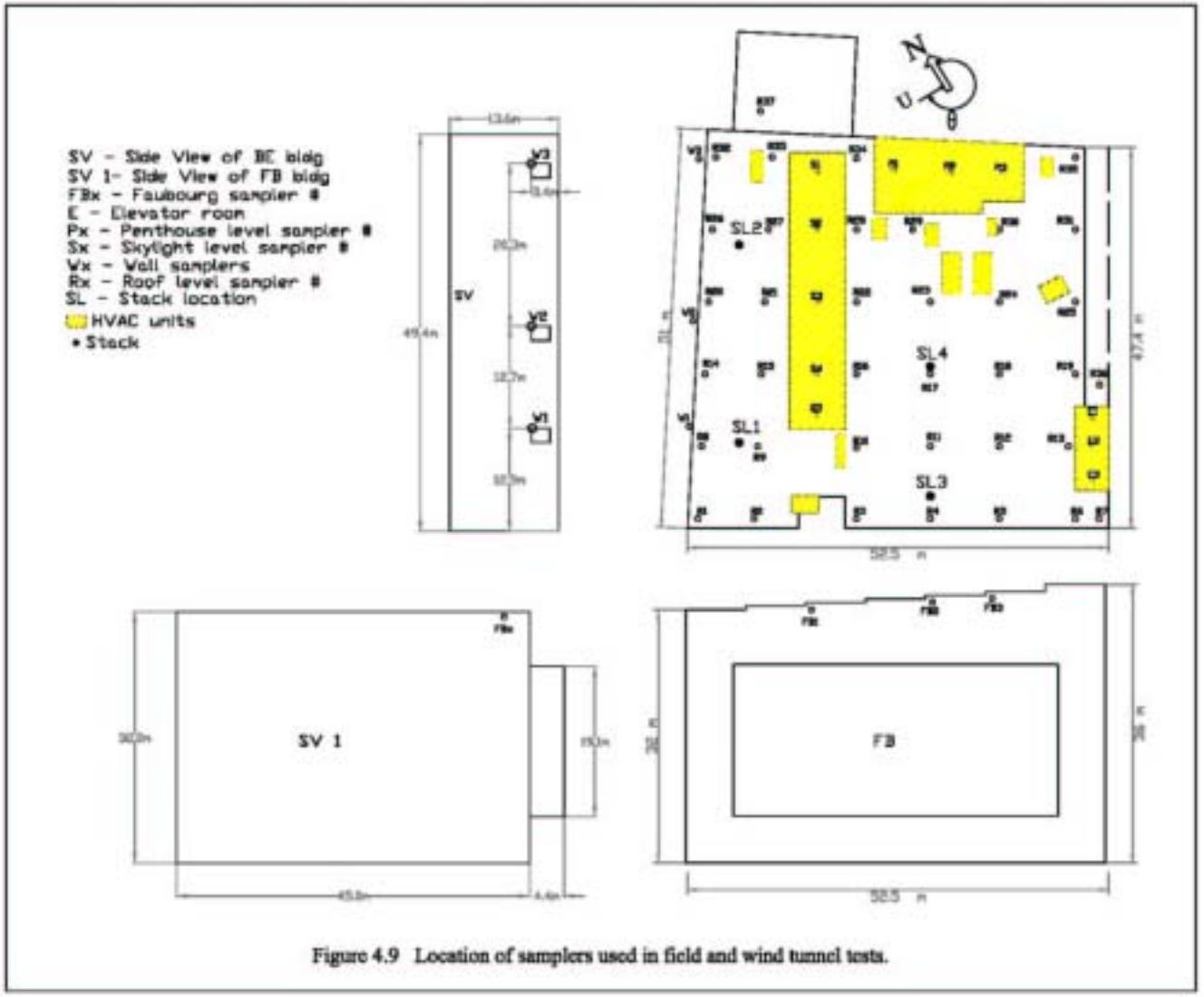

Figure 4.9 Location of samplers used in field and wind tunnel tests.

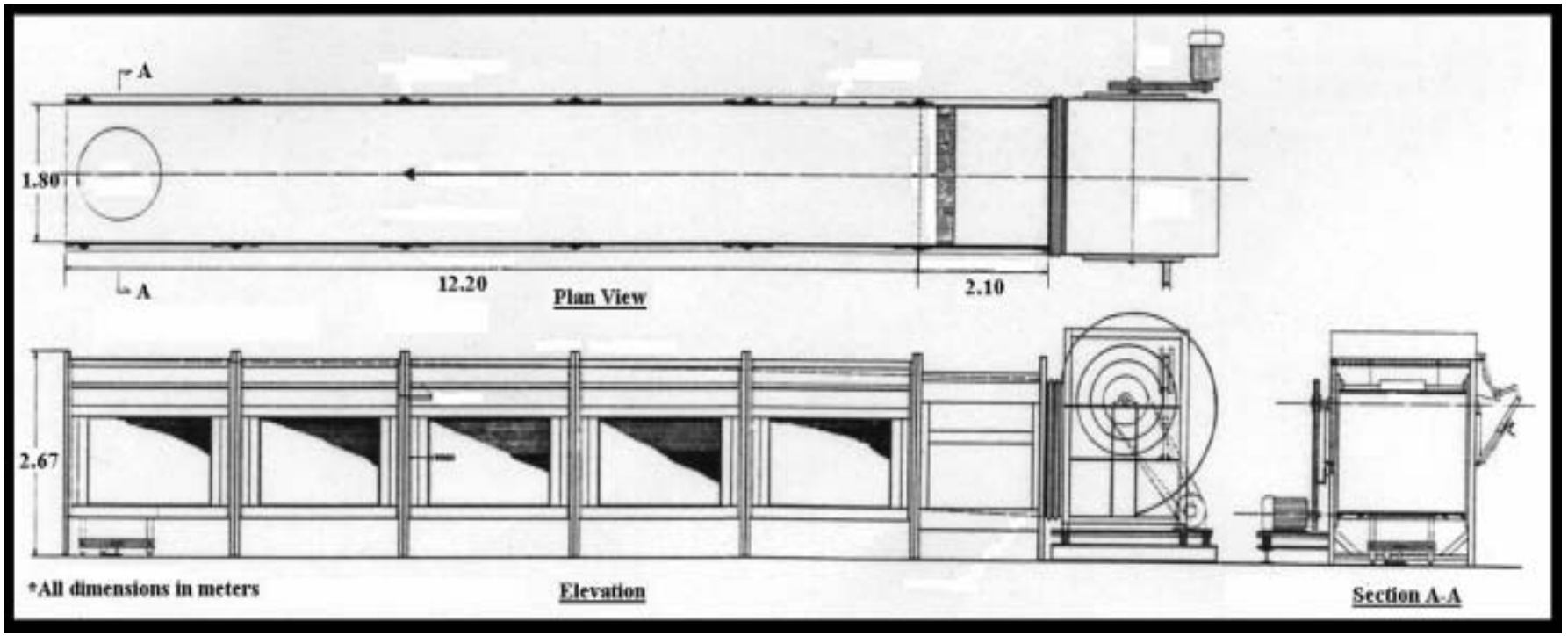

Figure 4.10 Concordia University boundary layer wind tunnel

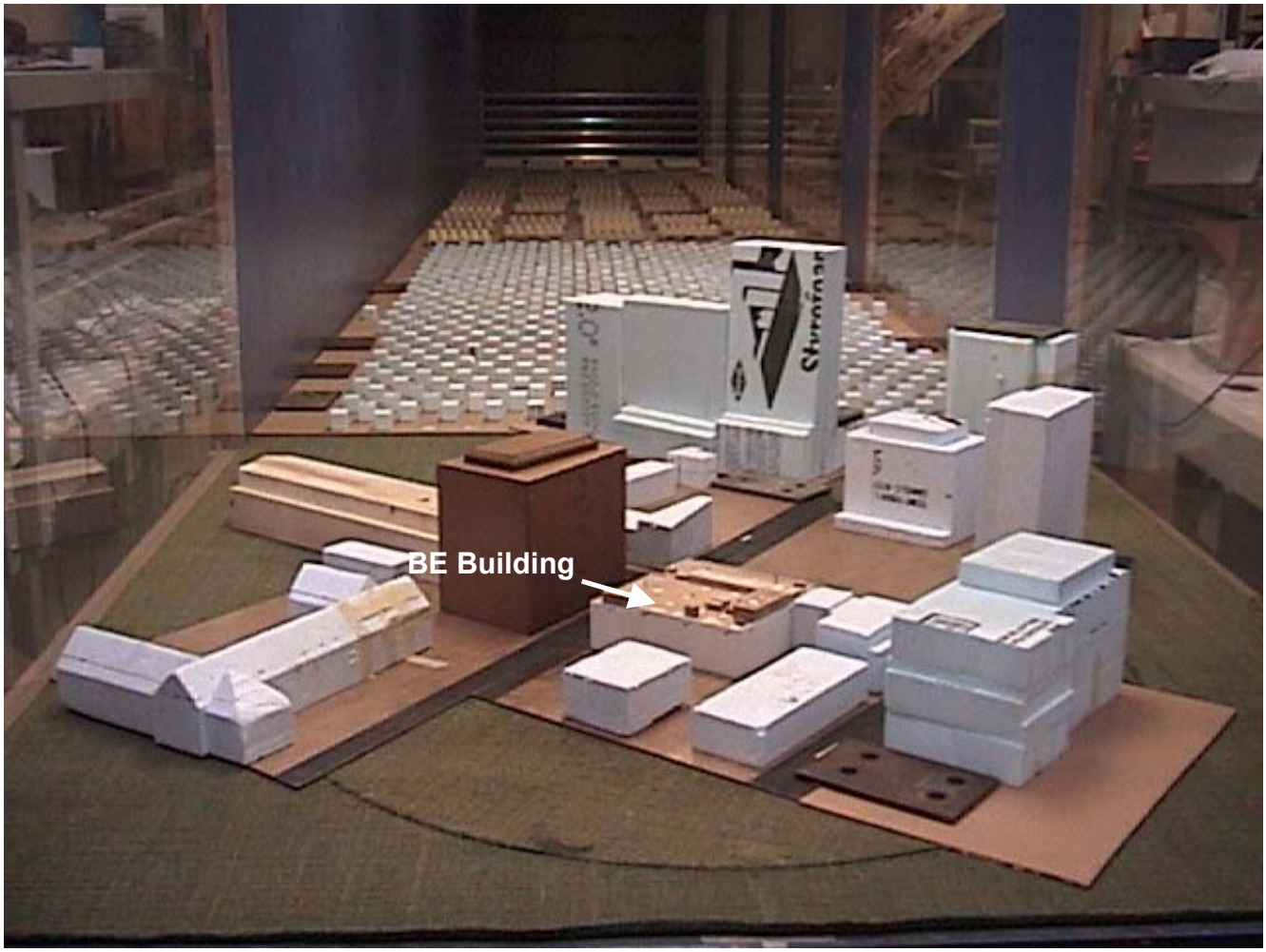

a) Westerly wind direction

Figure 4.11 Photograph of wind tunnel setup

b) Southwest wind direction

Figure 4.11 Photograph of wind tunnel setup

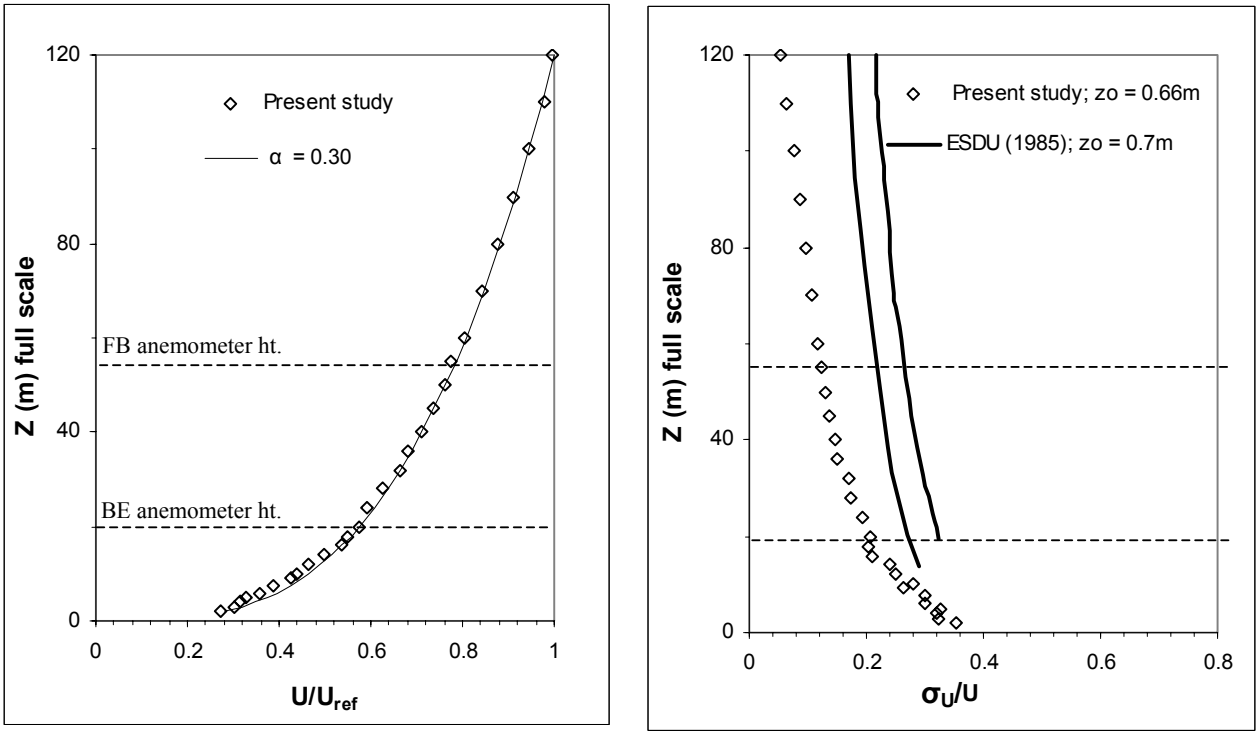

a) Mean velocity profile

b) Turbulence Intensity

Figure 4.12 Vertical profiles of mean wind velocity and turbulence intensity obtained with an urban exposure in the Concordia University boundary layer wind tunnel

Chapter 5

Experimental Results

In the present chapter, results of field and wind tunnel experiments are discussed. The chapter has been divided into two sections:

Tests performed with an open fetch. (stack locations 1, 2 and 4)
Tests performed with a tall upwind adjacent building (stack locations 3 and 4)

The results obtained in section 5.1 are suitable for comparison with Gaussian dispersion models recommended in ASHRAE (2003) since the plume traveled downwind. In such cases, receptor concentrations are largely dependent on their distance from the source. On the other hand, for tests discussed in section 5.2, the plume was trapped in the near-wake region of the upwind building. For this configuration, the plume initially travels upwind before being dispersed by the wake turbulence. Due to the complexity of the flow in building wakes, Gaussian dispersion models are not applicable for the prediction of dilution profiles on the roof of the emitting building and leeward wall of the adjacent building. A complex Gaussian wake model was developed by Wilson et al (1998) had relatively poor predictive capability but it was successful in demonstrating the trend of dilution associated with changes in M.

The following format will be followed in discussion of the results. First, an overview of the field data will be presented and will focus on the influence of exhaust momentum ratio (M) and stack height on concentration data. Secondly, the field results will be compared to the available dispersion models. Finally, the data will be compared with wind tunnel results.

The concentration data will be expressed in two forms:

normalized concentration (k),

dilution (D).

The normalized concentration is generally used in the scientific literature [e.g. Snyder (1994)]. On the other hand, the ASHRAE (1999) and ASHRAE (2003) dispersion models are in terms of dilution.

Tests with an open fetch

This section presents data for tests in which the upwind fetch was relatively open:

Stack 1 (all tests)

Stack 2 (all tests)

Stack 4 (Nov. 21, 2002 only)

Photographs of the upwind fetch for each stack location are shown in Figure 4.4. In each case, it is assumed that upwind buildings do not significantly influence the plume *trajectory* but may enhance plume *spread*.

5.1.1 Overview of field data (open fetch)

A total of thirteen 50-minute tests were performed with open fetch conditions (see Table 4.1). In this section, typical results from seven of these tests are discussed. Table 5.1 provides meteorological and stack parameters for the selected tests. The wind direction was generally southwesterly ($228^o < \theta < 260^o$) for stack 1, northwesterly ($280^o < \theta < 355^o$) for stack 2 and southeasterly ($\theta \sim 160^o$) for stack 4.

Figure 5.1 and Figure 5.2 show wind data obtained with the sonic anemometer at 5-minute intervals for the stack 1 and stack 2 tests, respectively. Also shown are wind speed and wind direction data obtained at Dorval Airport at a height of 10 m. An additional wind speed curve is shown which indicates predicted U values at the BE building based on Dorval measurements. In general, wind direction measured at Dorval compare well with θ values measured at the BE building. Likewise, the Dorval wind speeds, adjusted for measurement height and terrain, compare well with the BE data.

It was intended that the tests be performed in moderate to high winds to ensure neutral atmospheric stability, since this condition is simulated in the wind tunnel and assumed in the ASHRAE dispersion models. A further advantage to neutral conditions is that variations in wind direction during a 50-minute test are typically small, compared to those obtained in stable or unstable conditions. Although low wind speeds (< 2 m/s) were measured at the BE building during some tests (e.g. June 28.01, Aug. 29.01), neutral or near neutral conditions are assumed for all tests since the Dorval wind speed usually

exceeded 4 m/s. Low wind speeds at the BE building are due primarily to sheltering effects of upwind buildings and Mount Royal.

Table 5.1 Wind and stack data for selected open fetch tests

Date	Test No.	Stack Location	Stack Height (m)	M	U_H (m/s)	θ (deg)
10/12/00	1	SL1	1	5.4	3.3	240
	2	SL1	1	2.5	3.0	242
05/15/02	1	SL1	3	2.5	3.0	267
10/30/01	1	SL2	1	3.4	2.3	305
	2	SL2	3	3.6	2.1	316
11/21/02	1	SL4	1	5.6	1.5	160
	2	SL4	1	10.5	1.7	160

It should also be noted that large fluctuations in U and θ were measured by the BE anemometer on Oct. 12, 2000. The spikes in the data are believed to be a result of an occasional shift in the wind direction which caused the Faubourg building to be upwind of the BE building. Concentration measurements obtained during these periods are not representative of an open fetch configuration and therefore have not been included in the present analysis.

Figure 5.3 shows wind speed data for the tests performed with stack 4 on Nov. 21, 2002. The data were obtained with a cup anemometer located on the 4 m tall elevator housing at the south corner of the BE building. The measured wind speed compares well with Dorval data adjusted for height and terrain.

5.1.2 Effect of M (Field data)

The effect of exhaust momentum ratio, $M= w_e/U_H$, was investigated in the field tests by changing the exhaust velocity. Typically, a 50-minute test would be performed for a low or high value of w_e (~7.5 m/s or ~17.5 m/s) and the 2nd 50 minute test would be carried out using the other value of w_e. During some tests, especially those performed during light wind conditions (U_H < 2.5 m/s), the wind speed varied significantly during each test and consequently, M also varied significantly.

In comparing data of two tests performed on the same day, it is implicitly assumed that the wind conditions are similar during the two tests. This assumption was not always valid, however. Wind direction varied significantly during some tests and thus, the influence of M on k cannot be evaluated in such cases. For example, Figure 5.4 shows the variation in θ with time for the two 50-minute tests performed on June 28, 2001 with the stack at SL2. In this case, the mean wind direction for the two tests differed by approximately 20º. In each test, the range of 5-minute θ values was approximately 50º. Consequently, it is likely that a significant component of the variation in k is due to the variation in θ rather than M.

The Oct. 12, 2000 (SL2) tests are suitable for investigating the effect of M on k. In this case, the wind direction did not vary significantly during most sampling periods, disregarding the large fluctuations in θ that occurred intermittently (see Figure 5.1). These fluctuations are almost certainly due to a wind shift that caused the BE building to be in the wake of the Faubourg building. Sampling periods containing these θ spikes have not been included in the following analysis.

Typical time series plots of k obtained in the Oct. 12 test are shown in Figure 5.5. Results are shown for a nearby sampler located within 10 m of the stack on the roof (R15), a medium distance sampler on the skylight structure (S3) and one sampler located more than 40 m away on the penthouse (P2). Refer to Figure 4.9 for locations of samplers. The locations of the 15 samplers used in each of the field tests are also provided in Appendix A.

Figure 5.5a shows that at roof sampler R15, located near the stack at S~9 m, doubling the exhaust speed (or M-value) produces a similar reduction in k. The mean value of k at R15 for hour 1 (w_e=17.7 m/s, M=5.42) was approximately 1500. This compares to a k-value of 3000 for hour 2 when the exhaust speed was reduced (w_e=7.4 m/s, M=2.45).

Further away from the stack, the influence of M appears to be negligible. Figure 5.5b shows k-values obtained at sampler S3, located on the skylight structure at S~20 m. The mean values of k were approximately 1500 in each case. The relatively high k values obtained at S3 during the high flow test may be a result of the elevated position of the

sampler. Since the sampler was located at a height of 2 m above the roof, the effect of plume rise is small compared to that for rooftop samplers.

Figure 5.5c shows concentration data obtained at one of the farthest samplers, P2, located on the 4 m tall penthouse on the northeast side of the building (S~43 m). In this case, k values obtained with the high exhaust flow (M=5.4) were actually slightly greater than those obtained during the low flow test (M=2.4). The mean k value for the high flow case was approximately 350 while for the low flow test, mean k~200. Similarly, at rooftop samplers near the penthouse, k values obtained with M=5.4 were generally larger than those obtained with M=2.4. This indicates that for elevated and/or distant receptors, high exhaust velocity may not be beneficial and may in fact increase the severity of intake contamination. For elevated receptors, increasing M augments the momentum plume rise and as a result, elevated receptors may come in contact with the plume more frequently than would occur for a low M stack. For distant receptors at roof level, concentrations associated with a high M stack will be relatively high when the plume eventually makes contact with the roof.

A histogram showing the effect of M on mean k values for all samplers in the Oct. 12, 2000 test is plotted in Figure 5.6. The effectiveness of high exhaust speed in reducing k near the stack (S<20 m) is clearly evident. At larger distances, high M does not reduce k and may, in fact, increase k.

Variations in M are also produced by changes in wind speed. Therefore, the effect of M on k can be investigated by analyzing data from a single 50-min test that had significant variation in wind speed. Figures 5.7 and 5.8 show histograms of k for the Oct. 12, 2000 test (hr 1) and the May 15, 2002 test. As expected, the results show a relatively strong M-effect near the stack and a lesser effect at the distant samplers.

5.1.3 Effect of stack height (field data)

The influence of stack height on k values was investigated in the field study using a 1 m and a 3 m stack. Wind tunnel experiments were later carried out to obtain data for additional stack heights. These results are discussed in Sec. 5.1.5.

As with the effect of M on k, analysis of stack height effects was hampered by the large variation of wind direction during a test. Furthermore, wind speed variations also caused M to vary significantly. This is indicated in Figures 5.9 and 5.10, which show time series of θ and M for the Oct. 30, 2001 tests (stack loc. 2). During one 50-minute test, the wind direction varied by more than 60 deg. and M varied between 2.2 and 6.2.

Because of the variation of θ and M, the sample size used to evaluate stack height effects was small. Figure 5.11 shows a histogram of k values obtained in the Oct. 30 tests, for a sample size n=3 (3 periods of 5 minutes each) for which M~3 and θ~305 deg. For this limited sample, it appears that increasing the stack height from 1 m to 3 m, reduced k significantly, by as much as a factor of 5, near the stack (S<20 m). Some reduction in k

occurred at most of the other samplers, although the reduction was usually less than a factor of two.

Results were similar for the Nov. 15, 2000 test with the stack at SL1. Values of k at most samplers were highest with the 1 m stack. Increasing h_s to 3 m reduced k by less than a factor of 2 at most locations.

5.1.4 Comparison of field dilutions with ASHRAE model predictions

ASHRAE provides a number of models for the prediction of plume dilution at rooftop and wall receptors. In ASHRAE (1999), formulas are given for minimum dilution (D_{min}) for flush stacks and critical dilution (D_{crit}) for stacks with $h_s > 0$. ASHRAE (2003) recommends a new dilution formula, based on the Gaussian dispersion model, to predict roof-level dilution, D_r. As in the previous models, the ASHRAE (2003) model estimates dilution on the plume centre-line.

Descriptions of the ASHRAE dilution models have been provided in Chapter 3. Further details and assumptions used in the present study are given below.

D_r ASHRAE (2003) Assumptions: stack height = 0, no averaging time correction

Assumption No. 1: $h_s=0$

In applying the D_r model (Equs. 3-13-3-16), the final rise plume height, h, must be specified:

$$h = h_s + h_r - h_d$$

where h_s is stack height, h_r is plume rise and h_d is stack wake downwash. According to ASHRAE (2003), proper stack design suggests that h should be greater than the smallest height required to avoid a critical receptor, assuming a 5:1 slope of the plume (see Figure 3.3)**.** This smallest height is referred to as h_{small}.

ASHRAE (2003) specifies that:

"If the plume height is less than h_{small} but higher than any rooftop obstacle or recirculation zone (h_{top} in Figure 3.2), then only the physical height above h_{top} should be used to compute plume height rather than the full physical stack height."

If the plume height does not reach h_{top}, ASHRAE (2003) recommends the use of another dilution model (D_s) which does not consider plume rise.

In a design situation, the value of h_{small} depends on the location of the critical receptor (fresh air intake). It also depends on the exhaust velocity and the design wind speed, since these parameters determine the minimum plume rise (see Equ. 3-7). However, in the present study, it is simply assumed that h_{small} is large, as would be the case for a leeward wall intake, and thus, h is always less than h_{small}. It is also assumed that the momentum plume rise always exceeds the maximum height of the roof recirculation zones, h_{top}. Consequently, since $h_{top} < h < h_{small}$, stack height has not been included in the calculation of h.

The predicted recirculation zones corresponding to tests carried out with stack locations SL1 and SL2 are shown in Figure 5.12. Estimated values of h_{small} are indicated for intakes A, B and C, located on the leeward walls of the skylight structure, penthouse and main building, respectively.

Note that this figure is strictly applicable only for winds that are nearly normal to the northwest wall of the building. This condition was generally not satisfied for the SL1 tests (Oct. 12, 2000, Nov. 15, 2000), in which oblique winds likely produced conical vortices at leading edges of the building and roof structures. Nevertheless, Figure 5.12 will be used for the analysis of SL1 tests as well as SL2 tests, based on the assumption that the dimensions of recirculation zones for SL1 tests are roughly similar to those indicated.

Finally, it should be noted that the value of h used in Equ. 3-13 is assumed to be the height of the plume relative to the receptor height. Although elevated receptors are not mentioned in ASHRAE (2003), in the present study, the value of h is determined by subtracting the height of the receptor (rooftop structure) from the plume height. Thus, for a plume with a height of 10 m above the main roof, h=10 m for roof receptors and h = 6 m for receptors on the 4 m high penthouse.

Figure 5.12 indicates that the plume must rise to a height of 13.2 m to avoid being entrained in any of the rooftop or wake recirculation zones. This height is h_{small} for an intake on the leeward wall.

For the test on Nov. 21, 2002, the stack was at SL4 and the wind direction was southeasterly. Figure 5.13 shows the recirculation zones for this case. Note that, because SL4 is near the center of the roof, the minimum plume height required to avoid all recirculation zones (h_{small} = 9.6 m) is less than that for the stacks at SL1 and SL2, i.e. h_{small} =13.2 m. SL4 differs from SL1 and SL2 in that it is not located in the leading edge recirculation zone.

Assumption No. 2: no averaging time correction

The D_r model assumes an averaging time of 2 minutes. Values of lateral plume spread are adjusted for other averaging times using the 0.2 power law (see Equ. 3-14). However, if the stack tip and receptor are in the same recirculation zone, dilution is not expected to be sensitive to averaging time [ASHRAE (2003]. In the present study, since some samplers were in a roof recirculation zone with the stack, no averaging time correction has been made. Furthermore, the correction would be small anyway since the actual sampling time was only 5 minutes.

D_{min} ASHRAE (1999) Assumptions: stack height = 0, no averaging time correction, B_1 = 0.059.

Assumption No.1: h_s=0

The D_{min} model is applicable for exhaust vents that are flush with the roof and for stacks that do not exceed the height of rooftop structures [ASHRAE (1999)]. In the present

study, although the 3 m stack was slightly higher than the skylight rooftop structure, the effective stack height is considered to be zero for both 1 m and 3 m stacks.

Assumption No.2: no averaging time correction

The D_{min} model assumes an averaging time of 10 minutes. However, if the stack tip and receptor are in the same recirculation zone, dilution is not expected to be sensitive to averaging time [ASHRAE (1999]. In the present study, since some samplers were in a roof recirculation zone with the stack, no averaging time correction has been made.

Assumption No.3: $B_1 = 0.059$

The distance dilution parameter, B_1, is a function of the amount of turbulence in the approaching flow, as shown in Equ. 3.12. The recommended design value of B_1 for an urban area is 0.059, based on the assumption that $\sigma_\theta = 15^o$. Although σ_θ was not directly measured on the BE building, high values of longitudinal and lateral turbulence intensity measured during the tests indicate that $\sigma_\theta > 15^o$. Nevertheless, the default value of B_1 was chosen to provide conservative estimates of dilution.

ASHRAE dilution model comparisons

Field data from the tests at stack locations SL1, SL2 and SL4 have been used to evaluate the ASHRAE models. Recall that the ASHRAE models are not applicable for the SL3

tests, which were performed with the Faubourg building upwind. Except for the SL4 test (Nov. 21, 2002), the selected tests were generally performed in strong wind conditions.

Figure 5.14a shows 5-min dilution data plotted versus distance from the stack, located at SL1. The data were obtained with the 1 m stack and M=5.5 on Oct. 12, 2000. Also plotted are ASHRAE (2003) D_r curves for rooftop and skylight receptors and the ASHRAE (2001) D_{min} curve.

Relatively low values of dilution (100<D<200) were measured near the stack (S~10 m). At the most distant sampler, located on the 4 m high penthouse, the average dilution during the test was approximately 1000.

Generally, the D_{min} model provides an acceptable lower bound to the data, although dilution data obtained at one rooftop sampler and one skylight sampler were less than the predicted values. On the other hand, the D_r curve for rooftop samplers significantly overestimates the measured dilution values near the stack (S<25 m). The actual plume rise in this case may have been less than that predicted by the model due to high turbulence in the leading edge recirculation zone. Note, however, the D_r curve plotted for the skylight samplers fits the data well. The lower dilution indicated for the skylight samplers is due to the lower value of h, the height of the plume above the roof surface on which the samplers are located.

Figure 5.14b shows test results and model predictions for low M (SL1, M=2.5). In this case, the D_r model is conservative for both rooftop and skylight samplers – underpredicting the measured dilutions by approximately a factor of two at most locations. The D_{min} curve fits the data quite well.

Figure 5.15 shows data obtained in the May 15, 2002 test with the stack at SL1, for which h_s = 3 m and M=2.5. The ASHRAE models provide conservative predictions in this case. This conservatism is probably due to the assumption of zero stack height in both models. In addition, the underestimation of dilution may be partly due to the lack of receptors on the plume centre-line. The D_{min} curve provides a reasonable lower bound for the samplers located far from the stack (S>30 m), compared to the D_r model curves.

Figure 5.16a and 5.16b show data obtained with the 1 m and 3 m stacks, respectively, during the Oct. 30, 2001 tests (SL2, M~3.5). Minimum dilution values measured at each distance were generally similar for the two stacks. However, the tall stack produced numerous D values greater than 10,000 while the maximum dilution for the short stack was approximately 7000 at all locations.

The D_r curve for the rooftop samplers provides an acceptable lower bound near the stack (S<10 m). However, for S>20 m, D_r underpredicts the measured dilution by at least a factor of 5 for both the 1 m and 3 m stacks. The D_r curve for the skylight samplers is even more conservative. On the other hand, the D_{min} curve is less conservative, although it still

underpredicts the data by a factor of 3. It should also be noted that the D_{min} curve more accurately models the effect of distance on dilution than the D_r curves.

Figure 5.17 shows data obtained during the Nov. 21, 2002 tests with the 1 m stack at SL4 (M=5.6, M=10.5). Note that the 3 samplers farthest from the stack were wall samplers; the locations of these are shown in Figure 4.9. Comparing the two data sets, the effect of M (exhaust velocity) is evident. Near the stack (S~10 m), the minimum dilution at a rooftop sampler was approximately 300 for M=5.6. Increasing M to a value of 10.5 increased the minimum dilution at this sampler by a factor of 3 (D~ 1000). Further from the stack, the effect of M appears to be less significant. At S~30 m, minimum dilution obtained for M=10.5 is approximately 40% larger than that obtained for M=5.6. This appears to support the use of a two-component dilution model, like D_{min} that takes into account initial dilution near the stack and distance dilution.

The D_{min} model again provides an acceptable lower bound to the data, although it is overly conservative near the stack since it does not take into account the apparent dilution due to plume rise. The D_r curve for the skylight samplers fits the high M data well but is overly conservative for the M=5.6 data set. On the other hand, the D_r curve for the rooftop samplers fits the low M data reasonably well. However, the model is unconservative in predicting dilution at rooftop samplers for the high M case. The predicted values are approximately twice as large as the minimum dilutions measured at each location, indicating that the model overestimated the plume rise in this case.

The D_r model calculates momentum plume rise using Equ. 3-7, which was derived by Briggs (1984) for isolated stacks. The actual plume rise during some field tests may have been less than that predicted by Equ. 3-7 due to high turbulence in the approaching flow or downwash from rooftop structures. It should also be noted that the actual plume reaches its final height some distance from the stack. The D_r model assumes that plume rise occurs instantaneously and thus dilution values near the stack may be overestimated.

Finally, it should be noted that the D_r model would have been even more unconservative for the high M case if the stack height was considered. For M=10, the calculated plume height exceeds h_{small} for most receptors and consequently, the stack height should be included in calculating the plume height [ASHRAE (2003)]. If this were done, the predicted dilutions would have increased and the discrepancies between predicted and measured values would have been greater than those indicated in Figure 5.17b**.**

5.1.5 Comparison of field k values with wind tunnel data

The field concentration data, expressed as k values ($K = CU_HH^2(10^{-6})/Q_{SF6}$), have been compared to wind tunnel values for selected tests. Unless otherwise specified, the field data used in this comparative study are mean values for an entire 50-min test. In some cases, data for one or more of the 5 min sampling periods has been removed due to a large variation in wind direction or wind speed.

Diagrams showing wind tunnel and field k distributions on the BE building roof have been produced for all tests and are provided in Appendix B. Note that the wind tunnel

data were obtained for a limited number of M-values (M=2,3,4,5 etc.) which may not correspond exactly to the field value. Likewise, the wind direction in the wind tunnel was varied in increments of 10º. Therefore, in most cases the wind tunnel θ does not correspond exactly to the field value. It should also be noted that the field θ values have an expected uncertainty of ± 5º.

Figures 5.18 and 5.19 show wind tunnel and field k distributions obtained during the 1st and 2nd tests, respectively, of Oct. 30, 2001 (SL2). The M-value was approximately 3.5 in the field tests – slightly higher than the wind tunnel value (M=3). The wind direction used in both wind tunnel tests was 310º, which is within 6º of the estimated field values.

The wind tunnel k values agree reasonably well with the field data, although some degree of bias is evident. In both cases (h_s = 1m and 3 m), the wind tunnel overpredicted k near the stack, especially at the nearest skylight receptor, S3. For example, Figure 5.19 shows that when the stack was set at 3 m, k=705 at S3 in the wind tunnel. The corresponding field value was 320. Similar discrepancies are evident at the leeward edge of the building where wind tunnel k values at rooftop samplers in the path of the plume were 2 to 3 times the field values. Thus, the wind tunnel plume appears to be less dispersed than the field plume. This is also indicated by the somewhat higher k values measured in the field at the southwest edge of the building which is well off the plume centre-line. The field plume appears to be wider than the wind tunnel plume. The wind tunnel is unable to simulate the largest turbulence scales and so plume meander that is present in the field tests cannot

be reproduced in the wind tunnel, as discussed by Wilson (1995), Higson et al. (1994) and Mavroidis et al. (2003).

The bias of the wind tunnel data towards higher concentrations is evident in Figures 5.20 and 5.21 which show plots of field k values versus wind tunnel values. Although a number of data points lie on or near the 45 deg line, indicating good agreement, the majority of points are located below the line in each case.

Results obtained for a 1 m stack in the center of the roof (SL4) during the 2nd hour test on Nov. 21, 2002 are shown in Figure 5.22 (M=10.7, θ=160º). The comparison between wind tunnel and field concentrations is very good in this case, with the deviation between predicted and measured values less than 10% at several locations. At most, the wind tunnel value differed from the field k by a factor of 2.5. Concentrations obtained at the three leeward wall samplers in the wind tunnel were approximately twice as large as the field values.

Figure 5.23 shows a scatter plot and histogram of the k values shown in Figure 5.22. The scatter plot shows remarkable correlation between the wind tunnel and field data. Similar results were obtained for the 1st Nov. 21 test, for a lower M value (M=5).

Wind tunnel and field concentrations obtained during the May 15, 2002 test are shown in Figure 5.24. This test was carried out with a 3 m stack at SL1. The average M-value during the 50-minute test was only 2.5 due to a low exhaust velocity (w_e = 7.6 m/s).

The wind tunnel and field k values generally compare well, although the agreement is not as good as in the Nov. 21 test. The predicted concentrations are generally within a factor of 2 of the field values. Note the relatively large field concentration (k=489) measured on the roof near the stack (R9) which may be a result of stack tip downwash or high turbulence in the roof recirculation zone. The wind tunnel value was only 222, indicating the plume rise was greater in the wind tunnel.

Figure 5.25 shows the scatter plot and histogram of wind tunnel and field k values for the May 15 test. The discrepancies are much larger in this case than for the Nov. 21 test. This may be due to local instabilities in the approaching flow (both in the field and wind tunnel studies) produced by nearby buildings on May 15. In contrast, the approaching flow during the Nov. 21 tests may have been more stable since the southeast fetch is relatively open.

Although the wind tunnel simulated the field tests well in most cases, relatively poor agreement was obtained for the Oct. 12, 2000 and Nov. 15, 2000 tests, which were carried out with the stack at SL1. Wind tunnel and field concentrations obtained during the first Oct. 12, 2000 test are shown in Figure 5.26. In this case, field concentrations measured at rooftop samplers near the stack were large (e.g. k=1660 @ R15) due to the low stack height and strong wind. In contrast, wind tunnel k values at the rooftop samplers near the stack were small – sometimes less than 1% of the field value. On the other hand, wind tunnel k values measured on the penthouse were 3 to 4 times the field

values. It appears that the wind tunnel plume in this case had significantly greater plume rise and less lateral dispersion than the field plume.

For the Oct. 12, 2000 test, the minimum model value of Re_s was approximately 3000, which satisfies the criterion (Re_s >2000). The stack Reynolds No. criterion was also satisfied for the Nov. 15, 2000 model test (min Re_s ~ 5700). Thus, discrepancies between field and wind tunnel concentrations for these tests are not due to laminar flow in the model stack. It is more likely that the discrepancies are due to incorrect modeling of the upstream terrain. The turbulence intensity measured in the wind tunnel with a hot film probe at the location of the field anemometer (see Figure 4.2) was only 18% -- much less than the >40% turbulence intensities measured in the field tests of Oct. 12, 2000. Since flow patterns around buildings are strongly affected by the turbulence intensity of the approaching flow, it is not surprising that the wind tunnel and field dispersion patterns shown in Figure 5.26 are dissimilar. Further wind tunnel testing will be carried out with this configuration to determine the cause of the large discrepancies between wind tunnel and field values.

Figure 5.27a shows a scatter plot of field and wind tunnel k values obtained on the roof of the BE building for all open-fetch tests except Oct. 12, 2000. In general, the wind tunnel values compare well with the field data. Approximately 80% of the wind tunnel values are within a factor of two of the field results, as indicated by the 45º lines plotted on either side of the centre line. As discussed previously, the wind tunnel simulation of the

Oct. 12, 2000 test was not acceptable. Figure 5.27b shows that the wind tunnel significantly underestimated the field k values at most locations.

5.1.6 Effect of stack height (wind tunnel data)

The very good agreement between wind tunnel and field data for the Nov. 21 tests suggests that the effect of stack height can be predicted accurately by the wind tunnel for this stack location and wind direction (SL4, θ =160º). Figure 5.28 shows a histogram plot of k-values at the various receptors for stack heights of 1 m to 7 m for M=5.5. Compared to the 1 m stack, the 3 m stack reduces k by as much as a factor of 2 while the 5 m stack reduces k by approximately a factor of 3 at most locations. Very large reduction in k, by a factor of 10 or more, is achieved with the 7 m stack at most roof samplers. The effect of stack height is less significant at the wall samplers since the k values are relatively low, even for the 1 m stack.

Tests with the Faubourg building directly upwind of the BE building

A total of eight 50-min field tests were carried out with the Faubourg Building directly upwind of the BE Building. Tests were performed with the stack at SL3 on Aug. 12, Aug. 26 and Sept. 6, 2002. The stack was located at SL4 for the final two tests on October 1st, 2002.

Wind data were obtained with a YOUNG propeller anemometer on a 5 m mast near the southwest edge of the Faubourg roof. Figure 5.29 shows an elevation view of the BE and Faubourg buildings showing stack locations (SL3, SL4) and the anemometer location. It

should be noted that the Faubourg Building is not an isolated structure; it is connected to a long 4-storey structure on its southwest side.

Figure 5.30 shows time series of wind speed, wind direction and turbulence intensity for the four test days. Table 4.2 shows 50-min average values of the wind data for each test. Values of wind speed at the BE building height were derived from the Faubourg wind speed, U_{ref}, using the power law approximation with $\alpha = 0.30$. Note that winds were moderate to strong during all of the tests ($U_{ref} > 4$ m/s). Thus, the atmosphere could be classified as neutral or slightly unstable.

Stack parameters are shown in Table 4.3. The 50-min average M-values for the 8 tests, based on U_H, varied between 1.7 and 4.9. Figure 5.31 shows a photograph of a smoke test performed with the 3 m stack at SL3 on Sept. 6, 2002.

5.2.1 Overview of field data (Faubourg building upwind)

Time series of k obtained at three BE roof samplers during the two Aug. 12, 2002 tests are shown in Figure 5.32. For these tests, the 1 m stack was located near the leading edge of the building (SL3); the average M-values were 2.4 and 4.9. Figure 5.32a shows that near the stack (sampler R4), increasing M causes k to decrease. Although k shows large fluctuations in both tests, the peak value of k obtained for M=2.3 (k=2900) was significantly larger than that obtained for M=4.9 (k=900). On the other hand, M had little effect on k values obtained farther from the stack, as shown in Figures 5.32b and 5.32c

for the center roof (R23) and the northeast penthouse (P2) samplers, respectively. At both locations, the mean k values were similar for the two M-values.

Time series of concentration obtained at three wall samplers near the roof of the Faubourg building during the Aug. 26, 2002 are shown in Figure 5.33a and Figure 5.33b for M=1.7 and M=3.9, respectively. Note that in both cases, very high correlation between the samplers is evident. This suggests that, for emission sources in the near wake of the building, the location or size of a fresh air intake on the leeward wall has little influence on the amount of effluent that is entrained.

The effect of M on the wall concentrations is relatively small in this case. The 50-min mean k values at the middle sampler (FB2) were 394 for M=1.7 and 277 for M=3.9. Thus, an increase in M by more than a factor of 2 resulted in only a 40% reduction in k.

5.2.2 Comparison of field k values with wind tunnel data

Figure 5.34 shows the influence of wind direction on 5-min field values of k obtained at the center Faubourg wall sampler for low M ($2<M<3$) with the stack at SL3. Figures 5.34a and 5.34b show results obtained with the 1 m and 3 m stack, respectively. The field results do not show a significant trend over the range, $200^\circ < \theta < 235^\circ$, although the data show considerable scatter. Similarly, the wind tunnel k is relatively constant with respect to wind direction, although k reaches a maximum at $\theta = 220^\circ$ for the 1 m stack and shows a small increase with θ for the 3 m stack.

Figure 5.34 shows that the wind tunnel overpredicted k on the Faubourg building, on average, by a factor of 2 to 3. This suggests that plume rise may not have been modeled accurately in the wind tunnel. Other factors that may have affected the wind tunnel results are reduced values of turbulence intensity (T.I. = σ_u/U), and scale (L_x/D) due to the use of the large-scale model. For example, the wind tunnel T.I. was approximately 13% at the Faubourg anemometer height. This compares to values of 25% to 30% measured during the field tests. The relatively low turbulence in the wind tunnel may have reduced the lateral spreading of the plume, causing larger k values on the Faubourg wall.

Figure 5.35 shows the influence of wind direction on field and wind tunnel concentrations measured at a penthouse sampler (P2) for a 1m and 3 m stack at SL3. The field results indicate little influence of θ over the range $200^o < \theta < 235^o$ for the 1 m stack and $215^o < \theta < 235^o$ for the 3 m stack. On the other hand, the wind tunnel k shows some dependence on θ; in both cases, k reaches a maximum at $\theta = 220^o$. The wind tunnel k values at the BE penthouse are larger than the mean field value by approximately a factor of 2, on average, although in some cases, the wind tunnel data are lower than the field values for h_s = 1 m.

Figure 5.36a shows distributions of wind tunnel and field k (50-min avg.) on the roof of the BE Building and the leeward wall of the Faubourg building for the 1st test conducted on Aug. 12 for the 1 m stack at SL3. The exhaust speed of 18.0 m s^{-1} gave a relatively high M-value of 4.9. The wind tunnel data obtained on the roof of the BE Building were

generally similar to the field values except near the stack where the field k values were significantly larger. For example, at location 2, closest to the stack, the field value was approximately 4 times larger than the wind tunnel value. Note, however, that this trend is reversed for receptors on the leeward wall of the Faubourg, where wind tunnel k values are significantly larger than the field data, as shown previously in Figure 5.34. The leeward wall distributions will be discussed in more detail below.

Figure 5.36b shows wind tunnel and field k distributions obtained with low M (M~2.3). Compared to the high M case shown in Figure 5.36a, the concentrations obtained with low M are larger at all samplers. Near the stack, the field k values are much larger than the wind tunnel values.

Figure 5.37 shows the variation of k on the BE building roof in the along-wind direction for the Aug. 12 tests. Near the stack, the field values are significantly larger than the wind tunnel values. In particular, for the low M case (M_{field} =2.3), the field k is almost 10 times as large as the wind tunnel value. This discrepancy may be due to incorrect modeling of the model stack exhaust. For this case, the exhaust flow was laminar and consequently, the plume rise may have been too large in the wind tunnel.

For the M~5 case, the model plume rise is expected to be more accurately simulated since the exhaust flow was turbulent. Nevertheless, the field k exceeded the wind tunnel value by a factor of 4 at the near-stack sampler. It should be noted that good agreement between field and wind tunnel data is apparent further from the stack.

Figure 5.38 shows the variation of k with x for the Oct. 1 test when the stack location was near the center of the roof (x/L = 0.43) and the stack height was 1m. In this case, the field values near the stack were approximately two times the wind tunnel values. These discrepancies may again be attributable to excessive plume rise in the wind tunnel simulation. However, much better agreement between wind tunnel and field values was obtained at locations near the windward and leeward edges of the building and for higher M values.

Figures 5.37 and 5.38 indicate that the lowest k values on the roof of the BE Bldg. were measured near the leeward edge of the building. This suggests that for this building configuration, the optimum intake location is the northeast wall of the building.

Vertical distributions of k on the leeward wall of the Faubourg are shown in Figure 5.39 for the Aug. 26 test (hr 2). The stack location in this case was near the windward edge (x/L=0.08) and the stack height was 3 m. The exhaust momentum ratio was relatively large (M=3.9). k values obtained on the wall of the Faubourg in the wind tunnel were significantly larger than the field values except near the roof level of the emitting building. Near the roof of the Faubourg, the wind tunnel k values are approximately 2 to 3 times larger than the field values.

Similar results are shown in Figure 5.40 for the Oct. 1st test (hr 2) for which x/L=0.43, h_s = 1 m and M=3.7. As with the Aug. 26 test, the maximum k occurs near the roof of the Faubourg and the wind tunnel values are two to three times as large as the field values.

However, the values are less than those obtained with the upwind stack used in the Aug. 26 test. For example, the maximum k value obtained in the wind tunnel with the central stack (370) was 2 to 3 times less than the values obtained with the upwind stack ($750<K<1050$).

Wind tunnel experiments were carried out to evaluate the effect of stack height on k when the Faubourg building is upwind of the BE building. Figure 5.41 shows results obtained at three BE roof samplers and the Faubourg wall samplers for the stack at SL3 and M=2.2. The results obtained on both buildings show that even a 7 m stack provides little reduction in k. At most, the 7 m stack reduced k by a factor of two compared to the value obtained with the 1 m stack. Larger reductions may occur at larger M however.

Discrepancies between wind tunnel and field concentrations

The wind tunnel k values on the leeward wall of the Faubourg building were consistently larger than the field values, regardless of the M-value and model stack Reynolds number. This suggests that the wind tunnel did not accurately simulate the near-wake of the Faubourg building. The turbulence intensity measured above the Faubourg roof in the wind tunnel was less than 50% of the typical field value (see Table 4.4b) and consequently, flow characteristics of the modelled and full-scale wakes may be different. Furthermore, the absence of large scale turbulence in the wind tunnel may have reduced the lateral movement of the plume.

Figures 5.42a and 5.42b show scatter plots of wind tunnel and field k values measured on the BE roof and Faubourg wall, respectively, for tests performed with the Faubourg building upwind. The BE roof data generally show good agreement; most of the wind tunnel values are within a factor of two of the field results. As discussed previously, the wind tunnel underpredicted the field values at locations near the stack. Figure 5.42b shows that the wind tunnel consistently overpredicted k values on the Faubourg wall.

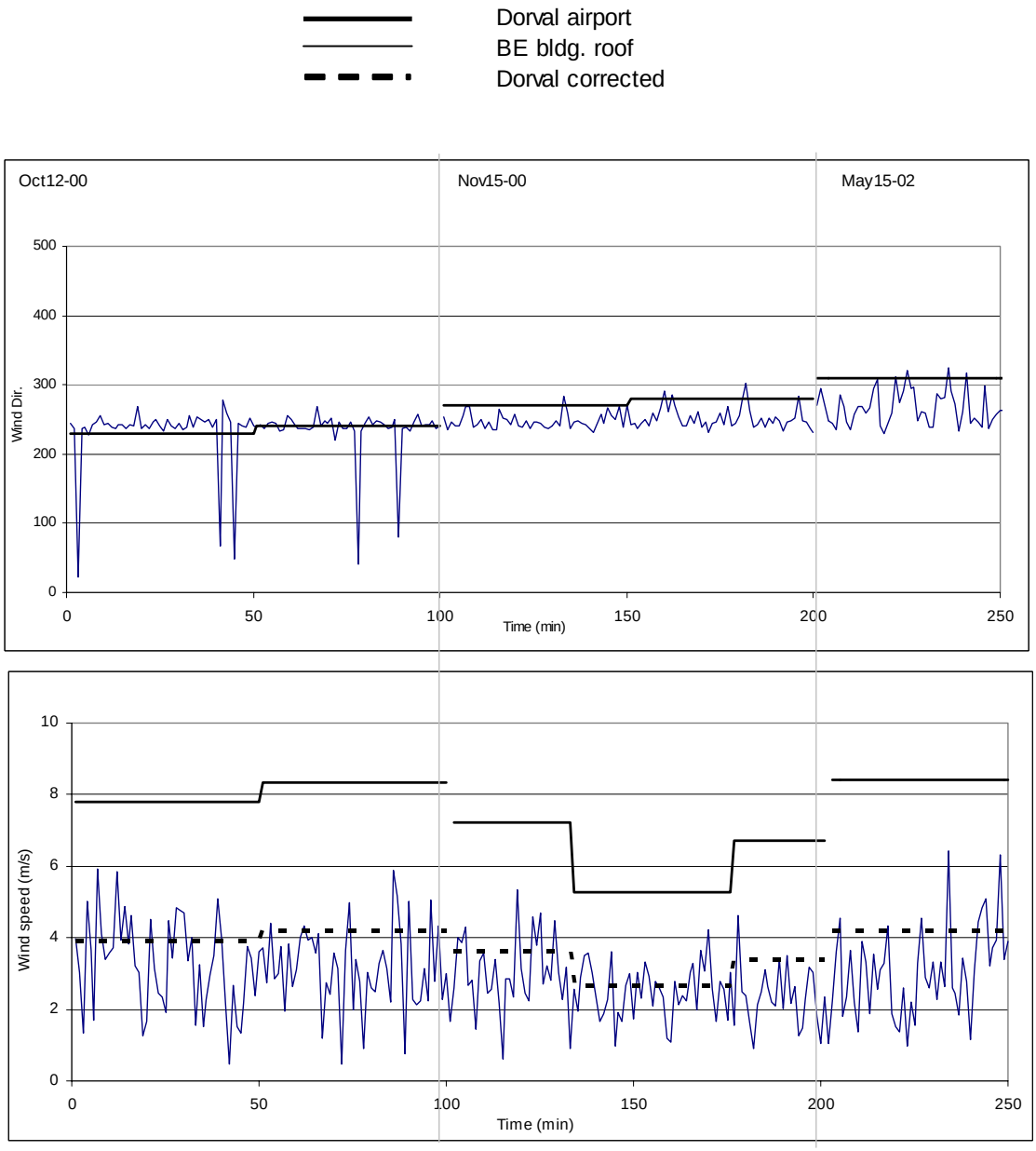

Figure 5.1 Wind data obtained for stack location 1

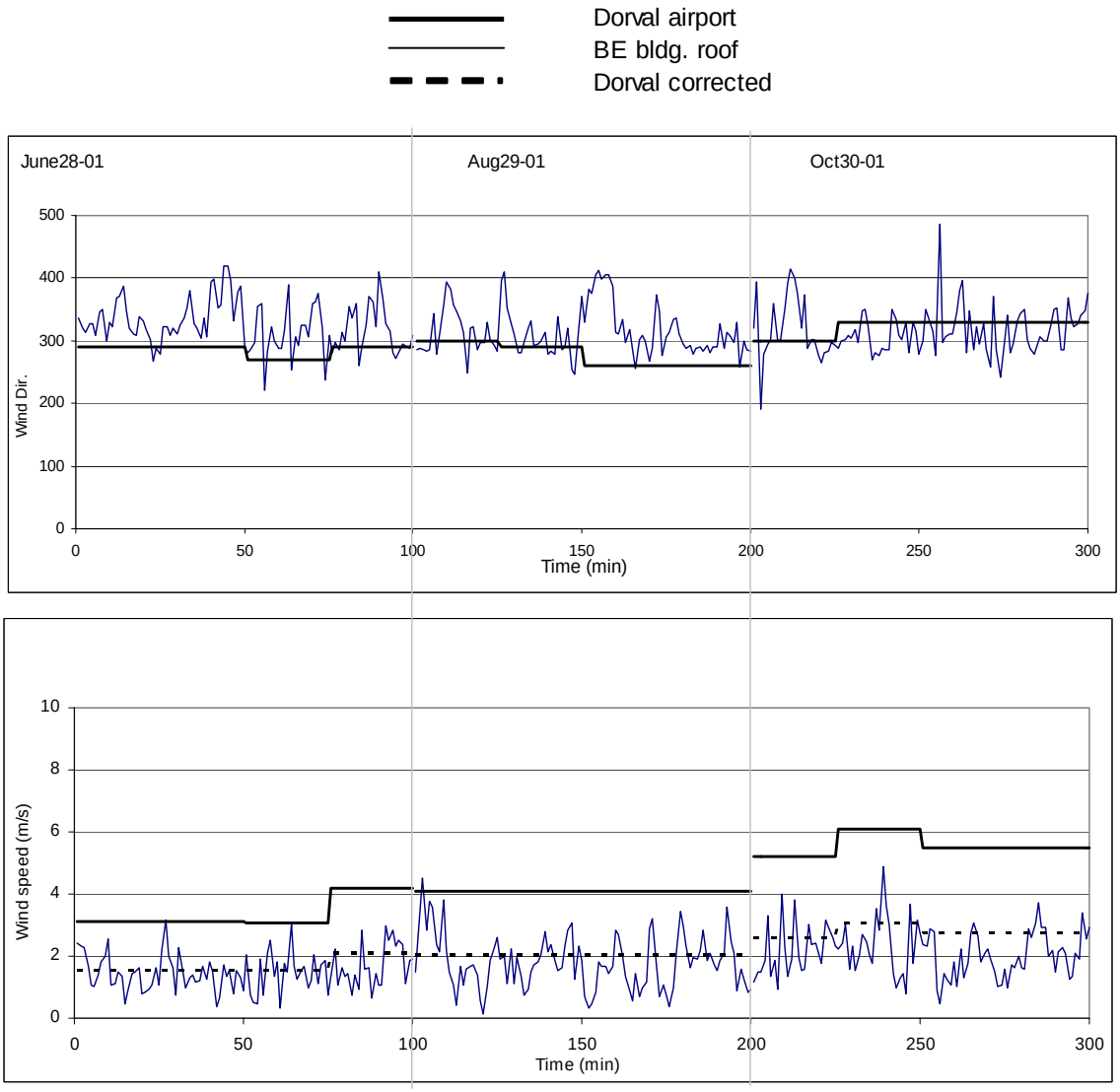

Figure 5.2 Wind data obtained for stack location 2

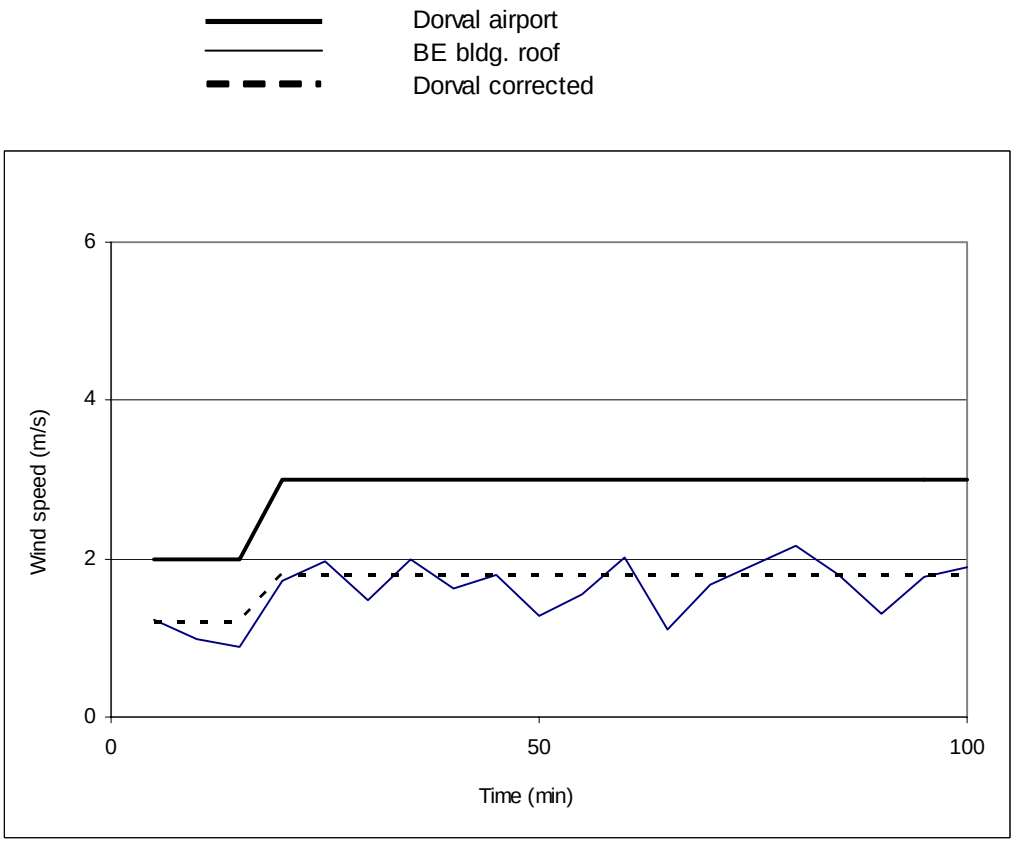

Figure 5.3 Wind data obtained for stack location 4 (Nov.21-02 field test)

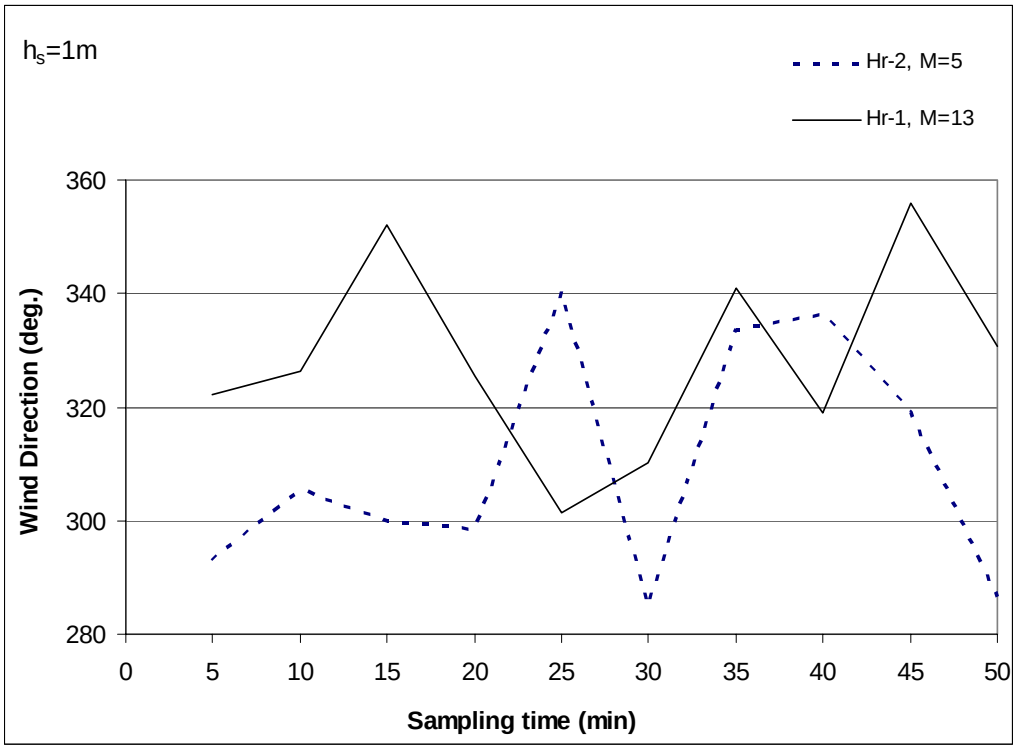

Figure 5.4 Variation of wind direction with time for June 28-01 field test: Stack location 2

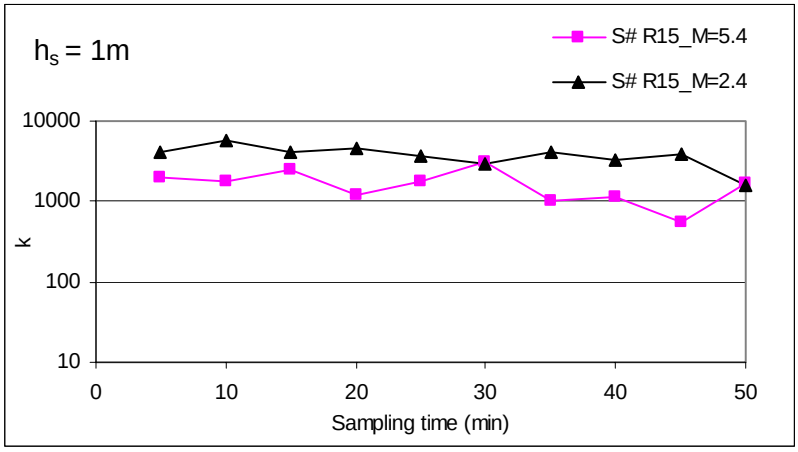

(a)

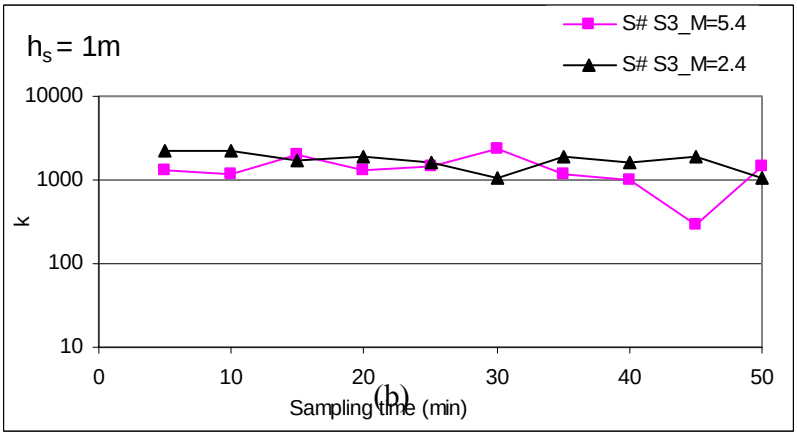

(b)

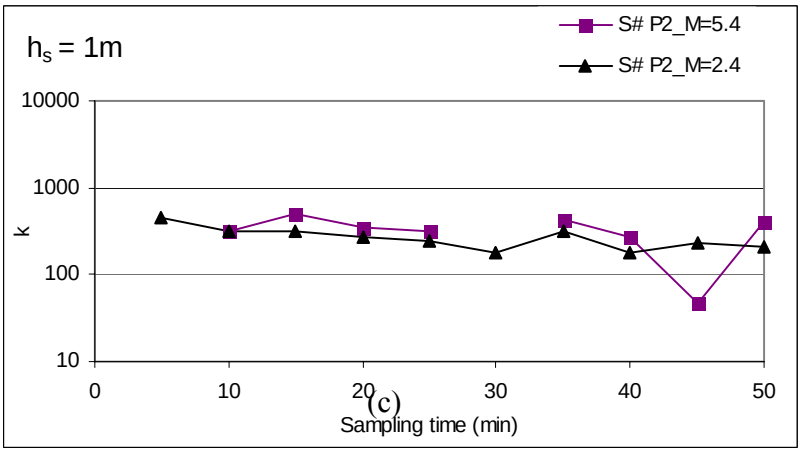

(c)

Figure 5.5 Concentration k time series for Oct12-00 field tests for near, mid and far sampler: Stack location 1

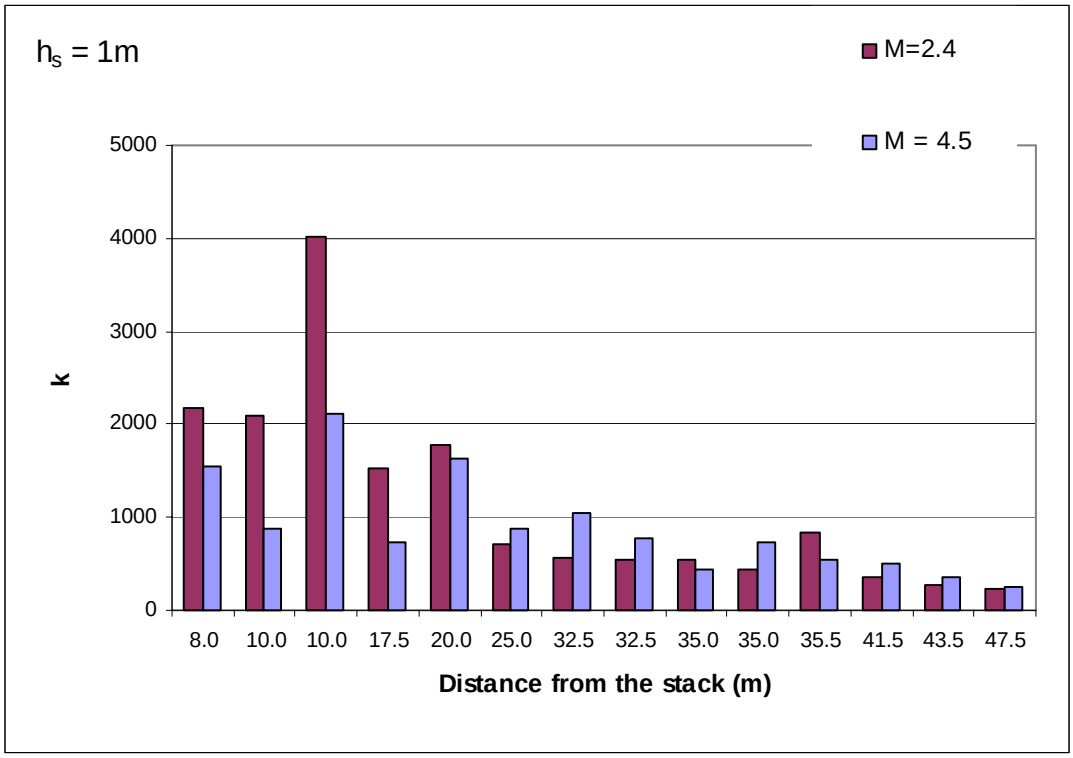

Figure 5.6 Effect of exhaust momentum (M) on k: Oct.12-00 field test: Stack location 1

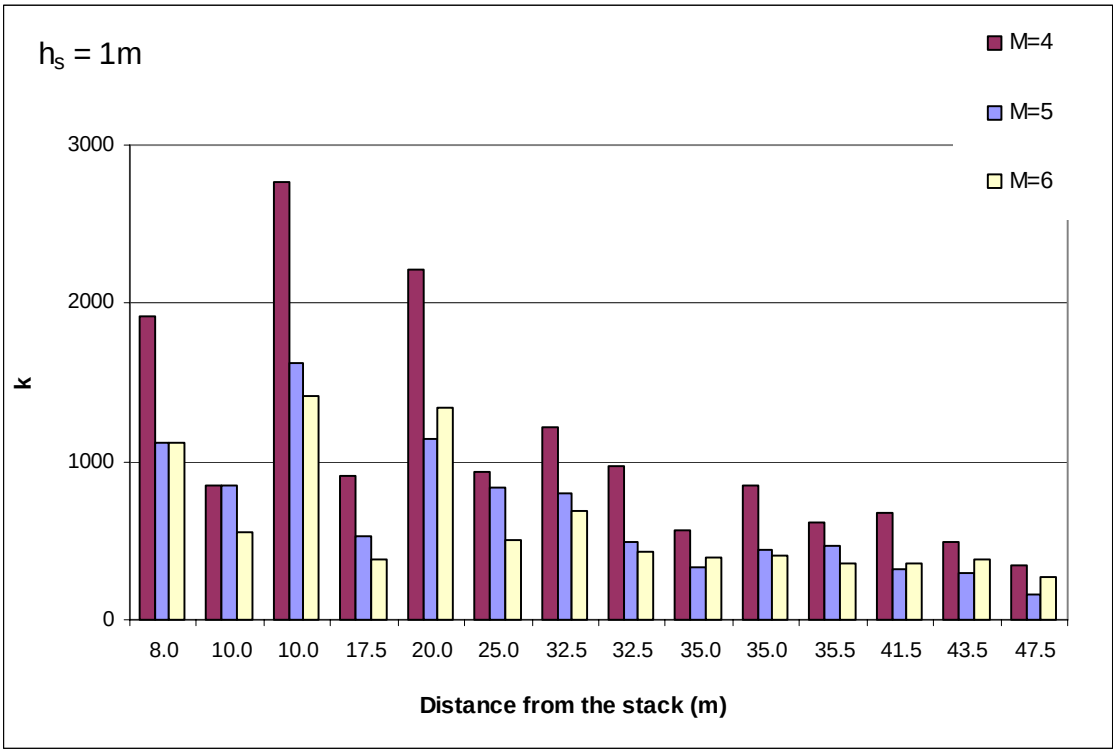

Figure 5.7 Effect of exhaust momentum (M) on k: Oct.12-00 field test: Stack location 1

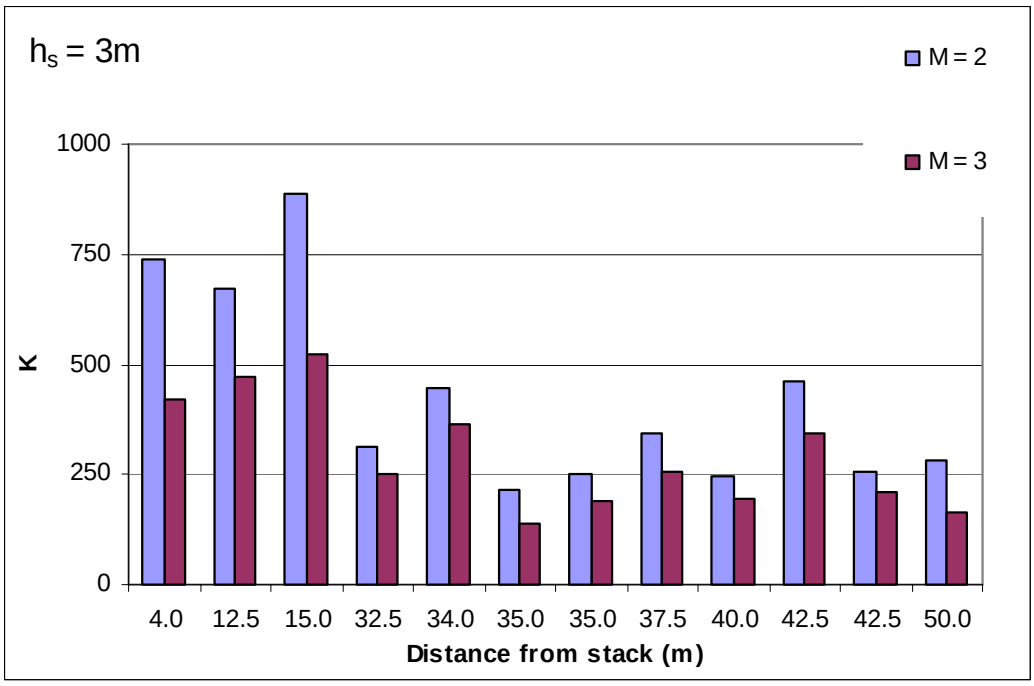

Figure 5.8 Effect of exhaust momentum (M) on k: May15-02 field test: Stack location 1

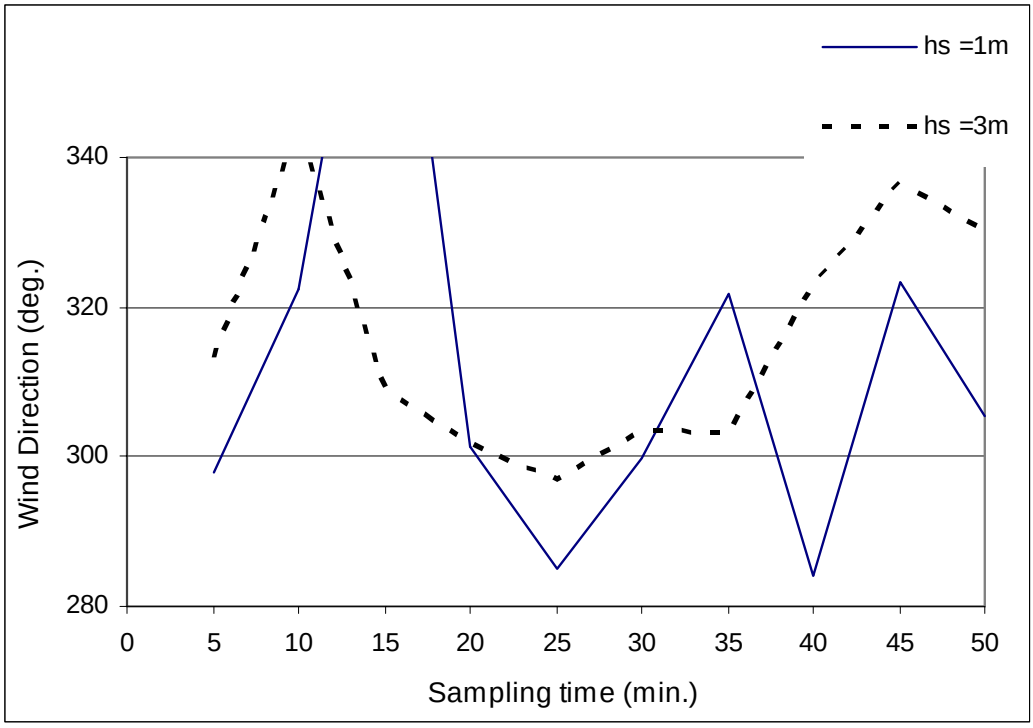

Figure 5.9 Variation of wind direction with time for Oct.30-01 field test: Stack location 2

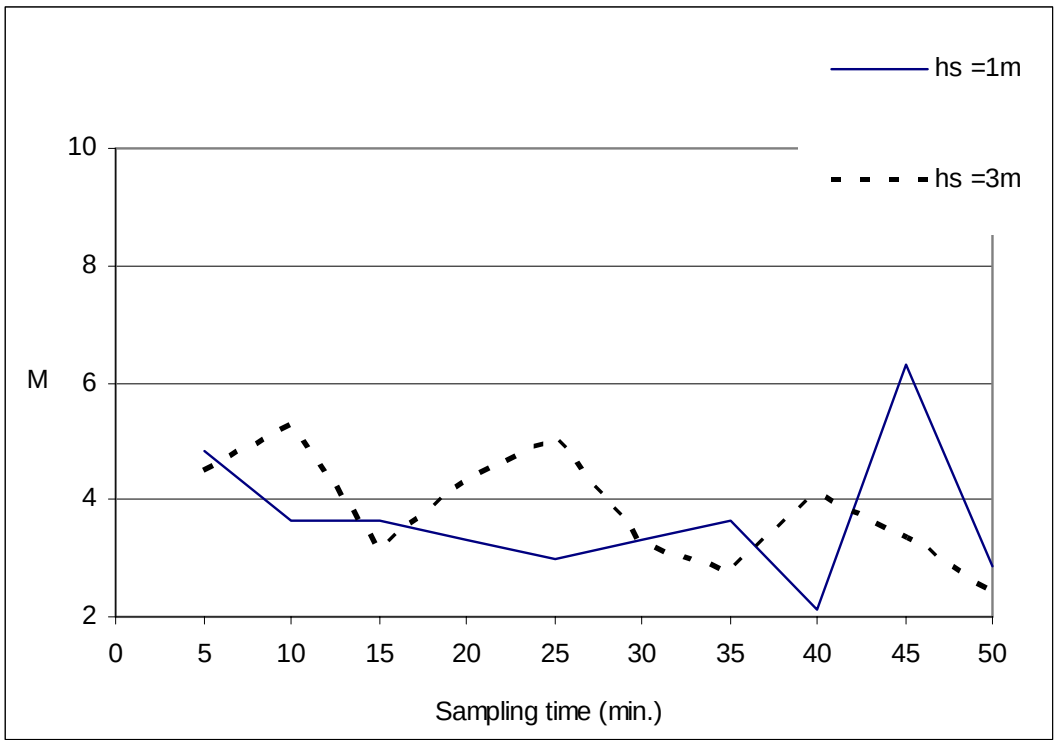

Figure 5.10 Variation of exhaust momentum (M) with time for Oct.30-01 field test: Stack location 2

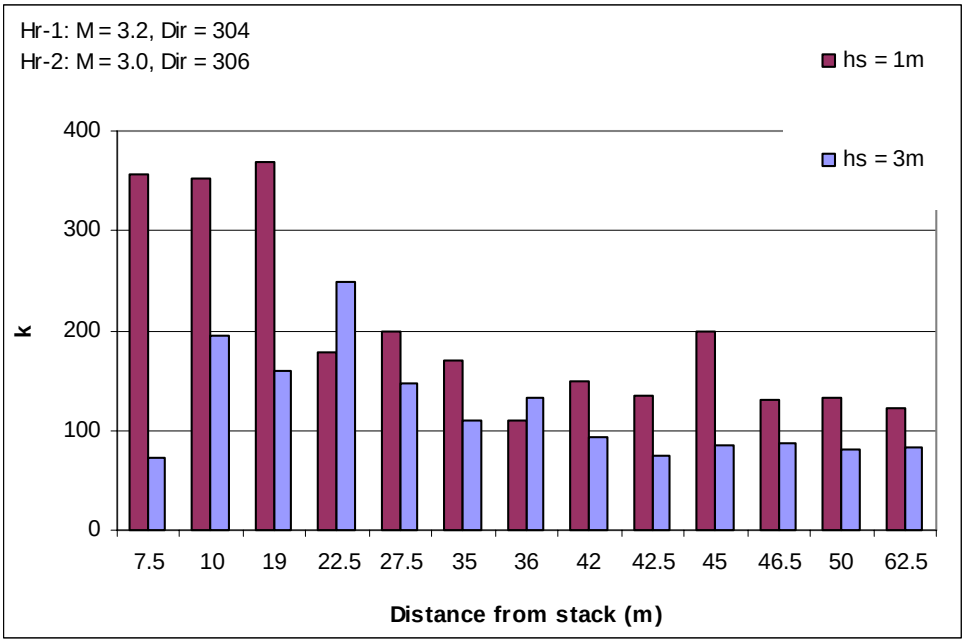

Figure 5.11 Effect of stack height on k for Oct.30-01 field test: Stack location 2

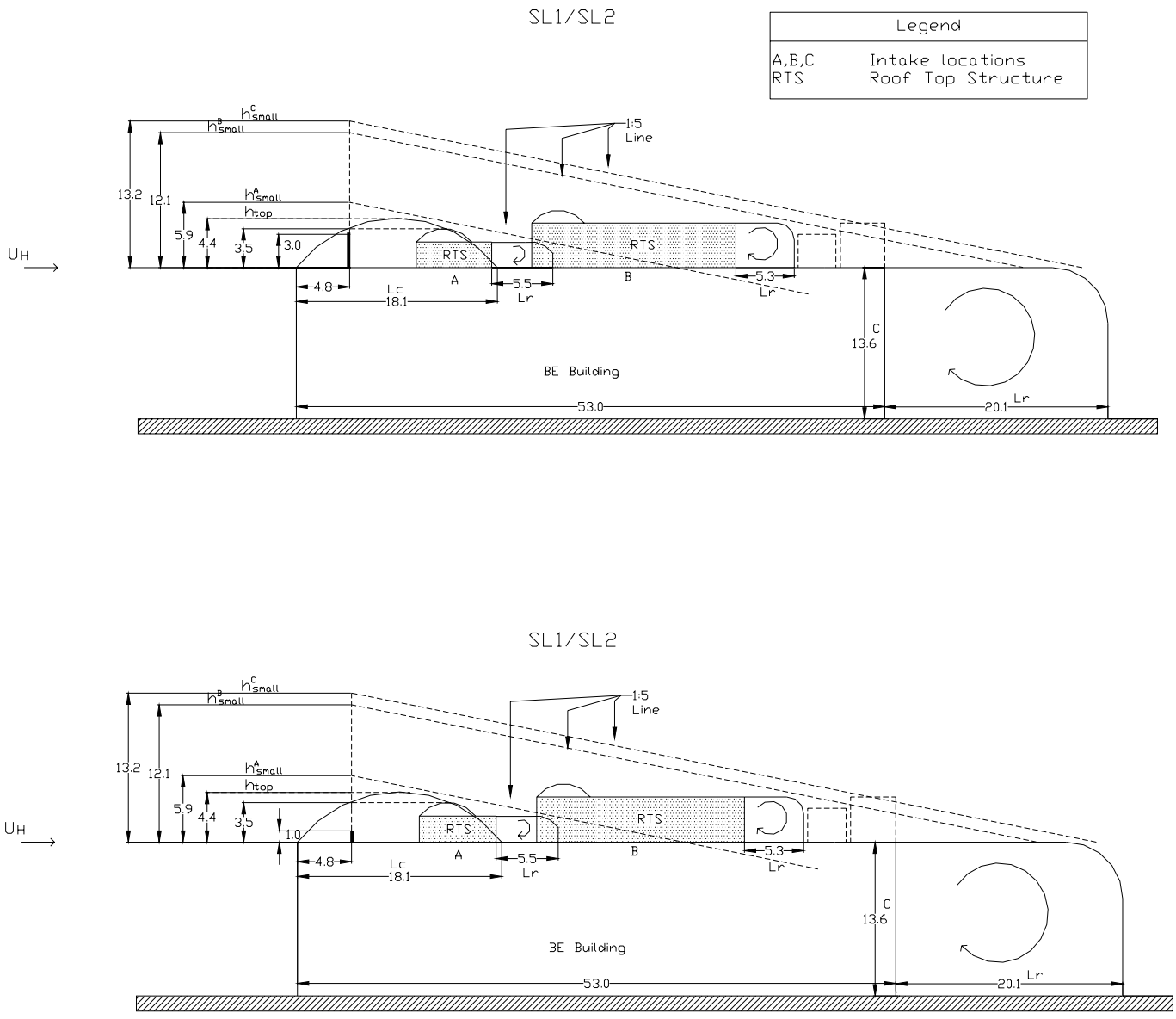

Figure 5.12 ASHRAE geometric design method for stack locations 1 and 2: stack height 3m and 1m

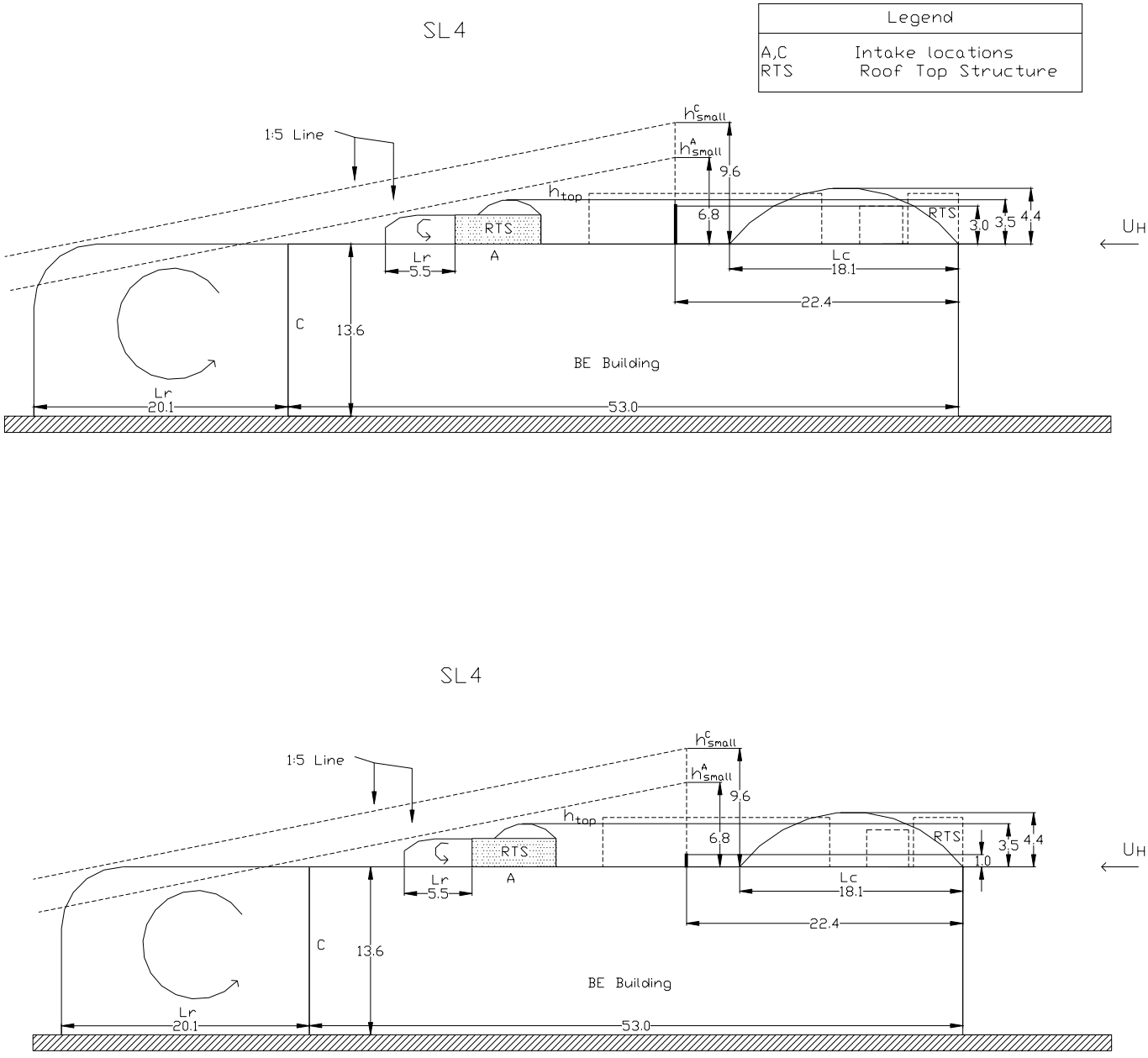

Figure 5.13 ASHRAE geometric design method for stack location 4: stack height 3m and 1m

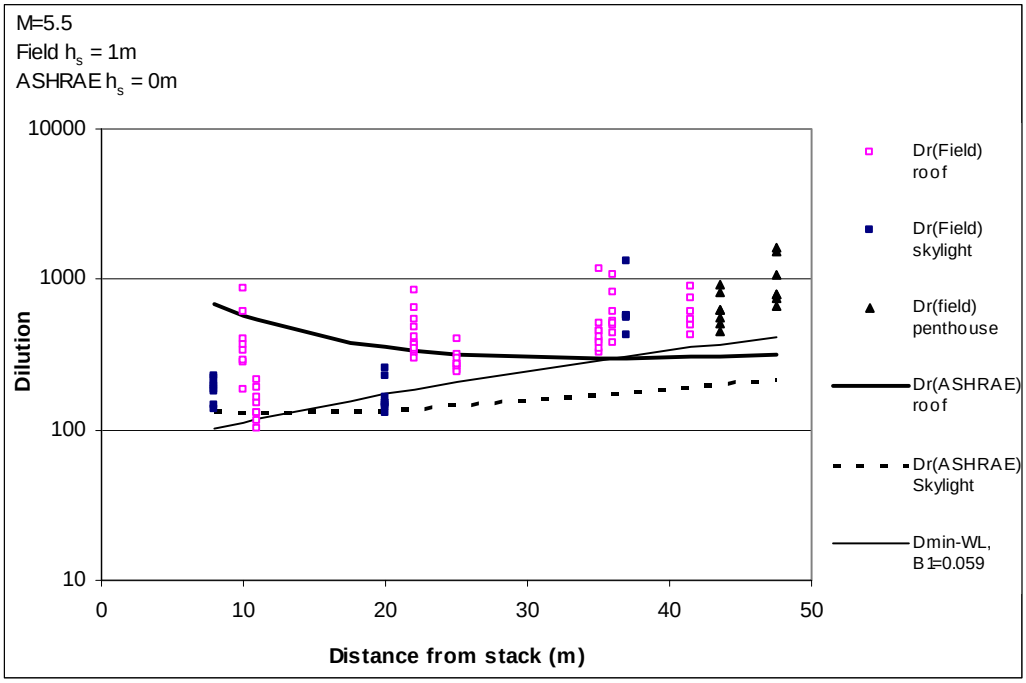

a)

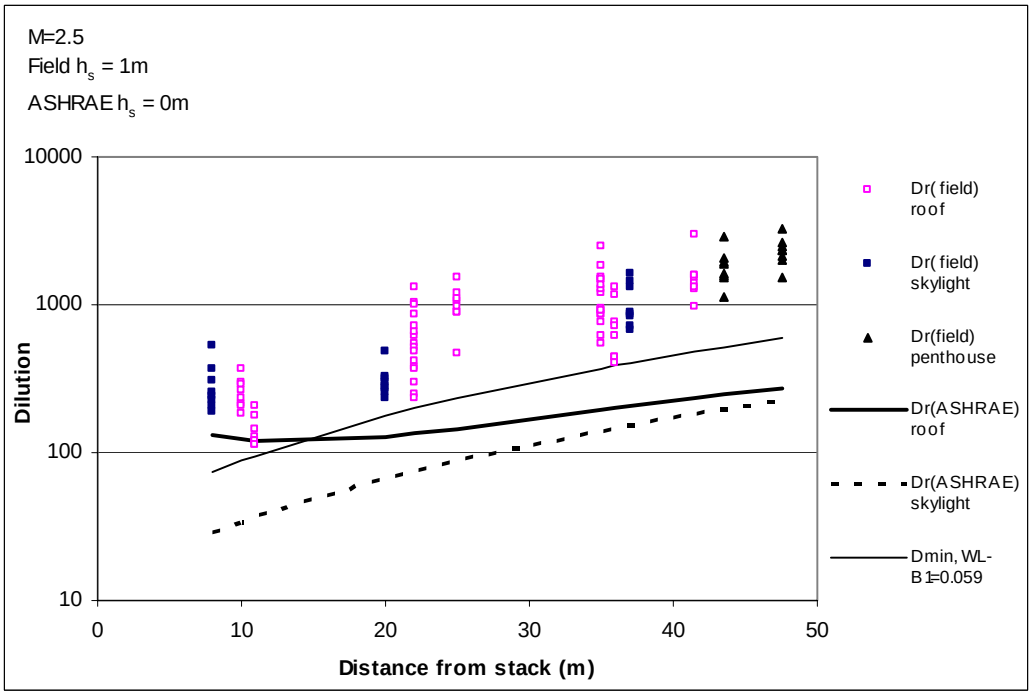

b)

Figure 5.14 Comparison of field test dilution data with ASHRAE (1999) D_{min} and ASHRAE (2003) Dr provisions: Oct.12-00: hour 1 and hour 2 test

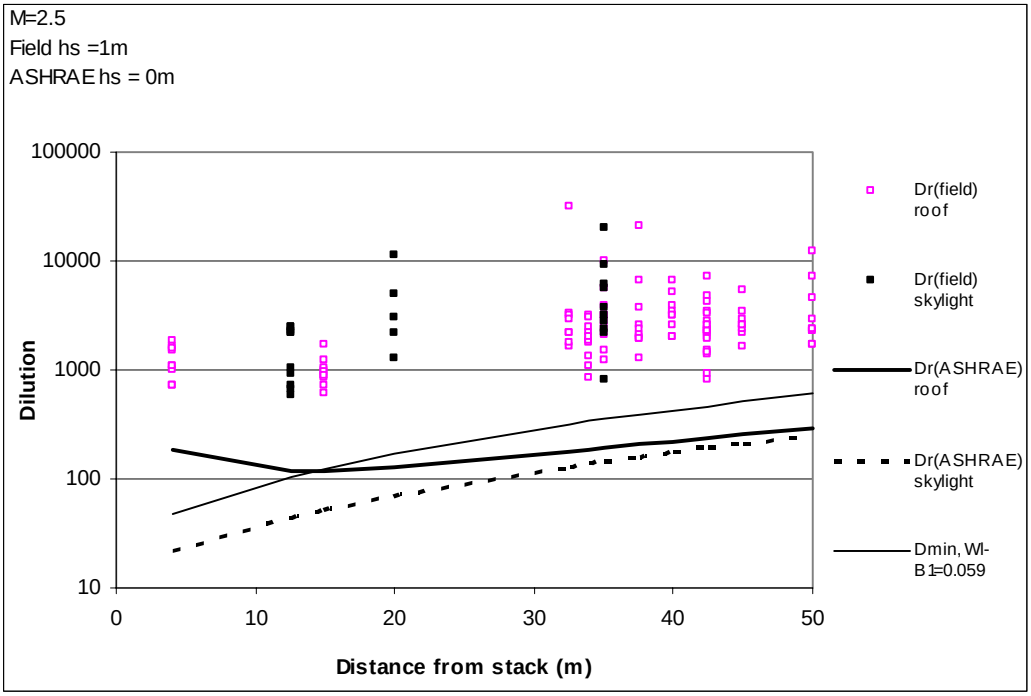

Figure 5.15 Comparison of field test dilution data with ASHRAE (1999) D_{min} and ASHRAE (2003) Dr provisions: May 15-02 test

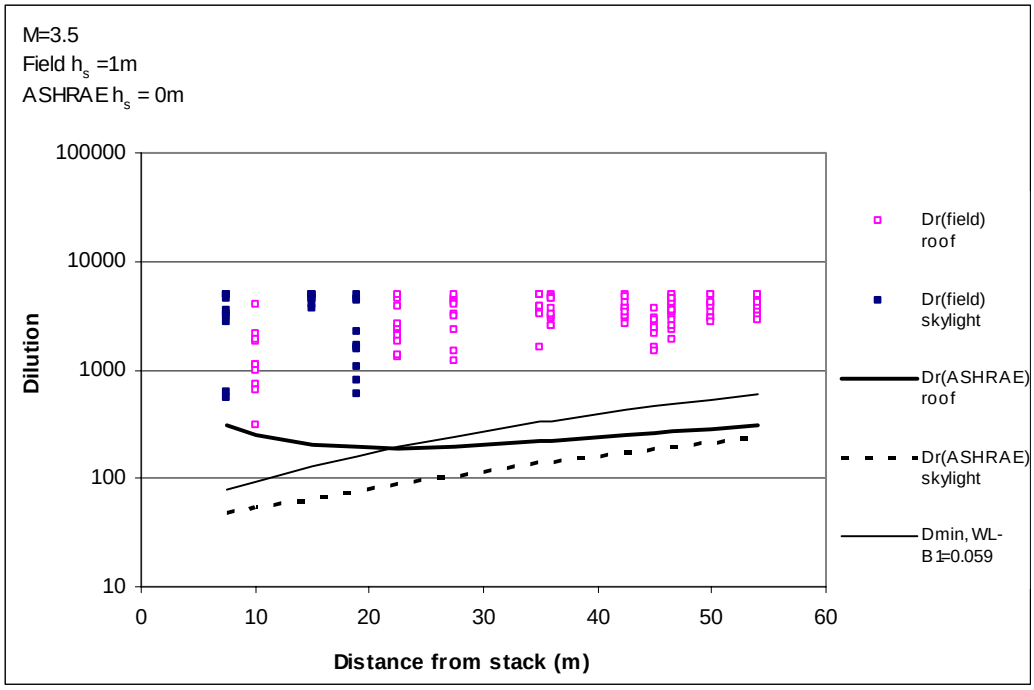

a)

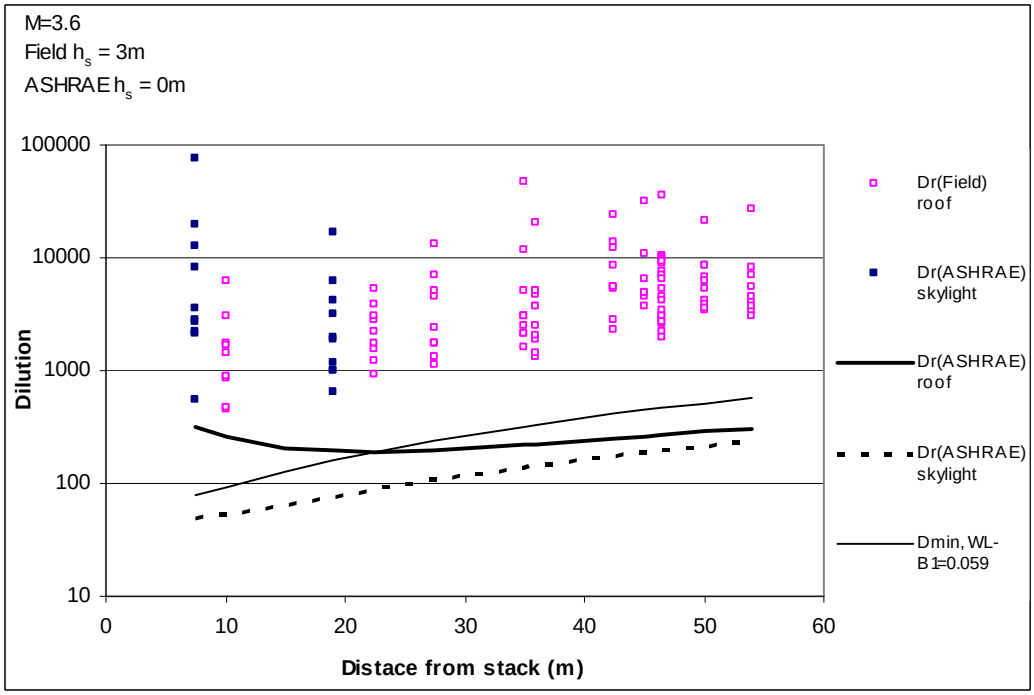

b)

Figure 5.16 Comparison of field test dilution data with ASHRAE (1999) D_{min} and ASHRAE (2003) Dr provisions: Oct.30-01: hour 1 and hour 2 test

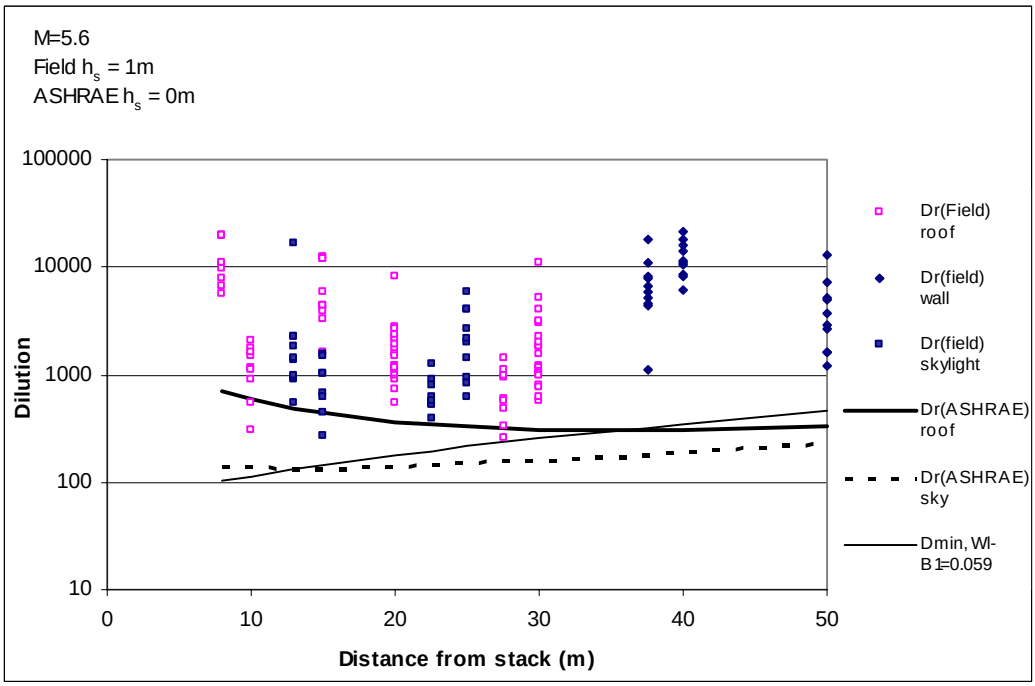

a)

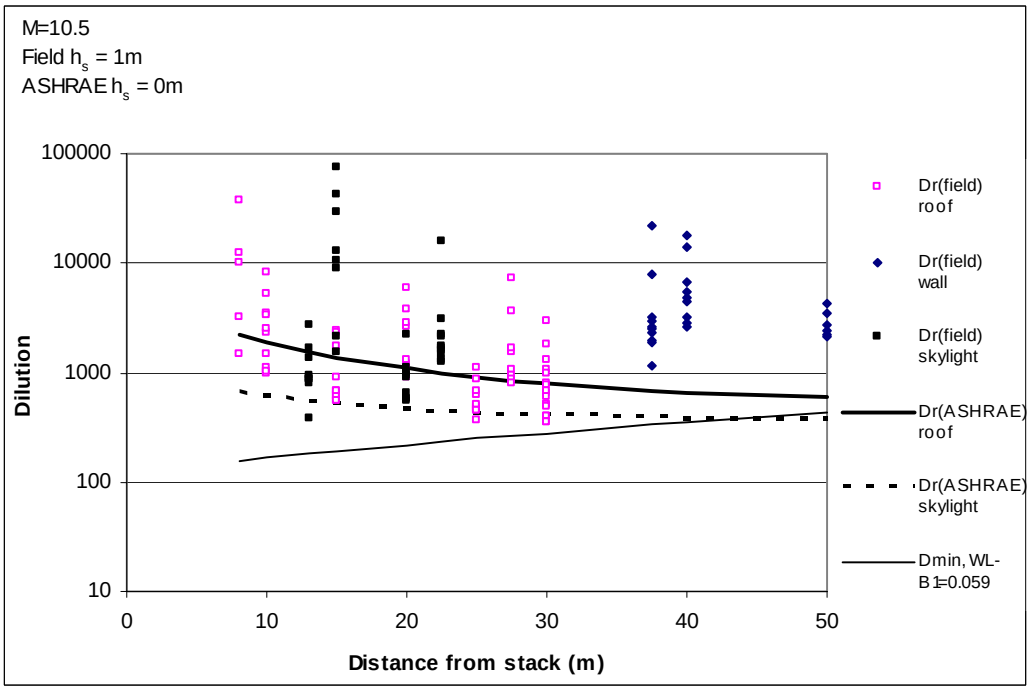

b)

Figure 5.17 Comparison of field test dilution data with ASHRAE (1999) D_{min} and ASHRAE (2003) Dr provisions: Nov.21-02 test: hour 1 and hour 2

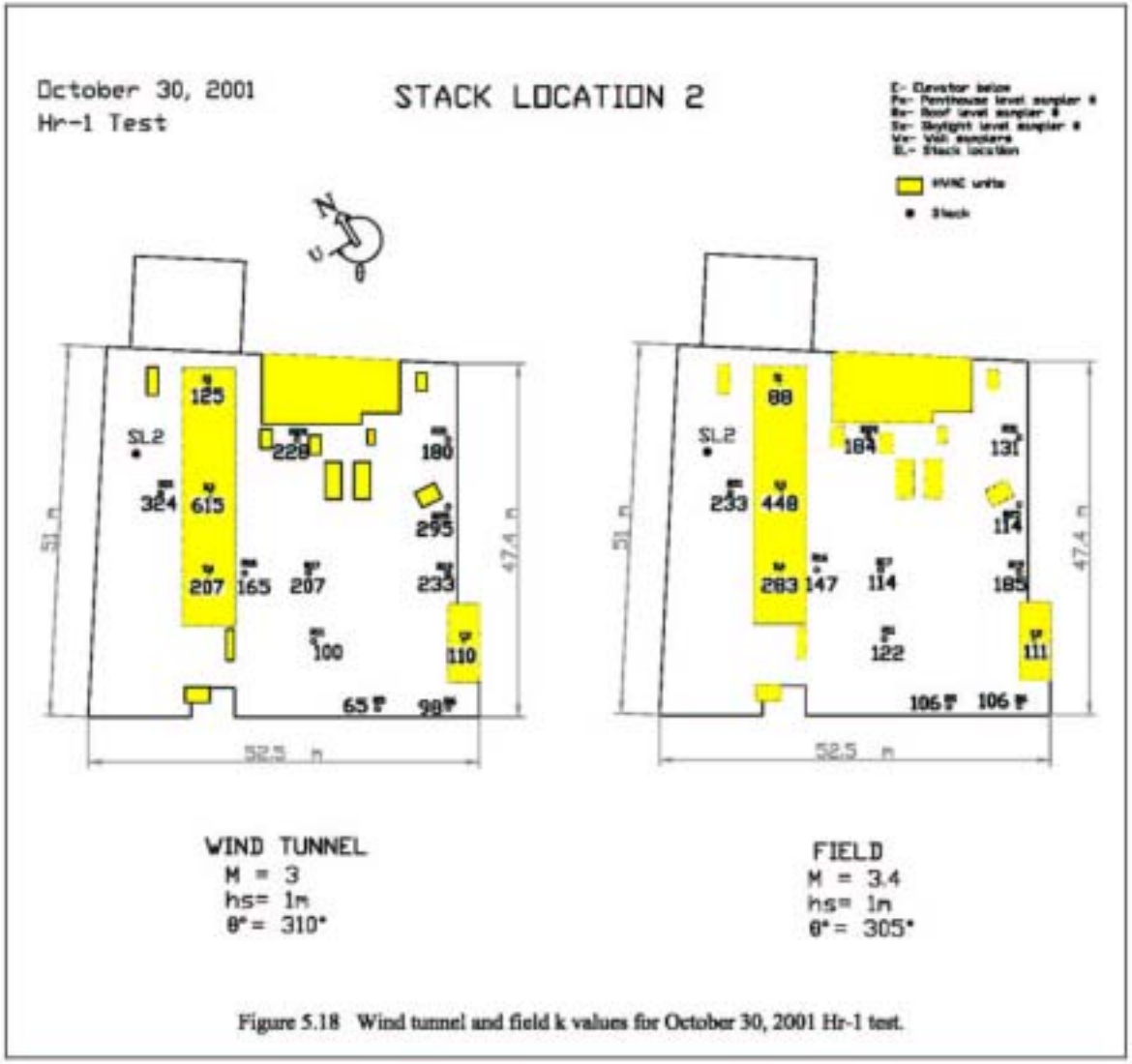

Figure 5.18 Wind tunnel and field k values for October 30, 2001 Hr-1 test.

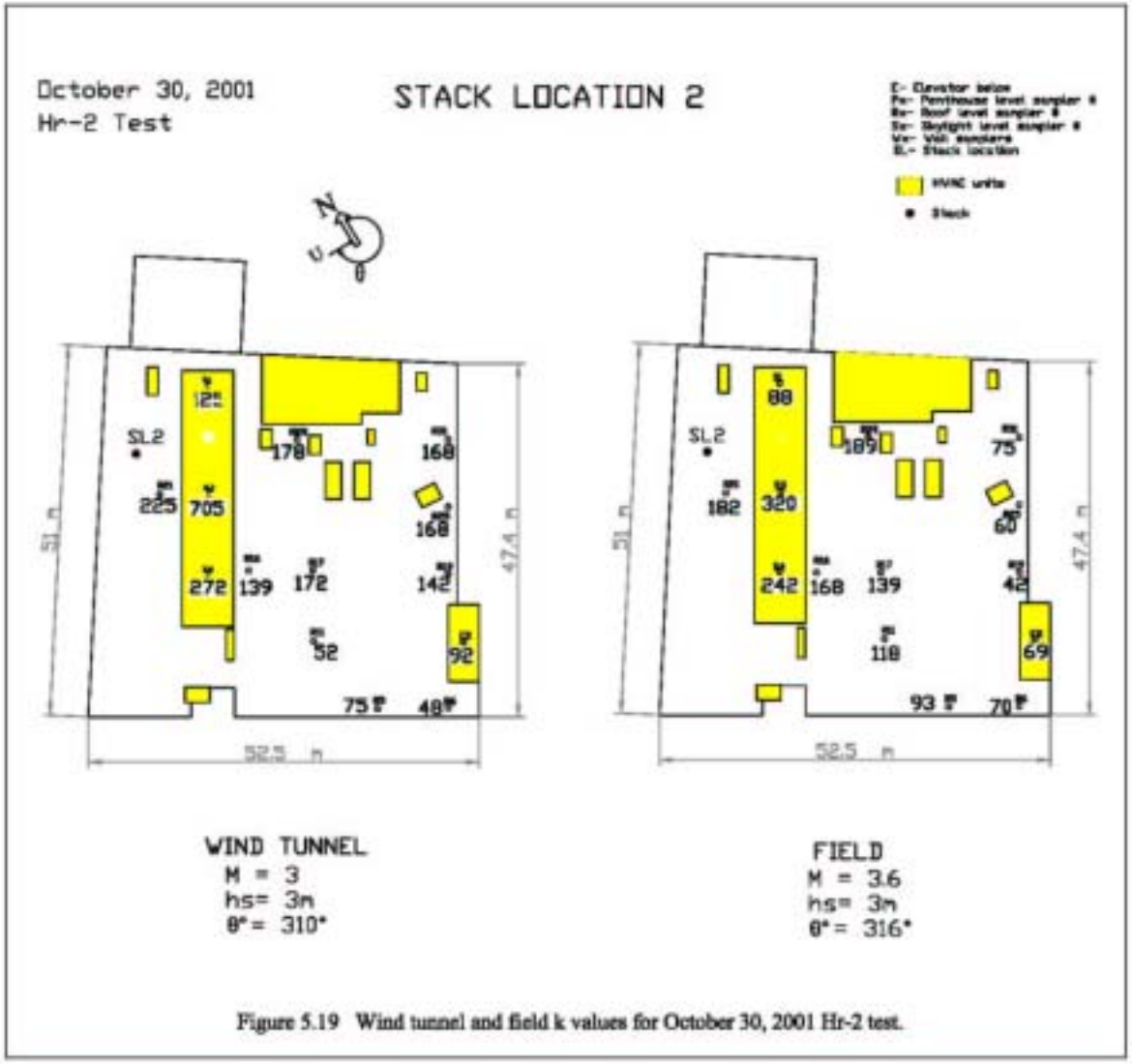

Figure 5.19 Wind tunnel and field k values for October 30, 2001 Hr-2 test.

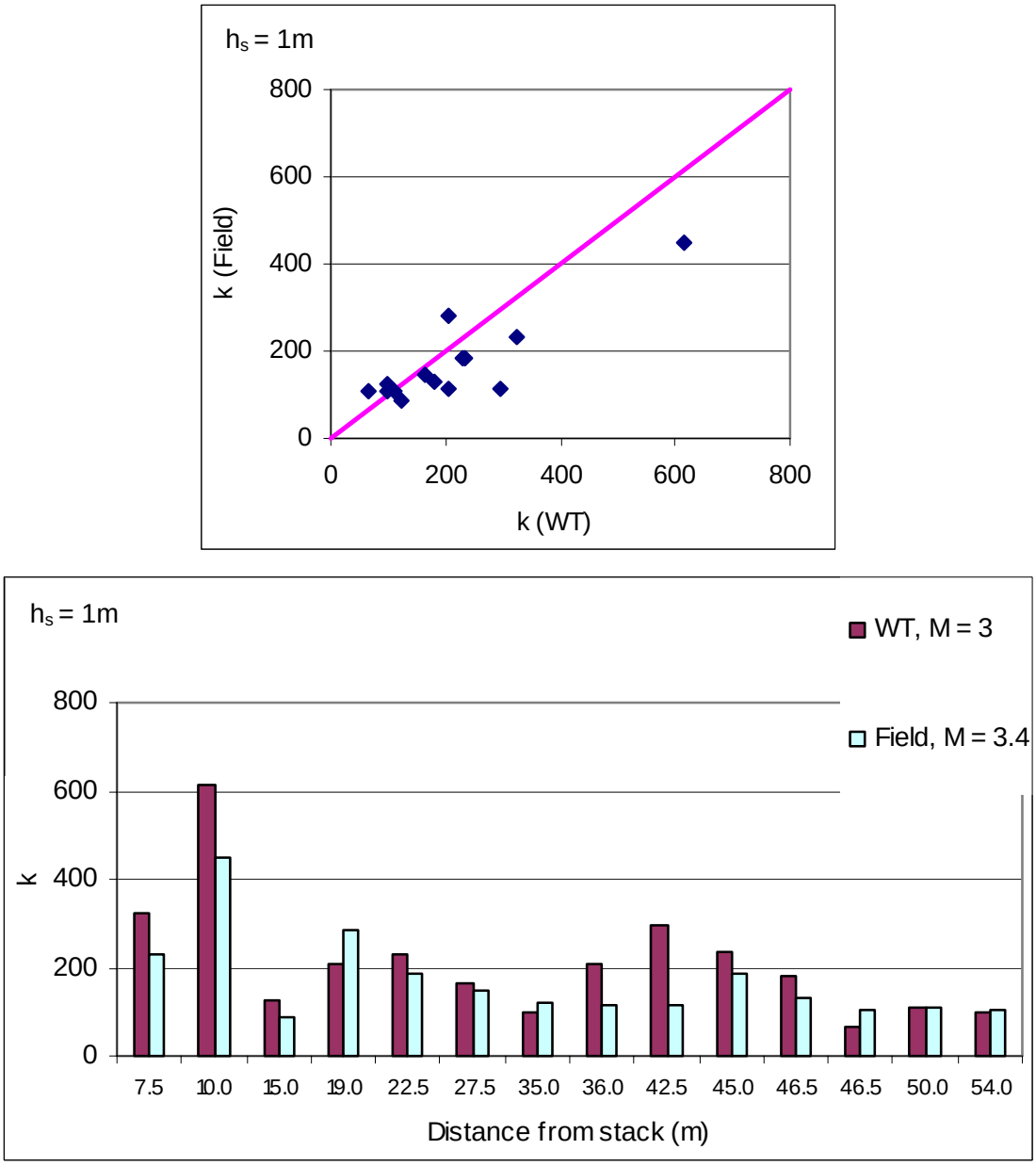

Figure 5.20 Field and wind tunnel data - Concentration scatter plot and histogram: Oct.30-01 test hour 1: Stack location 2

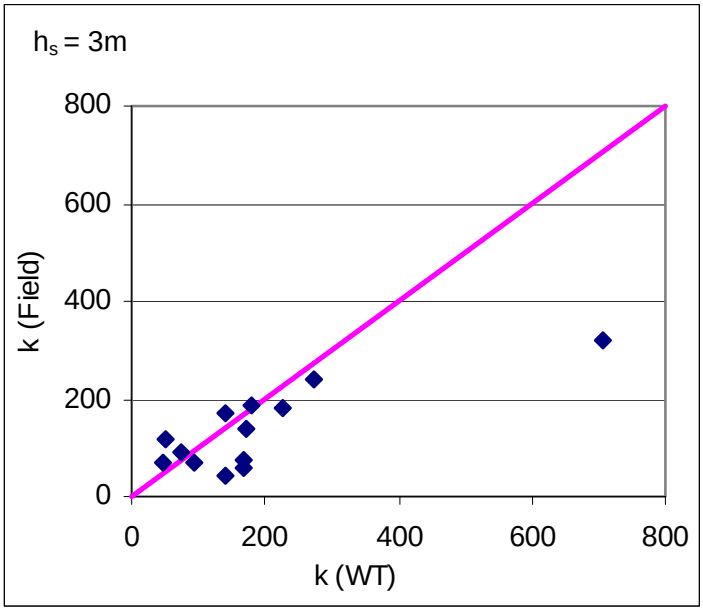

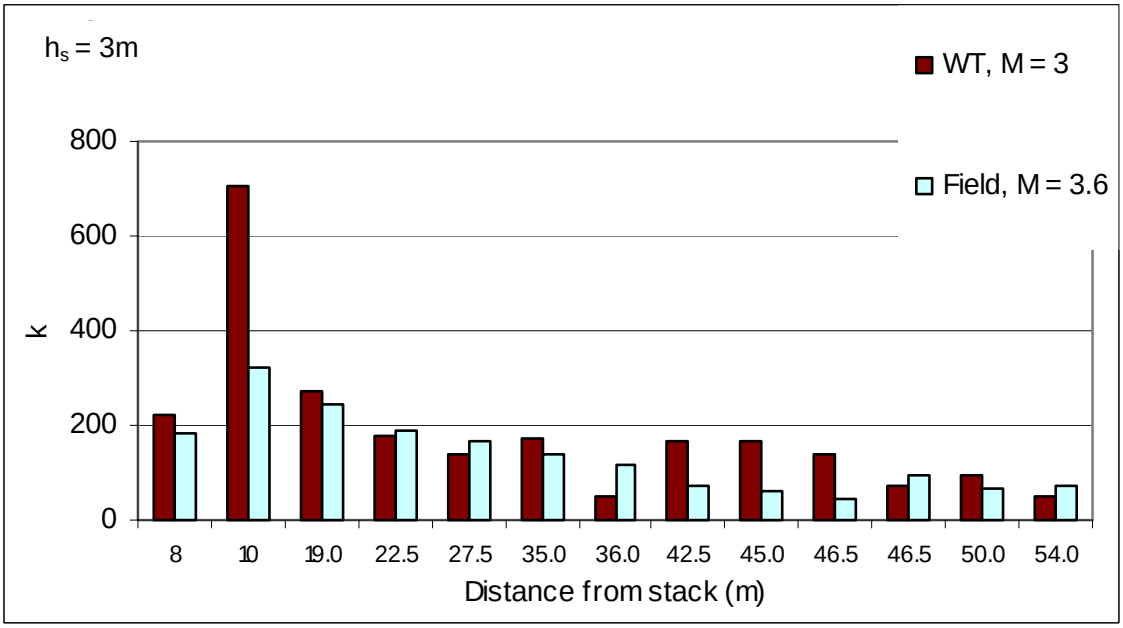

Figure 5.21 Field and wind tunnel data - Concentration scatter plot and histogram: Oct.30-01 test hour 2: Stack location 2

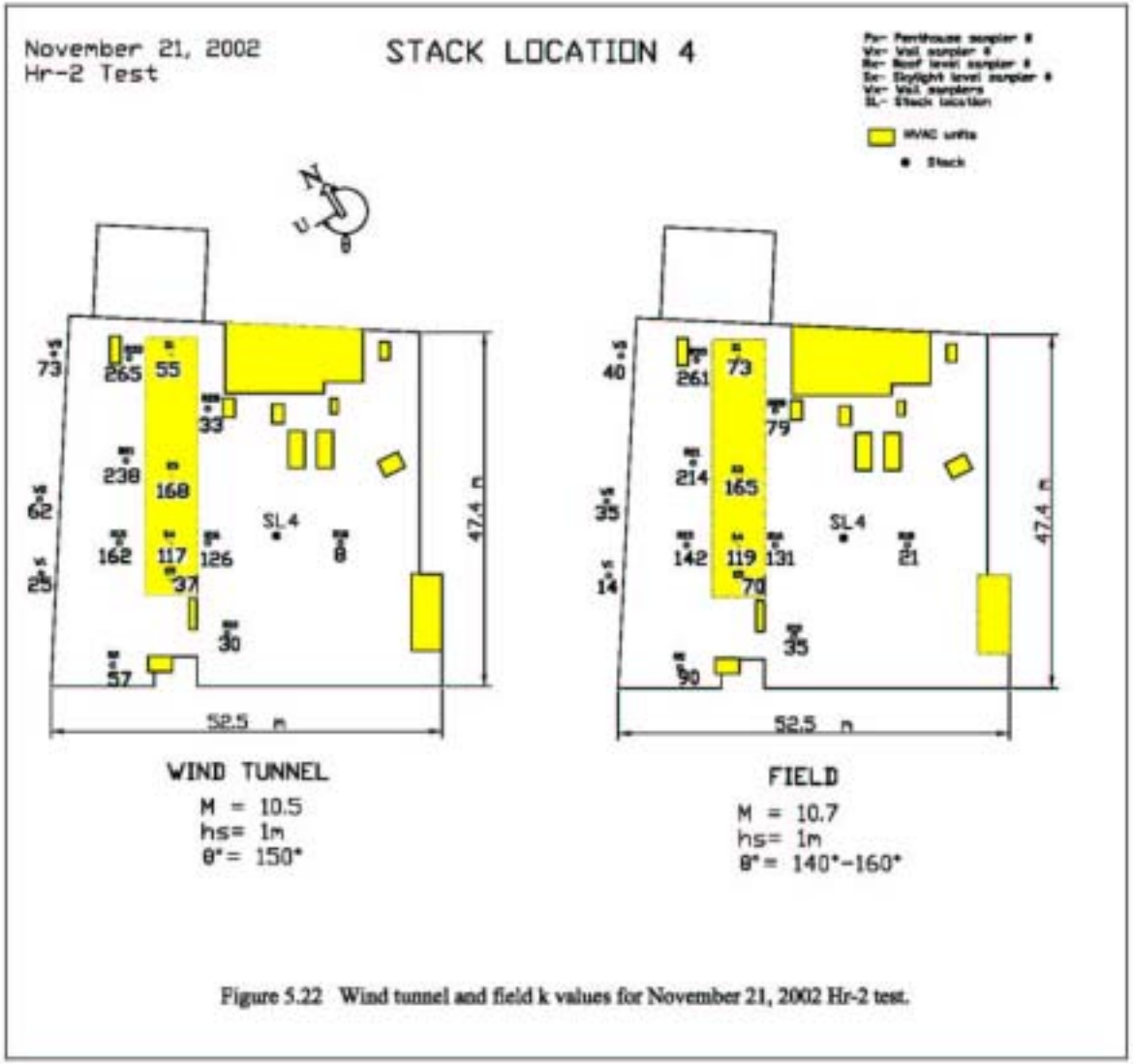

Figure 5.22 Wind tunnel and field k values for November 21, 2002 Hr-2 test.

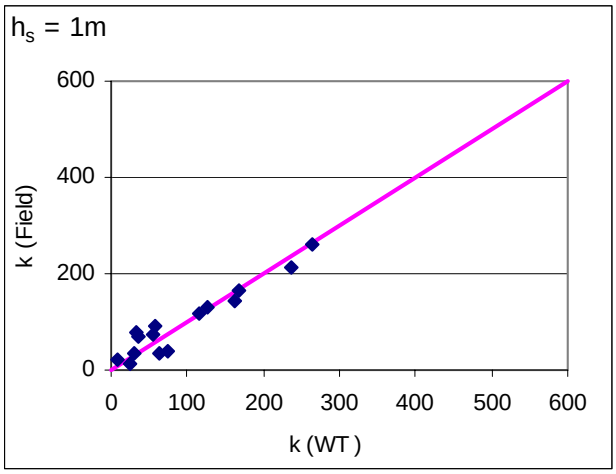

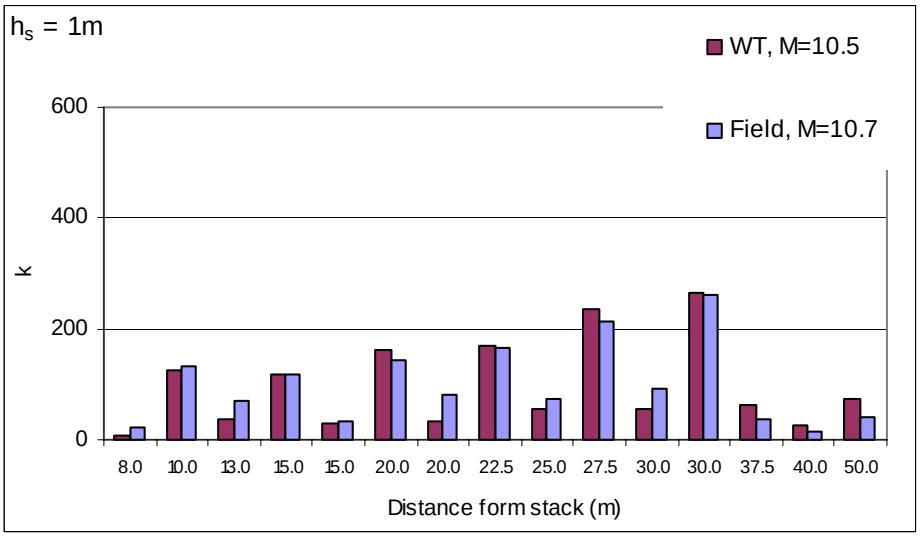

Figure 5.23 Field and wind tunnel data - Concentration scatter plot and histogram: Nov.21-02 test hour 2: Stack location 4

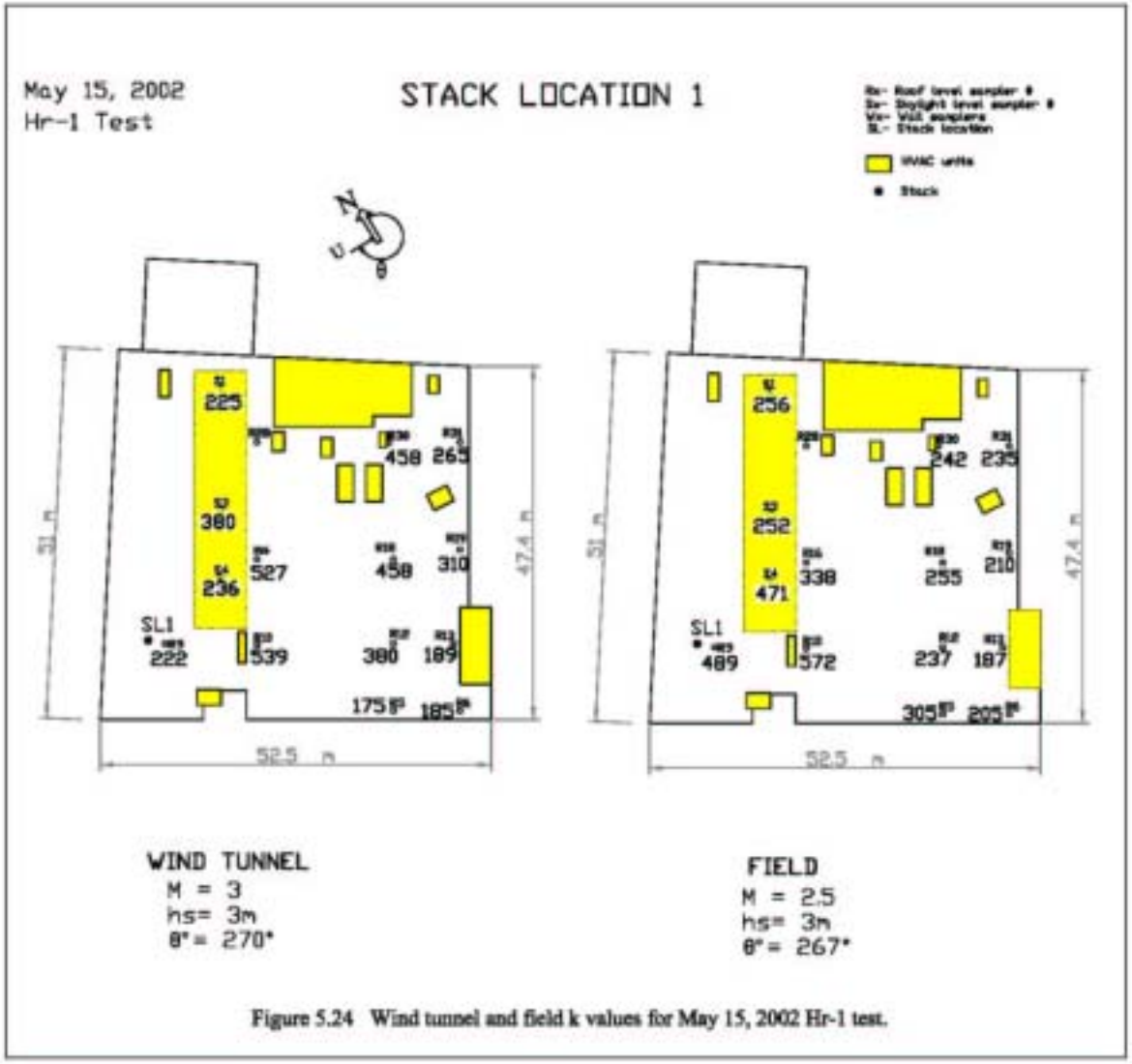

Figure 5.24 Wind tunnel and field k values for May 15, 2002 Hr-1 test.

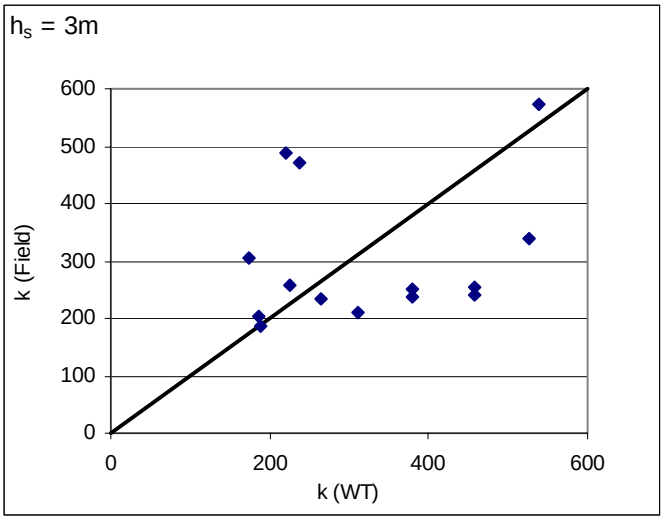

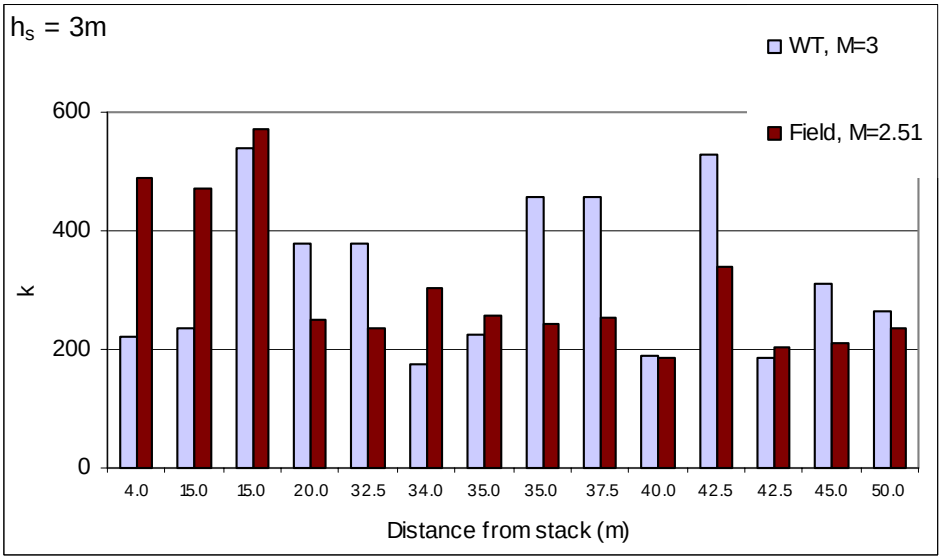

Figure 5.25 Field and wind tunnel data - Concentration scatter plot and histogram: May15-02 test: Stack location 1

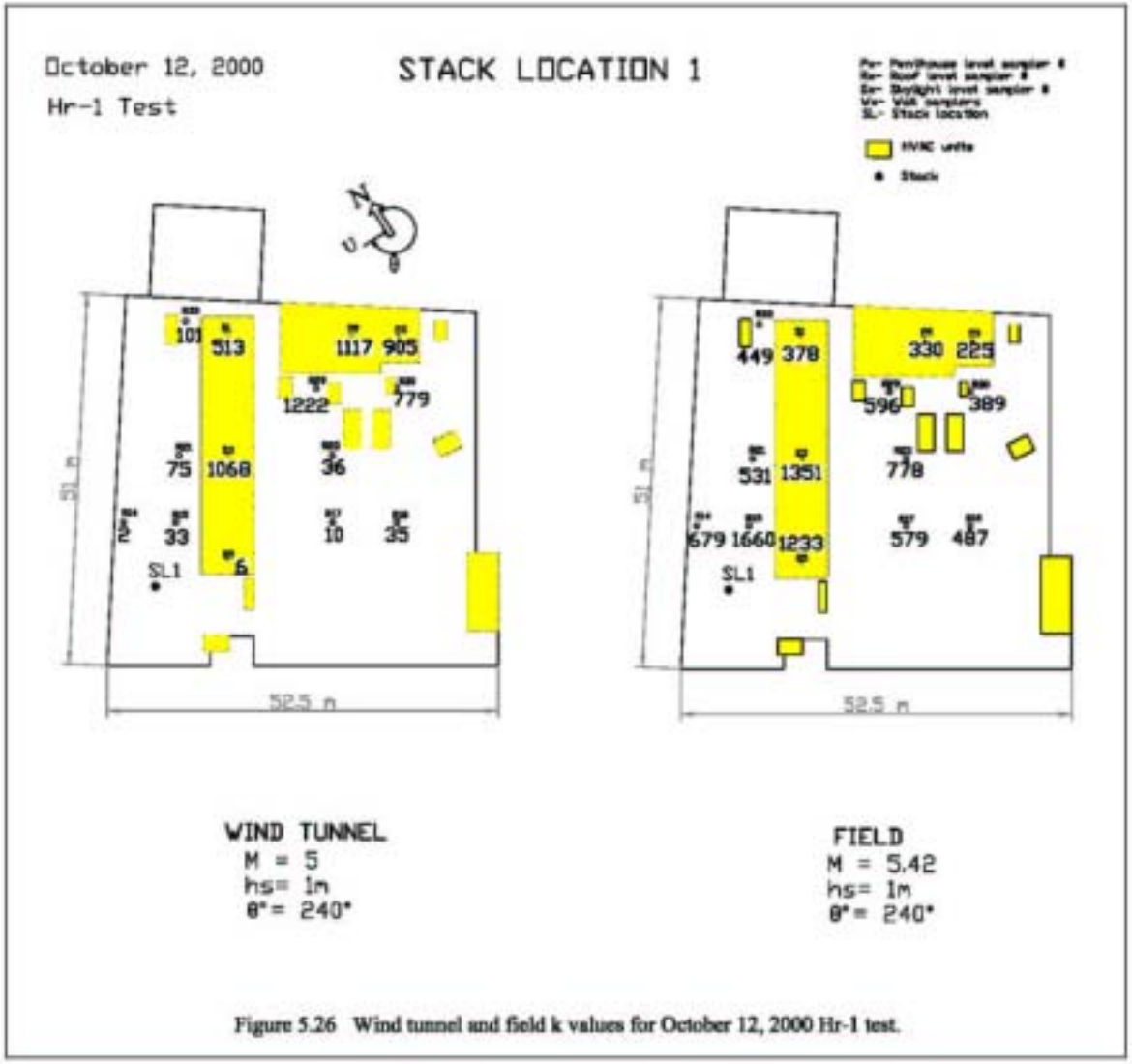

Figure 5.26 Wind tunnel and field k values for October 12, 2000 Hr-1 test.

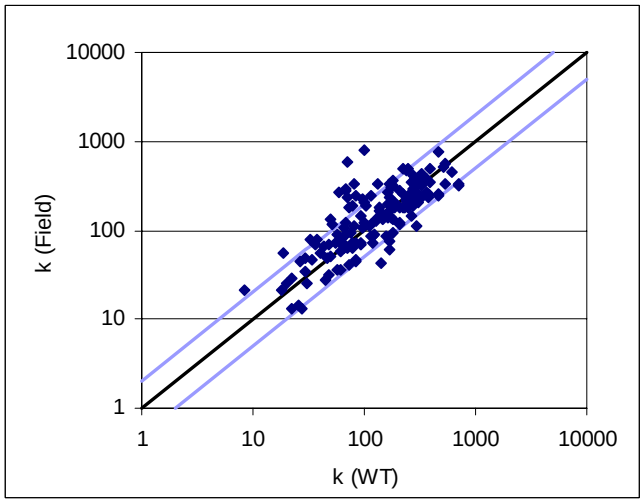

a) all tests except Oct. 12, 2000

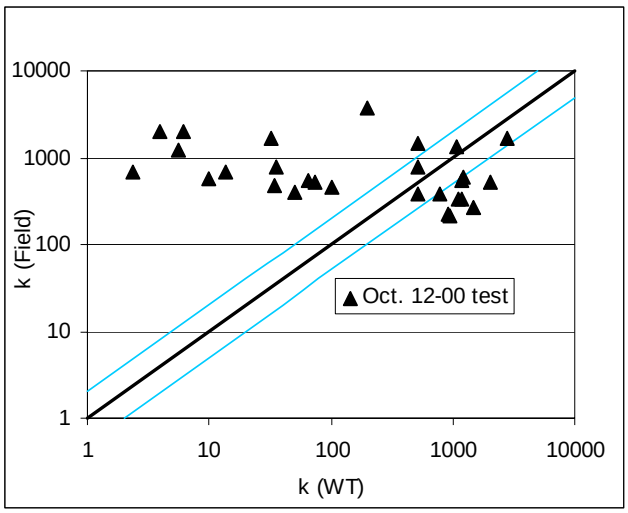

b) Oct. 12, 2000 test (2 hours)

Figure 5.27 Scatter plots of wind tunnel and field k data for open fetch tests

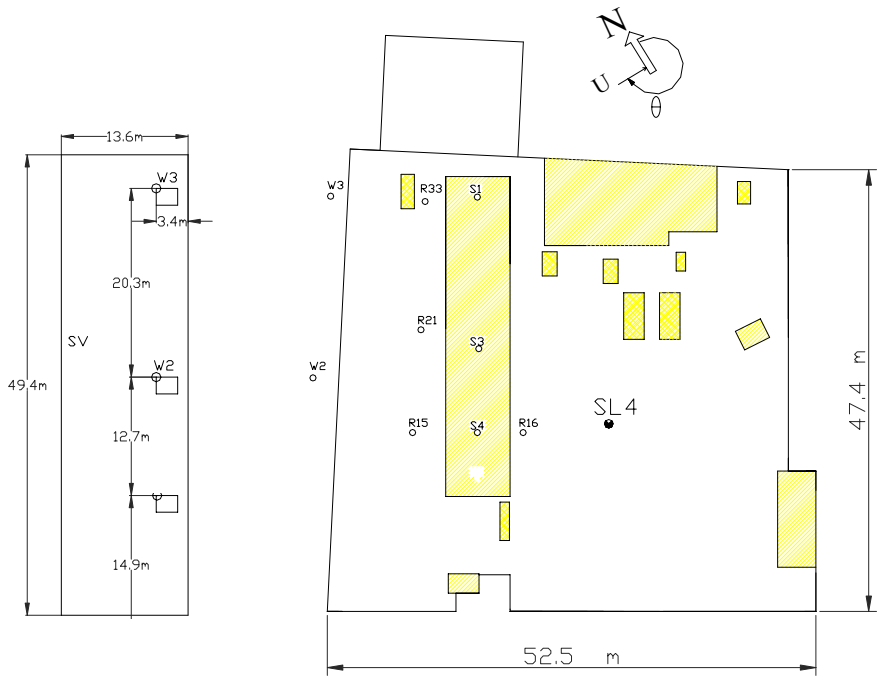

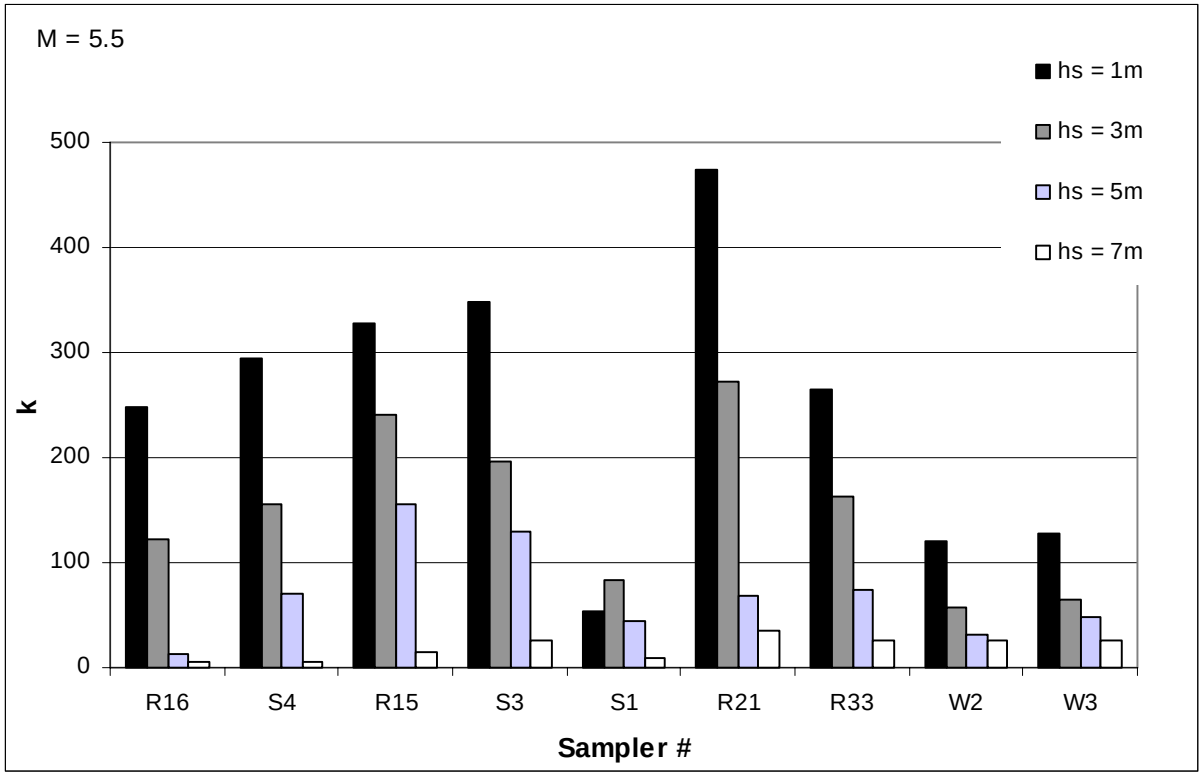

Figure 5.28 Histogram showing effect of stack height on k: Stack location 4, Wind direction = 150^{o}

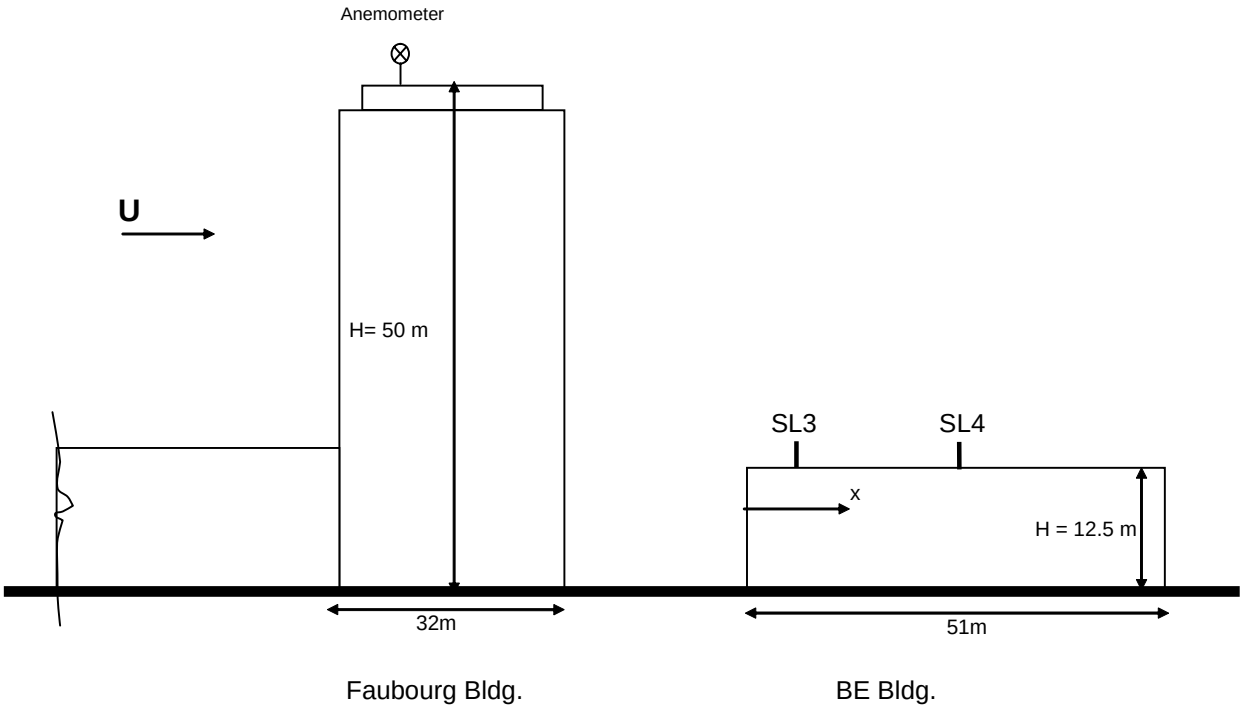

Figure 5.29 Elevation view of BE and Faubourg buildings

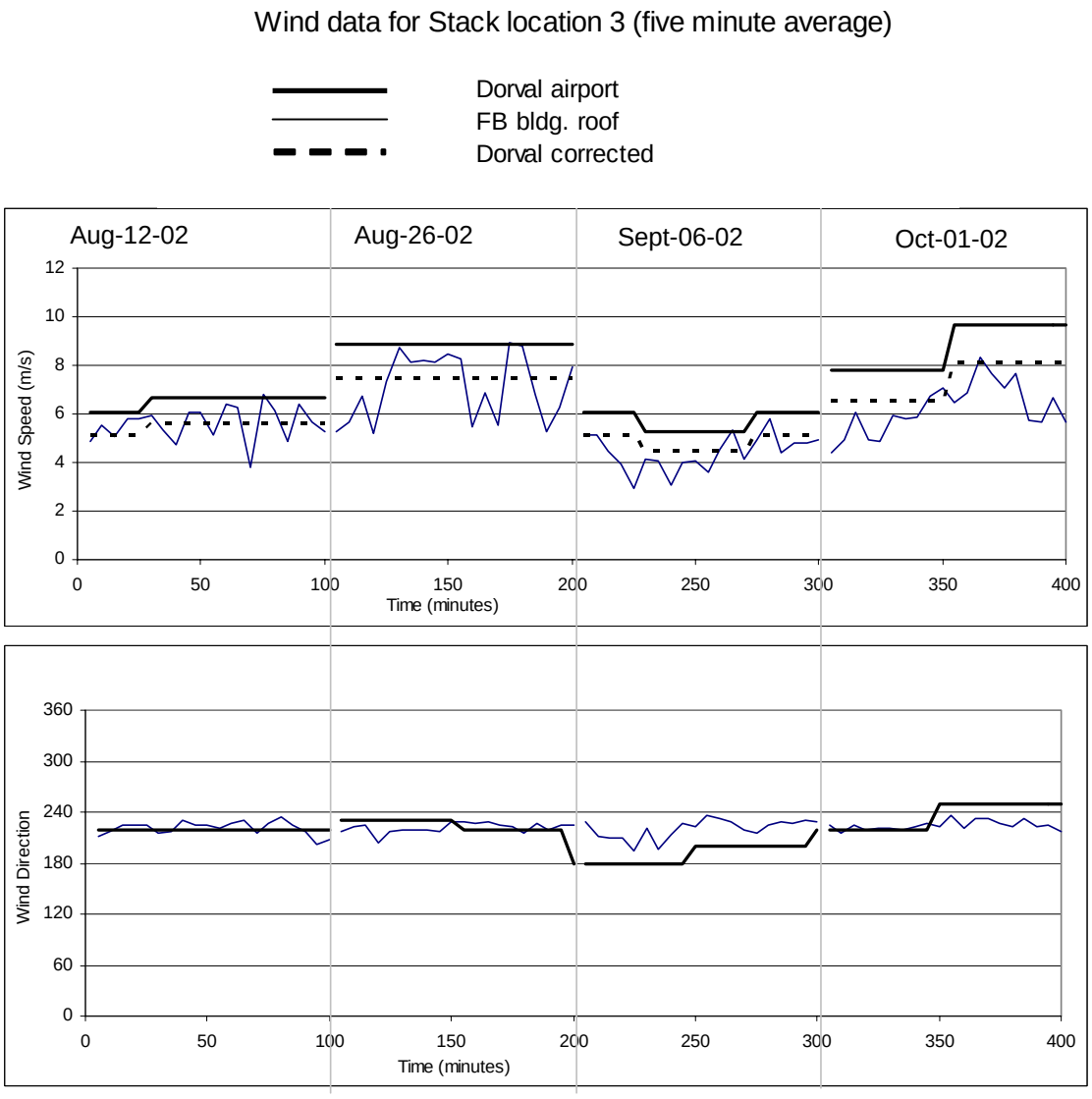

Figure 5.30 Field wind data obtained on the top of Faubourg building (BE building is in the wake)

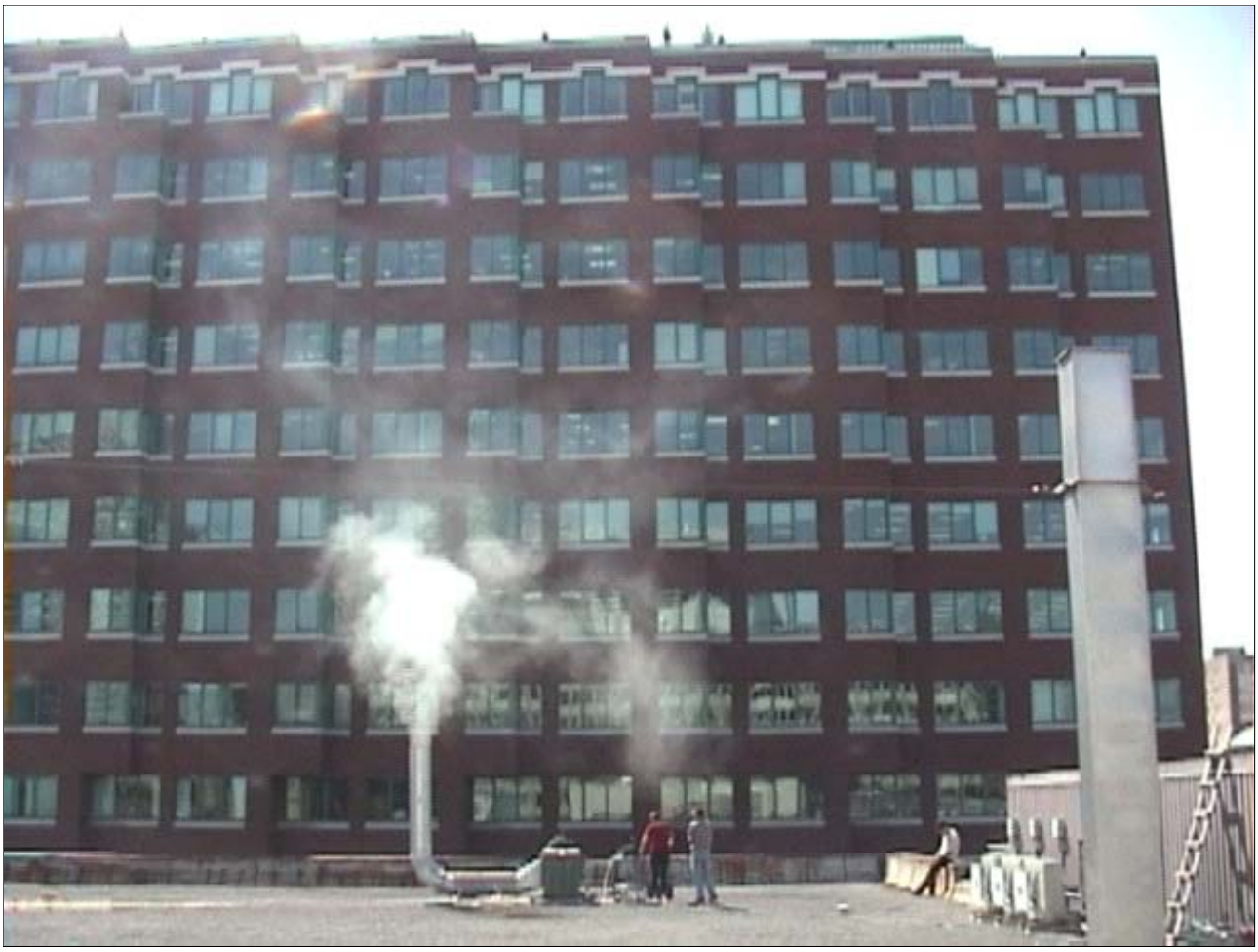

Figure 5.31 Smoke visualization test for September-06-02 hour 2 field test: Stack location 3

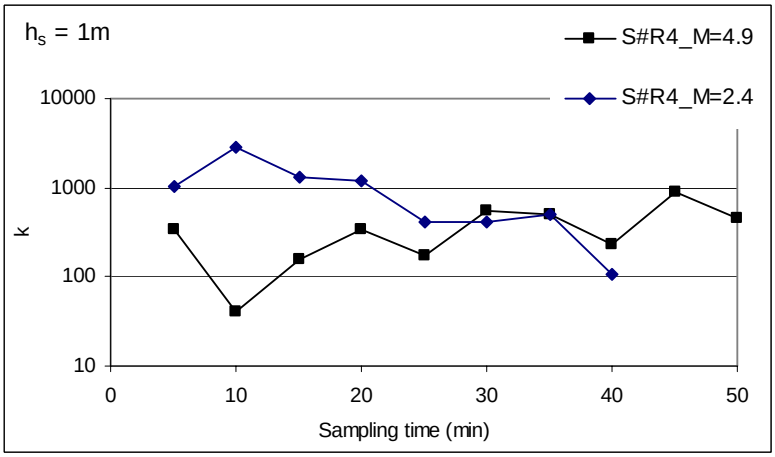

a) near

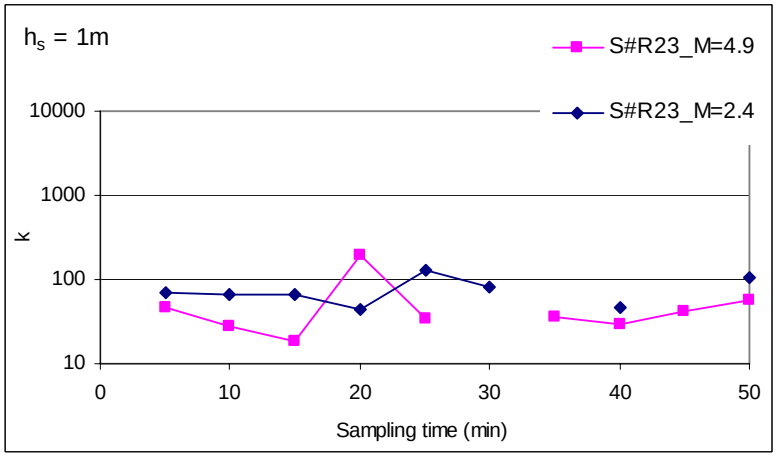

b) mid

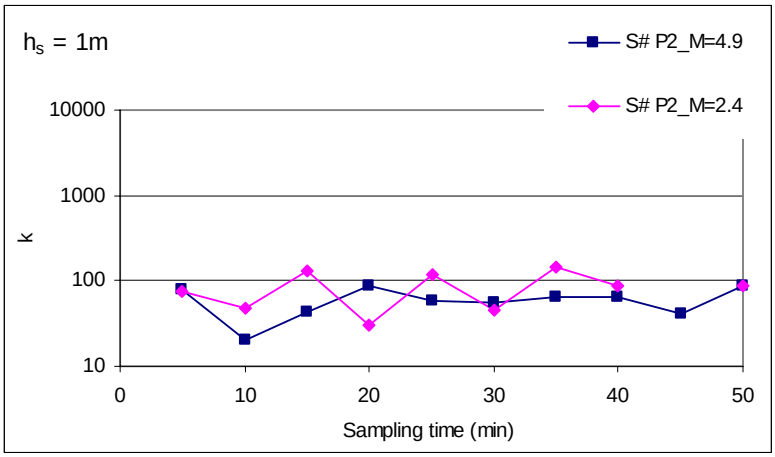

c) far

Figure 5.32 Concentration k time series for near, mid and far sampler on BE roof: Aug.12-02 field test: Stack location 3

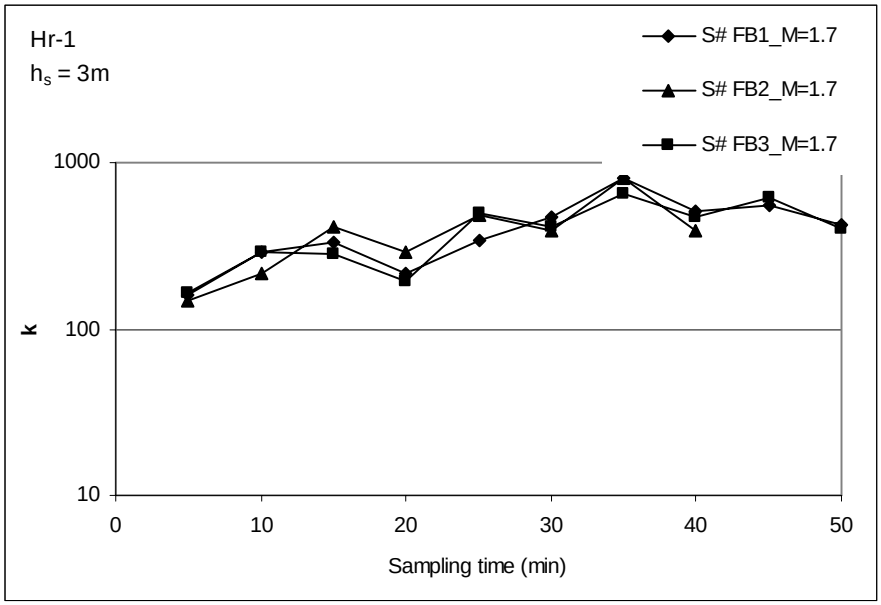

a)

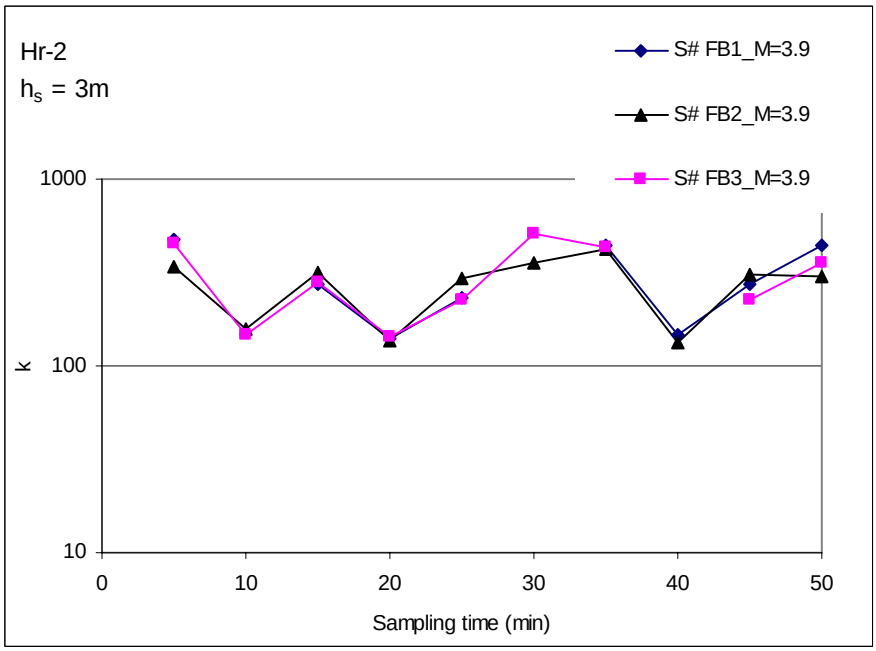

b)

Figure 5.33 Concentration k time series for samplers on FB wall, Aug.26-02 field test: Stack location 3

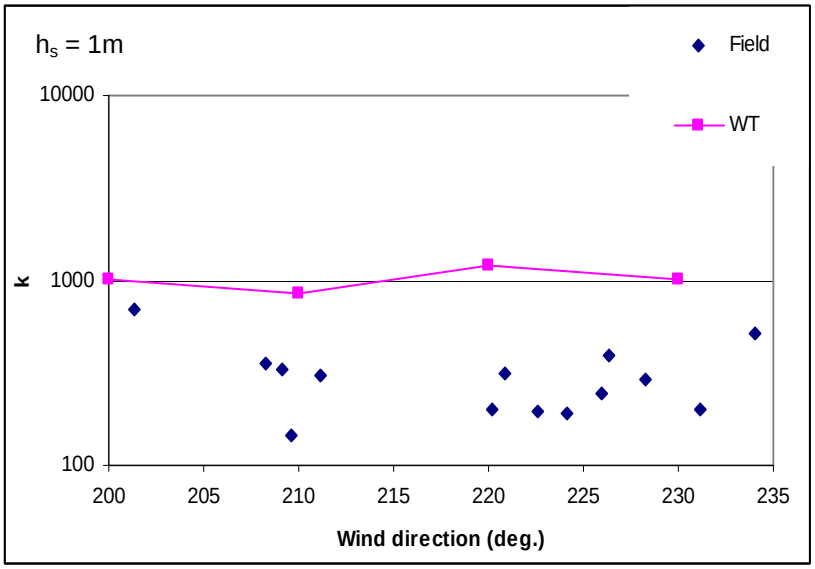

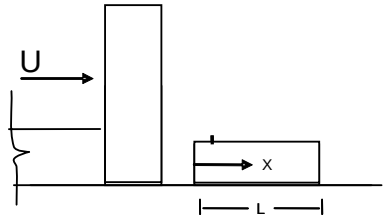

a) M_{field} = 2-3, M_{WT} =2.2

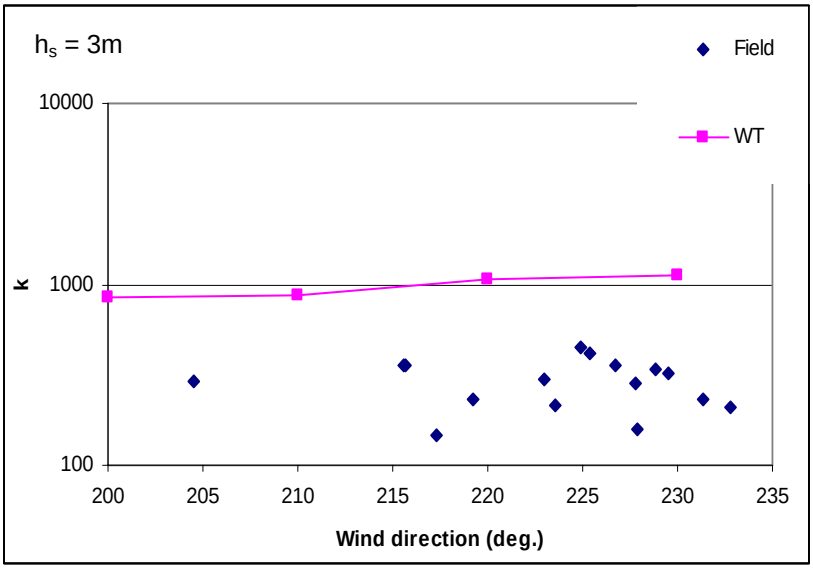

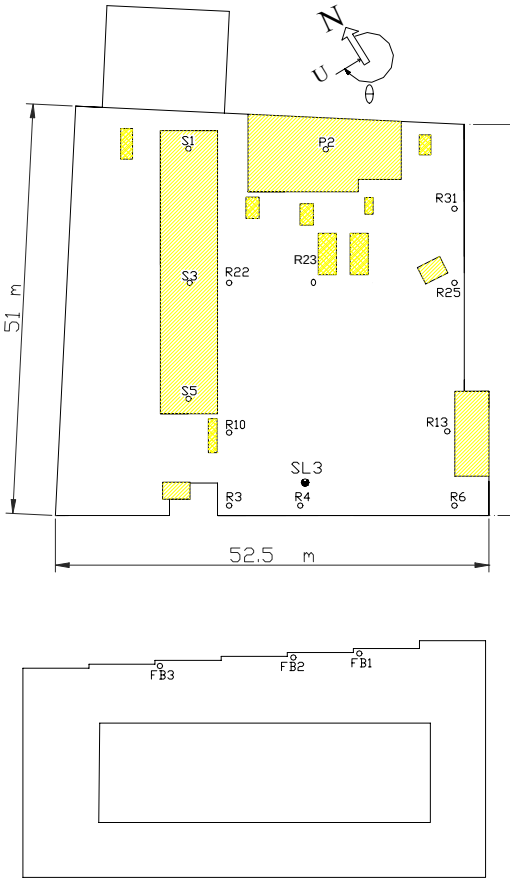

b) M_{field} = 2-3, M_{WT} =2.2

Figure 5.34 Effect of wind direction on k for Faubourg building wall sampler FB2: Stack location 3

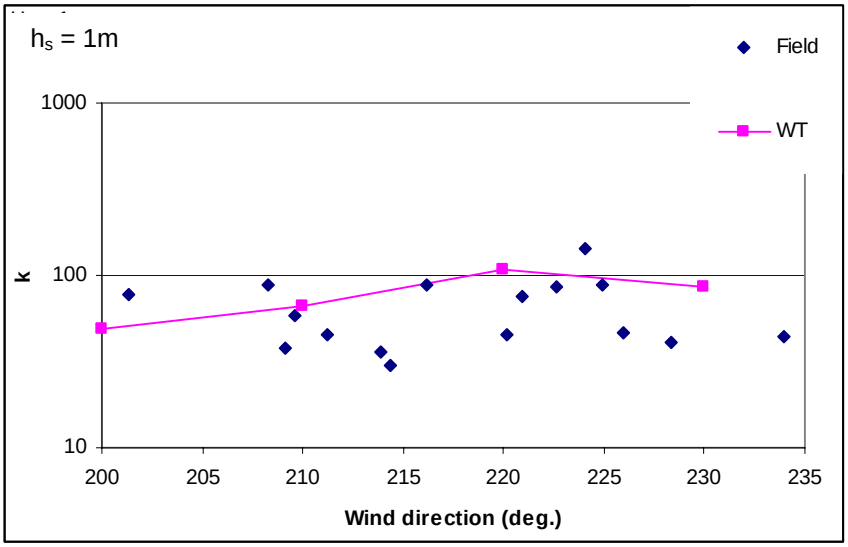

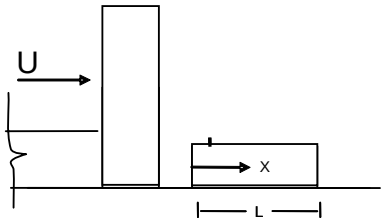

a) M_{field} = 1.5-2.5, M_{WT} =2.2

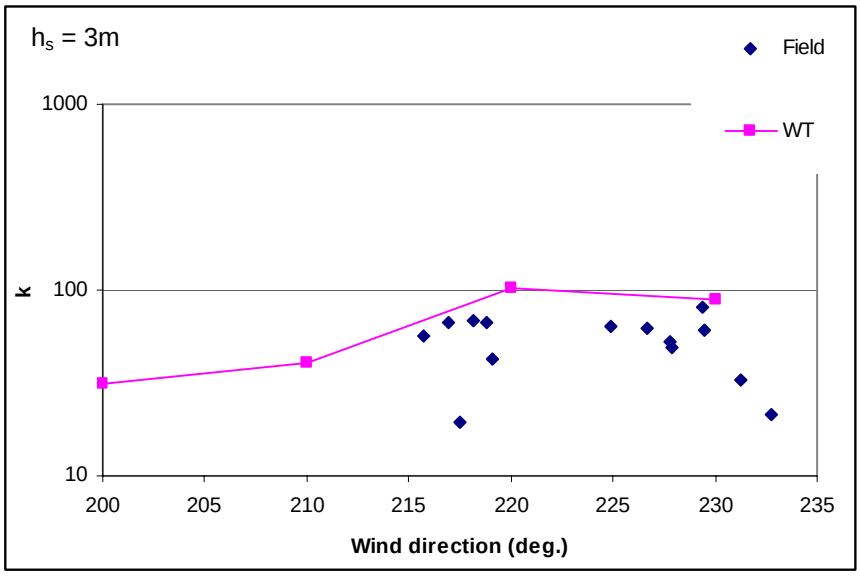

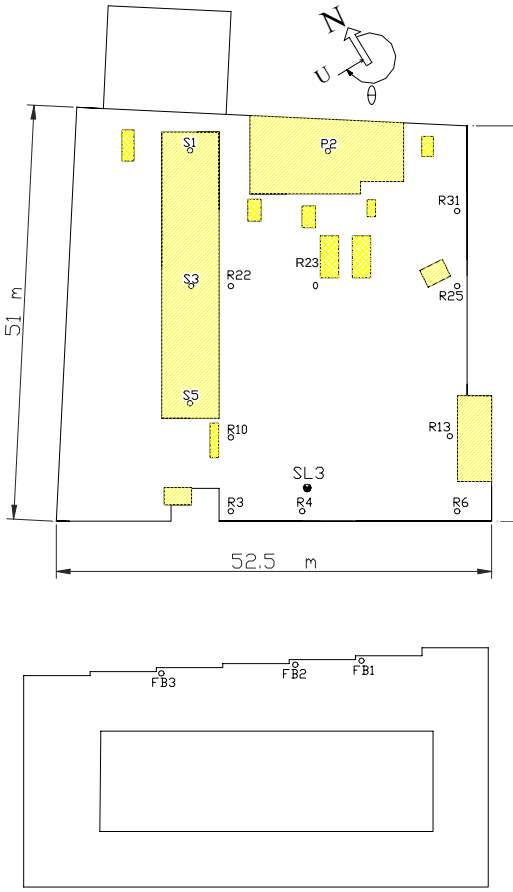

b) M_{field} = 1.5-2.5, M_{WT} =2.2

Figure 5.35 Effect of wind direction on k for BE building roof sampler P2: Stack location 3

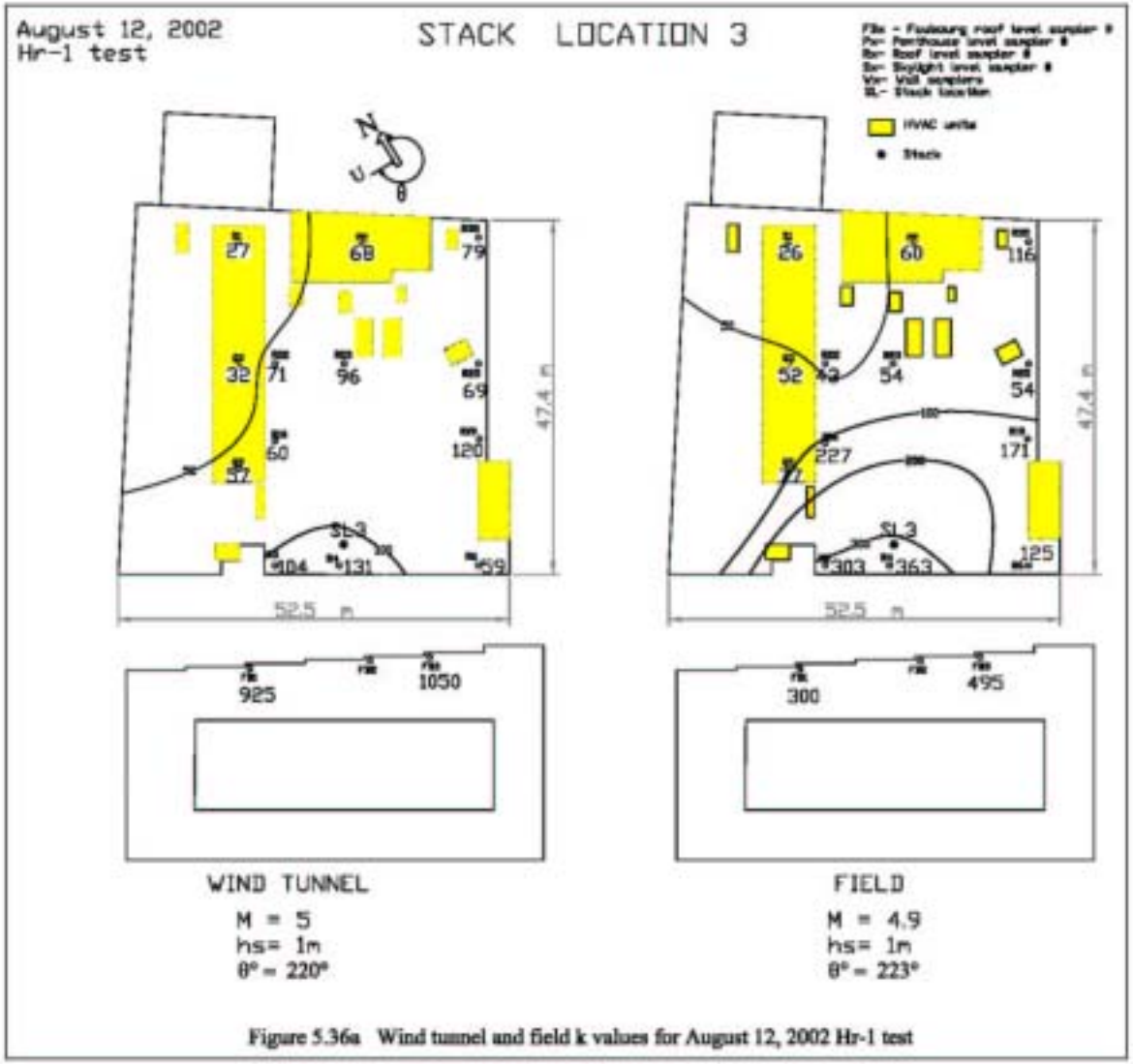

Figure 5.36a Wind tunnel and field k values for August 12, 2002 Hr-1 test

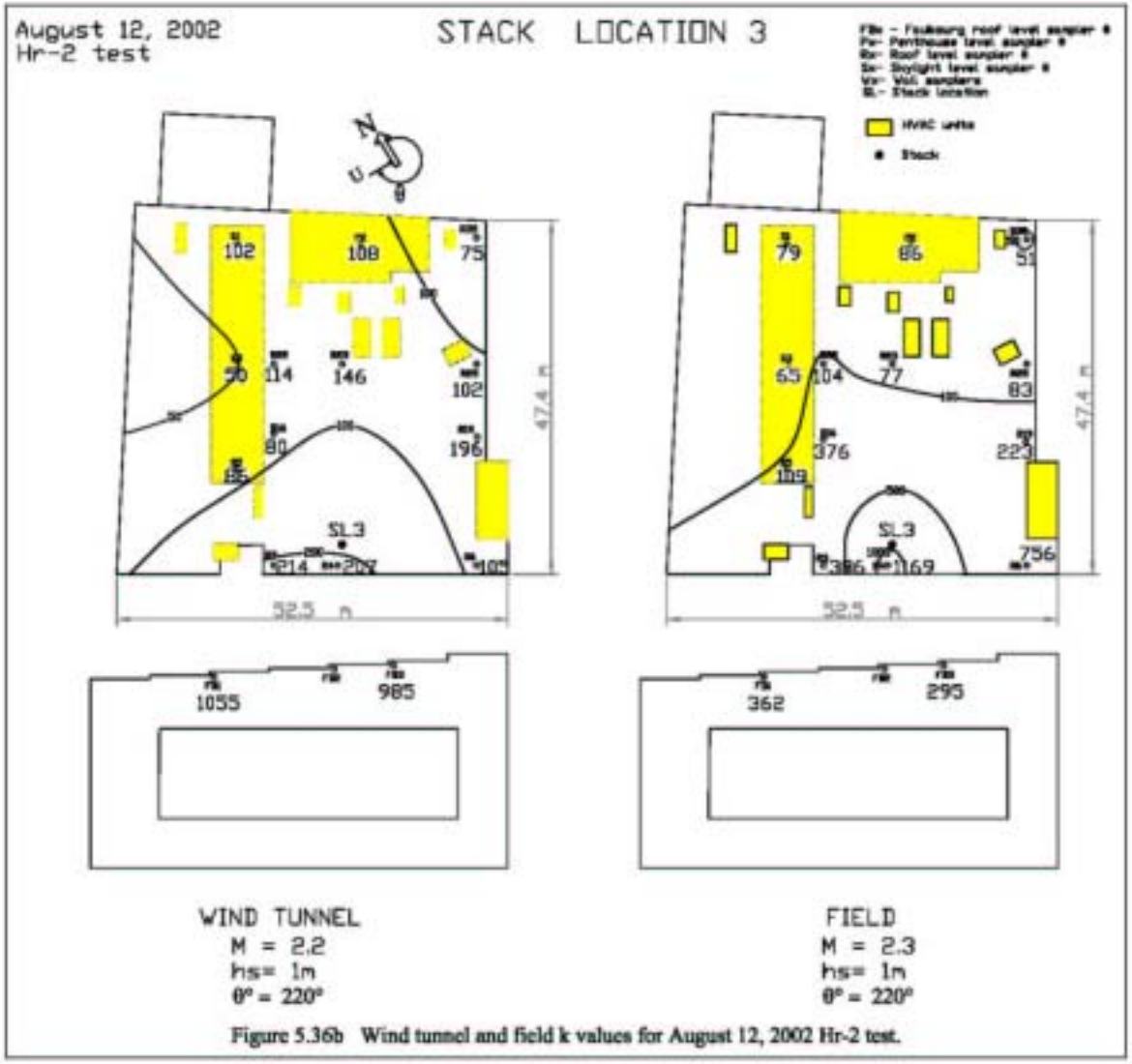

Figure 5.36b Wind tunnel and field k values for August 12, 2002 Hr-2 test.

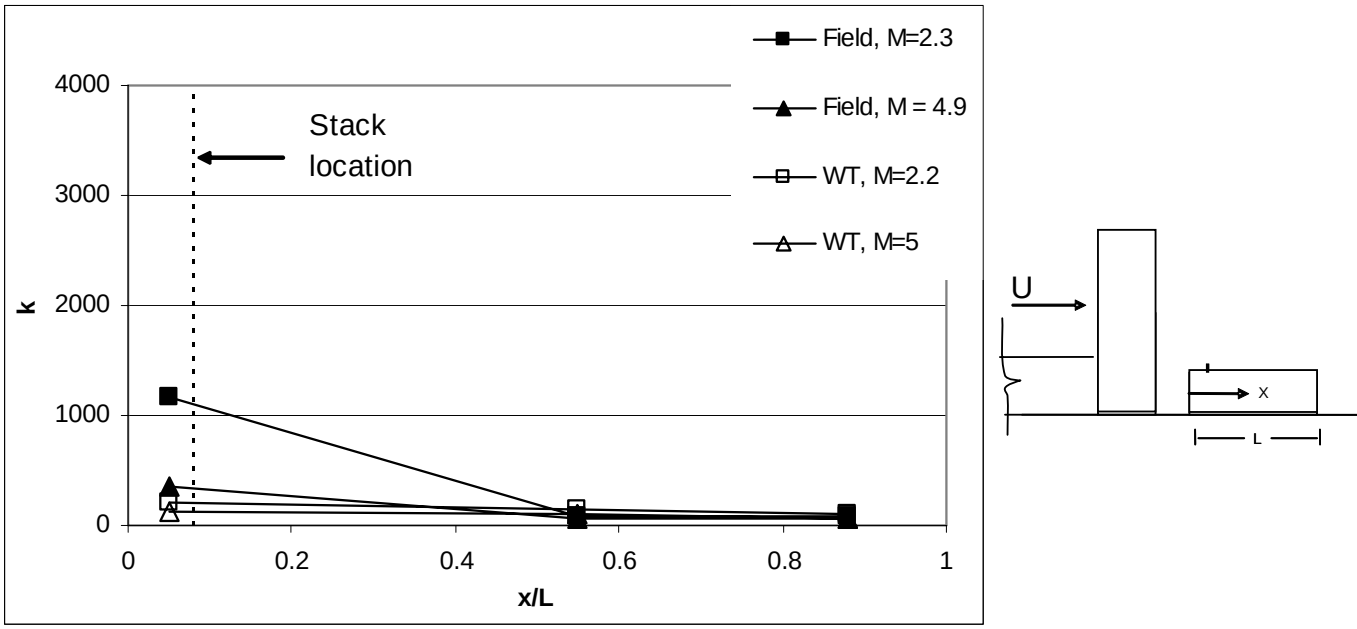

Figure 5.37 Variation of k with distance on BE roof, Aug.12-02 field test: Stack location 3

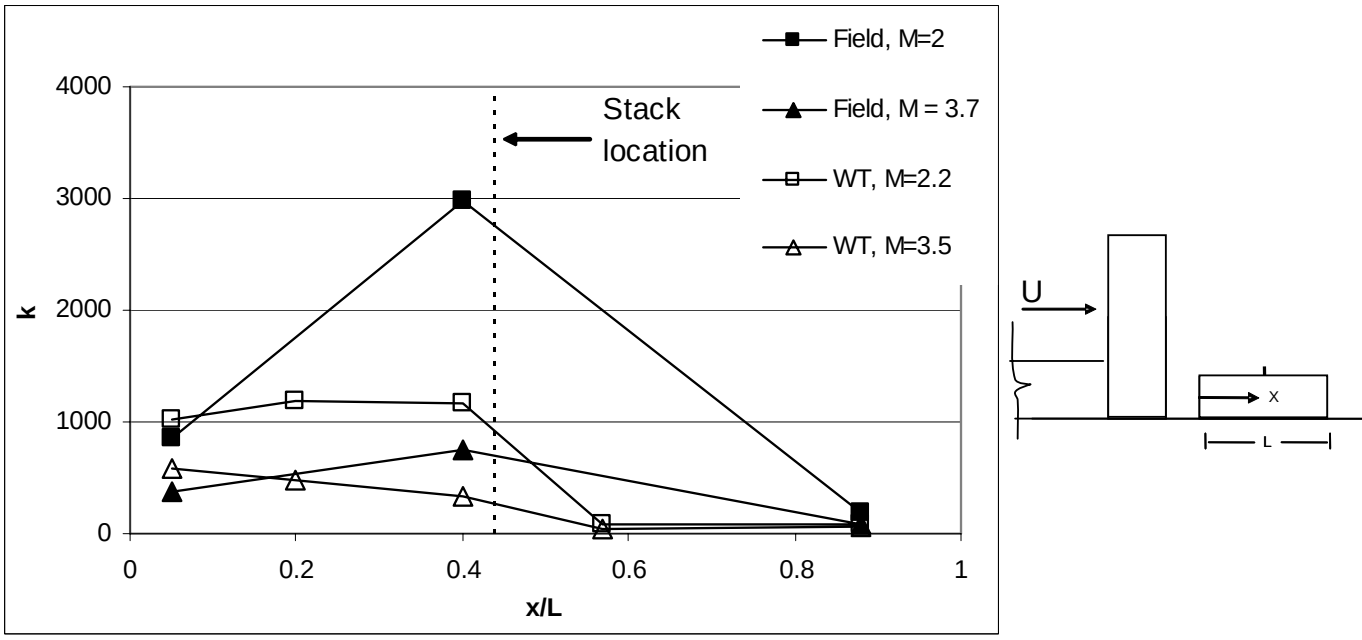

Figure 5.38 Variation of k with distance on BE roof, Oct.1-02 field test: Stack location 4

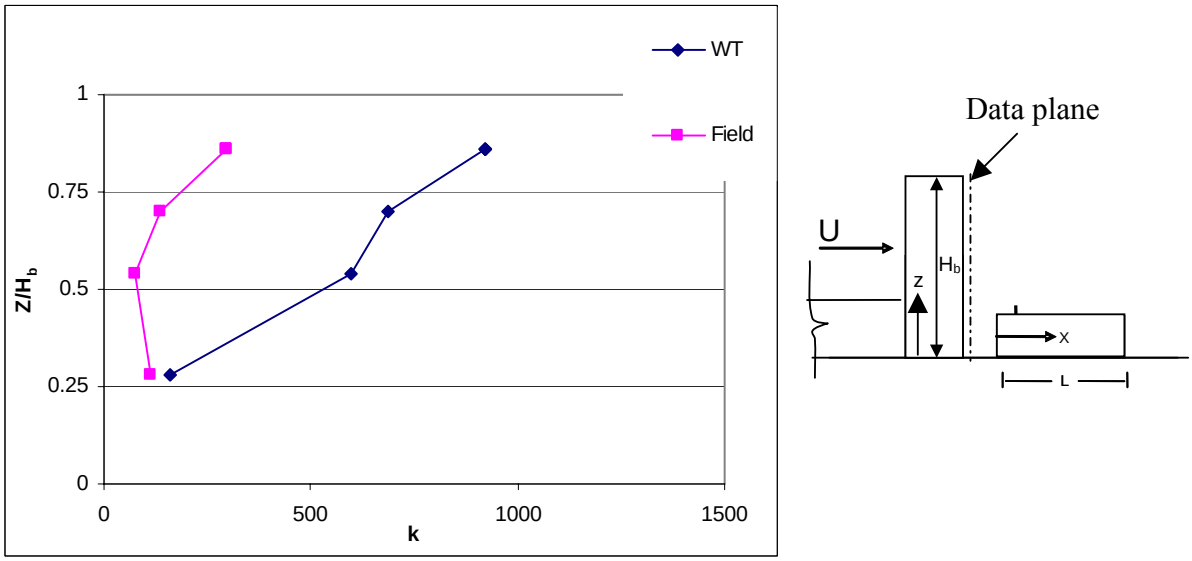

(M_{field} =3.9, M_{WT} = 4.5)

Figure 5.39 Vertical profiles of k on leeward wall of Faubourg building: Aug.26-02 test, h_s=3 m: Stack location 3

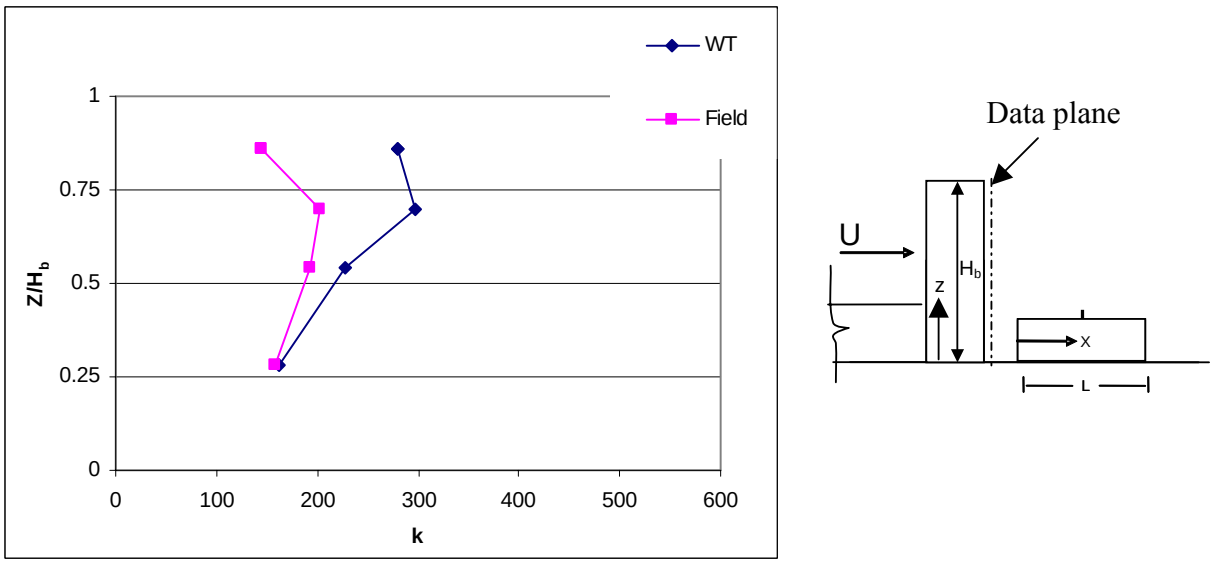

(M_{field} = 3.7, M_{WT} = 3.5)

Figure 5.40 Vertical profiles of k on leeward wall of Faubourg building: Oct.1-02 test, h_s=1 m: Stack location 4

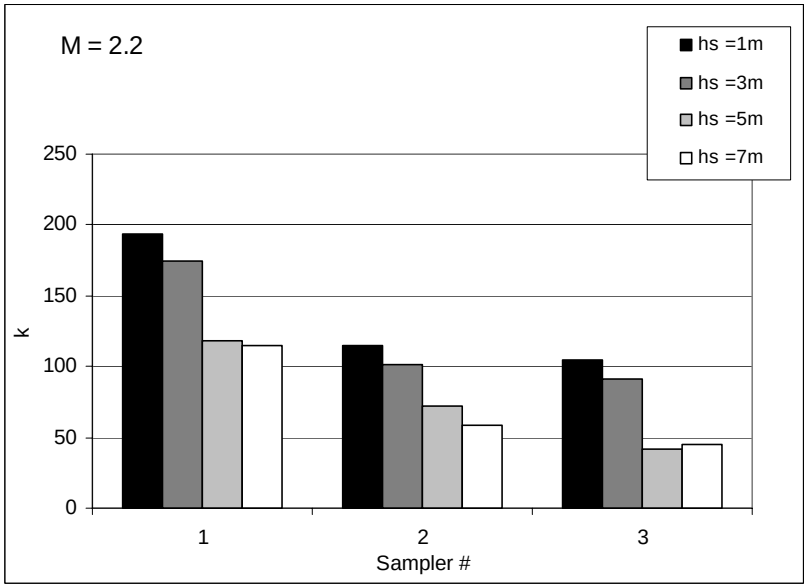

a) Roof samplers

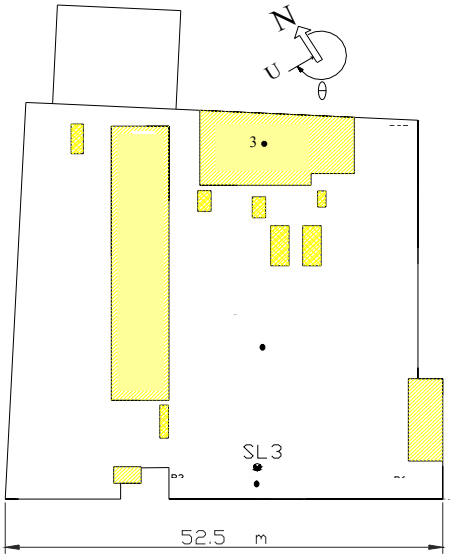

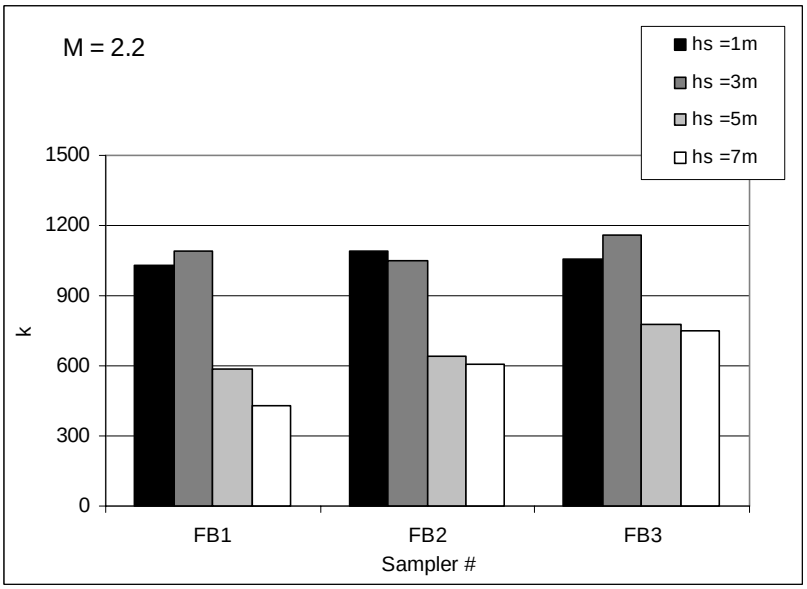

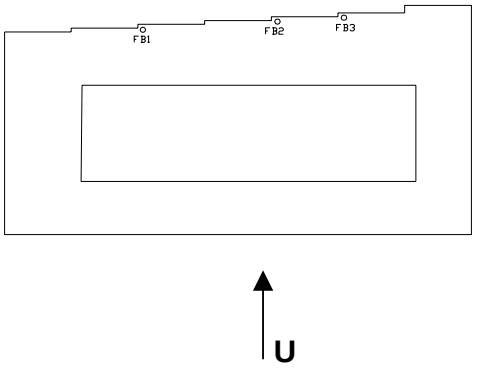

b) Faubourg wall samplers

Figure 5.41 Histogram showing effect of stack height on k for wind direction 220^{o}: Stack location 3

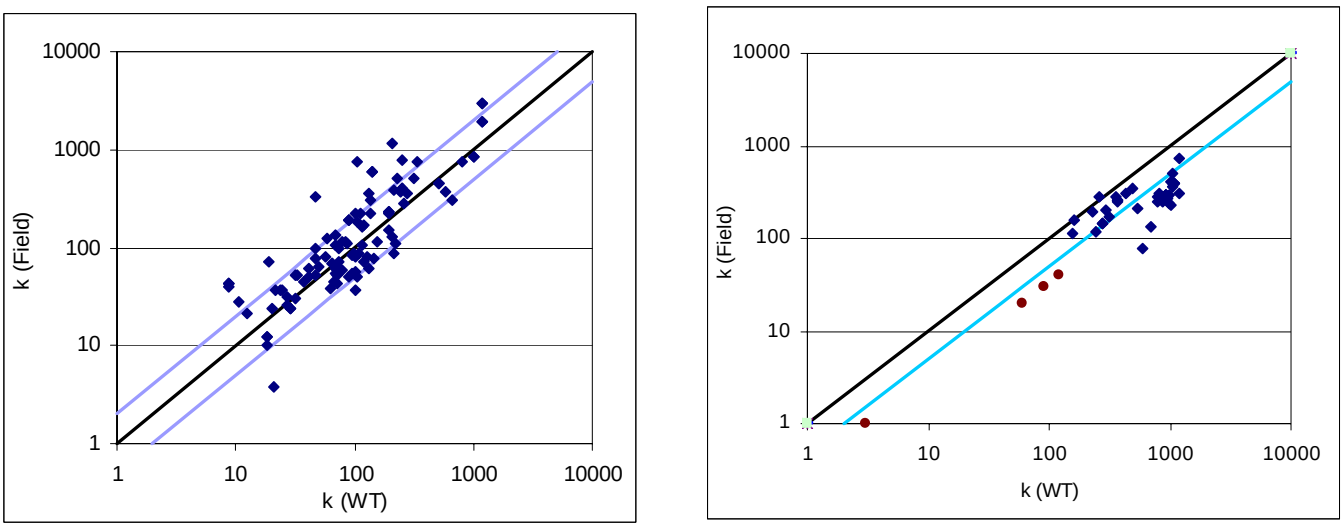

a) BE roof data

b) Faubourg wall data

Figure 5.42 Scatter plots of wind tunnel and field k data for Faubourg building upwind of BE building

Chapter 6

Design Guidelines

The following provides a summary of various design guidelines formulated on the basis of results obtained in the study:

Stack location: For open fetch situations, it is better to place the stack near the center of the roof. In this way, the leading edge recirculation zone is avoided, thus, maximizing plume rise. In addition, the required plume height to avoid contact with leeward wall receptors is minimized.

For the case of a taller building upwind of the emitting building, the center of the roof may not be the optimum stack location for receptors on the emitting building. Concentrations over most of the roof can be reduced by placing the stack near the leading edge. However, this stack location will result in higher concentrations on the leeward wall of the adjacent building.

Stack height: Increasing the stack height from 1 m to 3 m reduces concentrations near the stack by approximately a factor of two. Far from the stack ($x > 20$ m), the effect is negligible. A stack height of at least 5 m is required to provide significant reduction of k at such distances.

Stack exhaust speed: Increasing stack exhaust speed by a factor of 2.5 reduces concentrations near the stack by the same factor. For distant receptors ($x>20$ m), the

effect of exhaust speed depends on the M-value (the ratio of exhaust speed to wind speed). In the low M range (1.5<M<4.5), which is typical of wind speeds exceeding 5 m/s, increasing exhaust speed may not be beneficial for distant receptors because the plume rise may not be sufficient to avoid them. On the other hand, for light wind conditions, doubling the exhaust speed may cause M to be high enough so that concentrations are reduced over the entire roof.

ASHRAE (2003) vs ASHRAE (1999) model: The ASHRAE (1999) D_{min} model is less conservative than the ASHRAE (2003) D_r model and significantly better for distant samplers (S>30m).

For the **typical design situation** of low M cases (2.5<M<3.5), the ASHRAE (2003) D_r model appears to be overly conservative, especially for distant samplers – it underestimates dilution by a factor of 10 for receptors located more than 30 m from the stack**.** However, for high M values (M=10), the D_r model is unconservative for samplers near the stack.

Placement of fresh air intakes: The case of an emitting low building in the wake of a taller building was particularly investigated. For wind coming from the direction of the taller building:

- intakes should not be placed on leeward wall of upwind building.
- intakes on emitting building should be placed on its leeward wall if possible.

Chapter 7

Conclusions

In addition to the design guidelines formulated and summarized in Chapter 6, the following conclusions stem from this study.

- Wind tunnel predictions of concentration were generally within a factor of 2 of the field values and often within 10-20%
- Some discrepancies between wind tunnel and field data occurred for the emitting building in the wake of a taller building. This may have been due to the low level of turbulence in the wind tunnel for some configurations but the data need further examination.
    - concentrations on the leeward wall of the tall building were consistently too large in the wind tunnel, by approximately a factor of 3 on average;
    - wind tunnel concentrations measured near the stack on the emitting building were too small, especially for low M cases;
    - wind tunnel and field concentrations on the emitting building roof were similar for samplers far from the stack.
- For the open fetch configurations tested, the D_{min} model [ASHRAE (1999)] more accurately predicted minimum dilutions on the roof, compared to the D_r model [ASHRAE (2003)]. This demonstrates the usefulness of the two-component dilution model in which initial dilution and distance dilution are taken into account.

The results are encouraging because they demonstrate the general adequacy of the wind tunnel data to represent real design situations and the limitations of the ASHRAE models to predict real dilutions for particular building configurations and stack locations. The design guidelines provided in this report will be very helpful to the typical ventilation design engineer to tackle a multi-faceted complicated problem, for which codes and standards are either mute or extremely general to apply to particular real conditions.

Acknowledgments

The authors would like to gratefully acknowledge the contribution of Mr. Yves Beaudet, Mr. Rodrigue Gravel and Mr. Claude Létourneau of IRSST for their excellent work regarding the collection of the field data and Mrs Lucie Renée for the analysis of the samples.

The following students in the Department of Building, Civil and Environmental Engineering, Concordia University assisted with the field and wind tunnel experiments: Heather Knox, Joseph Caporicci and Enrico Yu.

Finally, the authors are very appreciative of the comments of the reviewers. Many of the comments have been addressed in the final report.

References

ASCE (1999) “Wind Tunnel Studies of Buildings and Structures”, Manual of Practice No. 67, American Society of Civil Engineers, Reston, VA, 20191-4400, USA.

ASHRAE (1999) Chapter 43, “Building Air Intake and Exhaust Design”, ASHRAE Applications Handbook American Society of Heating, Refrig. and Air-Cond. Eng., Inc., Atlanta.

ASHRAE (2003) Chapter 44, “Building Air Intake and Exhaust Design”, ASHRAE Applications Handbook, American Society of Heating, Refrig. And Air-Cond. Eng., Inc., Atlanta.

Briggs. (1984) “Plume rise and buoyancy effects”, in Atmospheric Science and Power Production. Randerson. Ed, U.S. Department of energy D.O.E./TIC-27601 (DE 84005177), Washington, D.C.

Engineering Sciences Data Unit (1985) “Characteristics of atmospheric turbulence near the ground, Data Item 85020, ESDU International Ltd., London.

Georgakis, K., Smith, J., Goodfellow, H. and Pye, J. (1995) “Review and evaluation of models estimating the minimum atmospheric dilution of gases exhausted near buildings”, Journal of the Air & Waste Management Assoc., Vol. 45, pp. 722-729.

Higson, H. L., Griffiths, R.F., Jones, C.D. and Hall, D.J. (1994) “Concentration measurements around an isolated building: a comparison between wind tunnel and field data”, Atmospheric Environment, Vol. 28, No. 11, pp. 1827-1836.

Mavroidis, I., Griffiths, R.F. and Hall, D.J. (2003) “Field and wind tunnel investigations of plume dispersion around single surface obstacles”, Atmospheric Environment, Vol. 37, pp. 2903-2918.

Meroney, R. N. (2003) Personal communication.

Meroney, R. N., Leitl, B., Rafailidis, S. and Schatzmann, M. (1999) “Wind-tunnel and numerical modeling of flow and dispersion about several building shapes,” Journal of Wind Engineering and Industrial Aerodynamics, 333-345.

Petersen, R. and LeCompte J. (2002) “Exhaust contamination of hidden versus visible air intakes – Final Report”, ASHRAE Research Project 1168-TRP, American Society of Heating, Refrig. and Air-Cond. Eng., Inc., Atlanta.

Saathoff P., Stathopoulos T., Lazure L, Peperkamp H. (2002) “The influence of roof top structure on the dispersion of exhaust from a rooftop stack”, ASHRAE Transactions,108

Schulman and Scire, J. (1991) “The effect of stack height , exhaust speed, and wind direction on concentrations from a rooftop stack”, ASHRAE Transactions, volume 97, pp 573-582 part 2.

Snyder, W, H., (1994) “Downwash of plumes in the vicinity of buildings: a wind tunnel study”, Recent Research Advances in the Fluid Mechanics of Turbulent Jets and Plumes, Kluwer Academic Pub. , 343-356.

Stathopoulos T., Lazure L, Saathoff, P. (1999) “Tracer gas investigation of reingestion of building exhaust in an urban environment", IRSST research report R-213, Institut de recherche Robert-Sauvé en santé et en sécurité du travail, Montreal, Canada

Stathopoulos T., Lazure L, Saathoff, P. and Wei. X. (2002) “Dilution of exhaust from a roof top stack on a cubical building in an urban environment", Atmospheric Environment 36, 4577-4591.

Turner, D.B. (1994) Workbook of Atmospheric Dispersion Estimates, 2nd Ed., CRC Press.

Wieringa, J. (1993) “Representative roughness parameters for homogeneous terrain,” Boundary-Layer Meteorology, 63, 323-363.

Wilson, D (1979) “Flow patterns over flat-roofed buildings and application to exhaust stack design”, ASHRAE Transactions, 85, part 2, 284-295.

Wilson, D.J. and Lamb, B., (1994) “Dispersion of exhaust gases from roof level stacks and vents on a laboratory building”, Atmospheric Environment, 28, 3099-3111.

Wilson, D.J., Fabris, I., Chen, J. and Ackerman, M. (1998) “Adjacent building effects on laboratory fume hood exhaust stack design”, ASHRAE Research Report 897, American Society of Heating and Refrigerating and Air-conditioning Engineers, Atlanta Ga.

Wilson, D.J. (1995) Concentration Fluctuations and Averaging Time in Vapor Clouds, Center for Chemical Process Safety, American Institute of Chemical Engineers, New York.

APPENDIX A

Stack and sampler locations for field tests

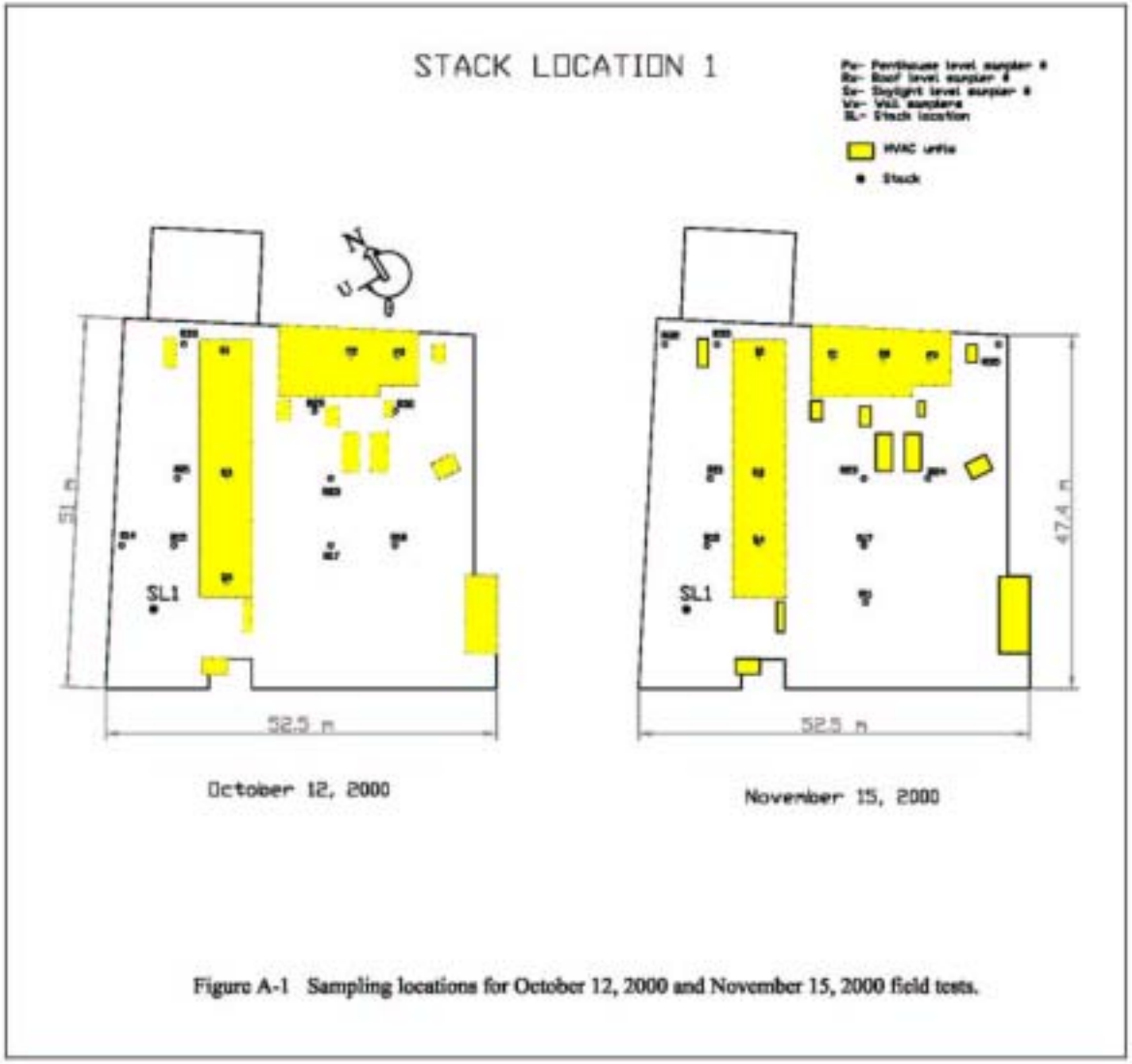

Figure A-1 Sampling locations for October 12, 2000 and November 15, 2000 field tests.

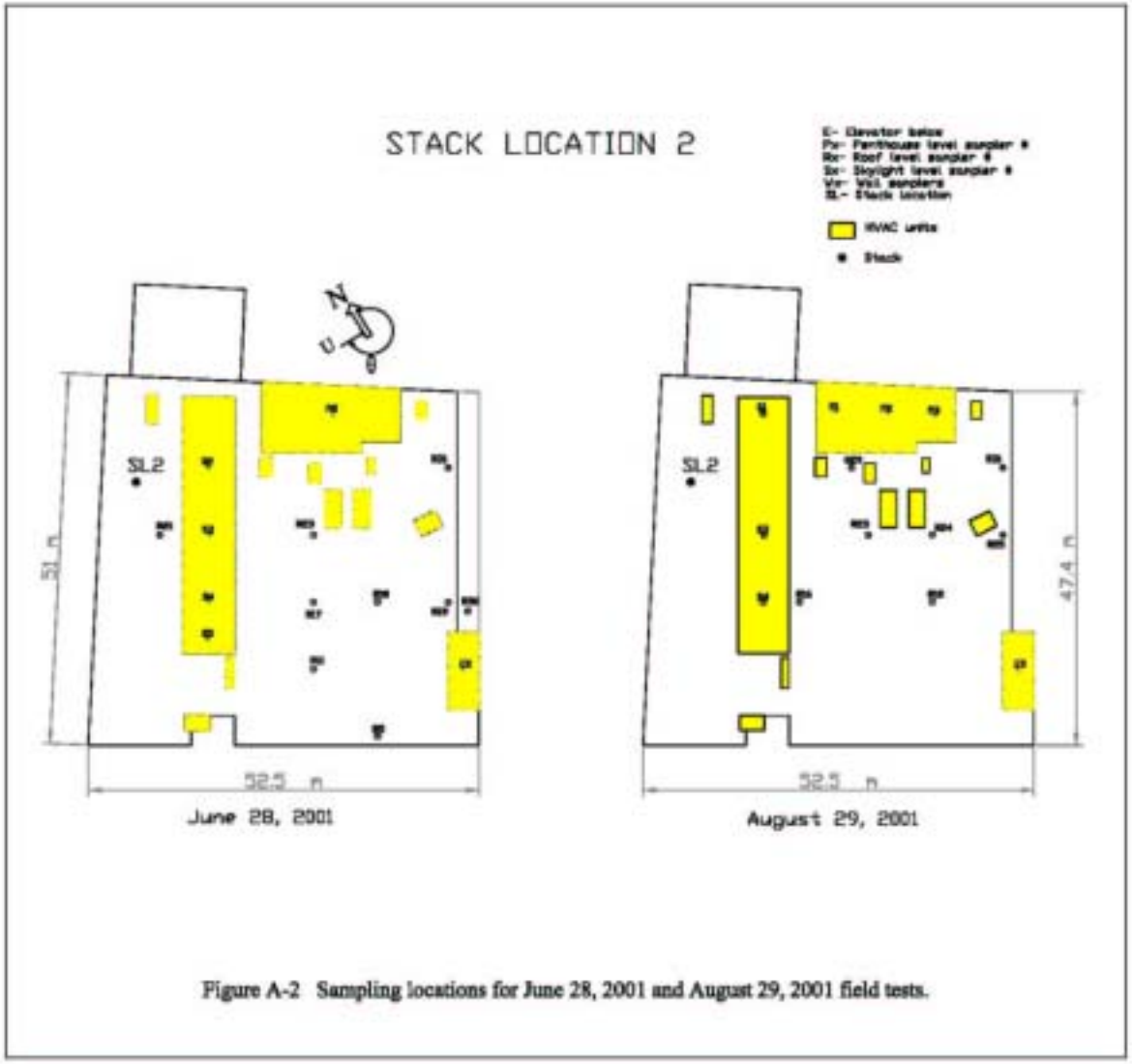

Figure A-2 Sampling locations for June 28, 2001 and August 29, 2001 field tests.

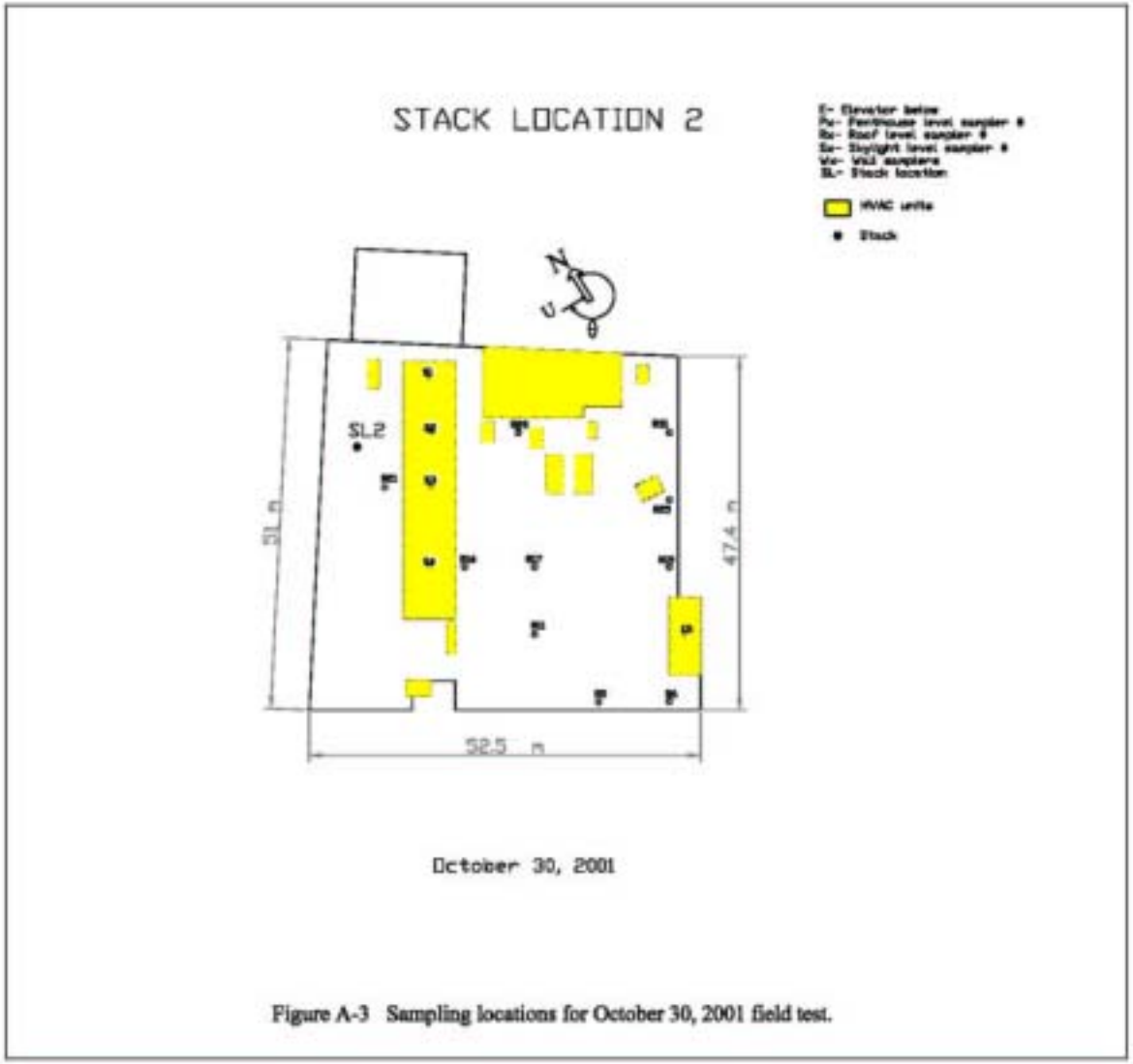

Figure A-3 Sampling locations for October 30, 2001 field test.

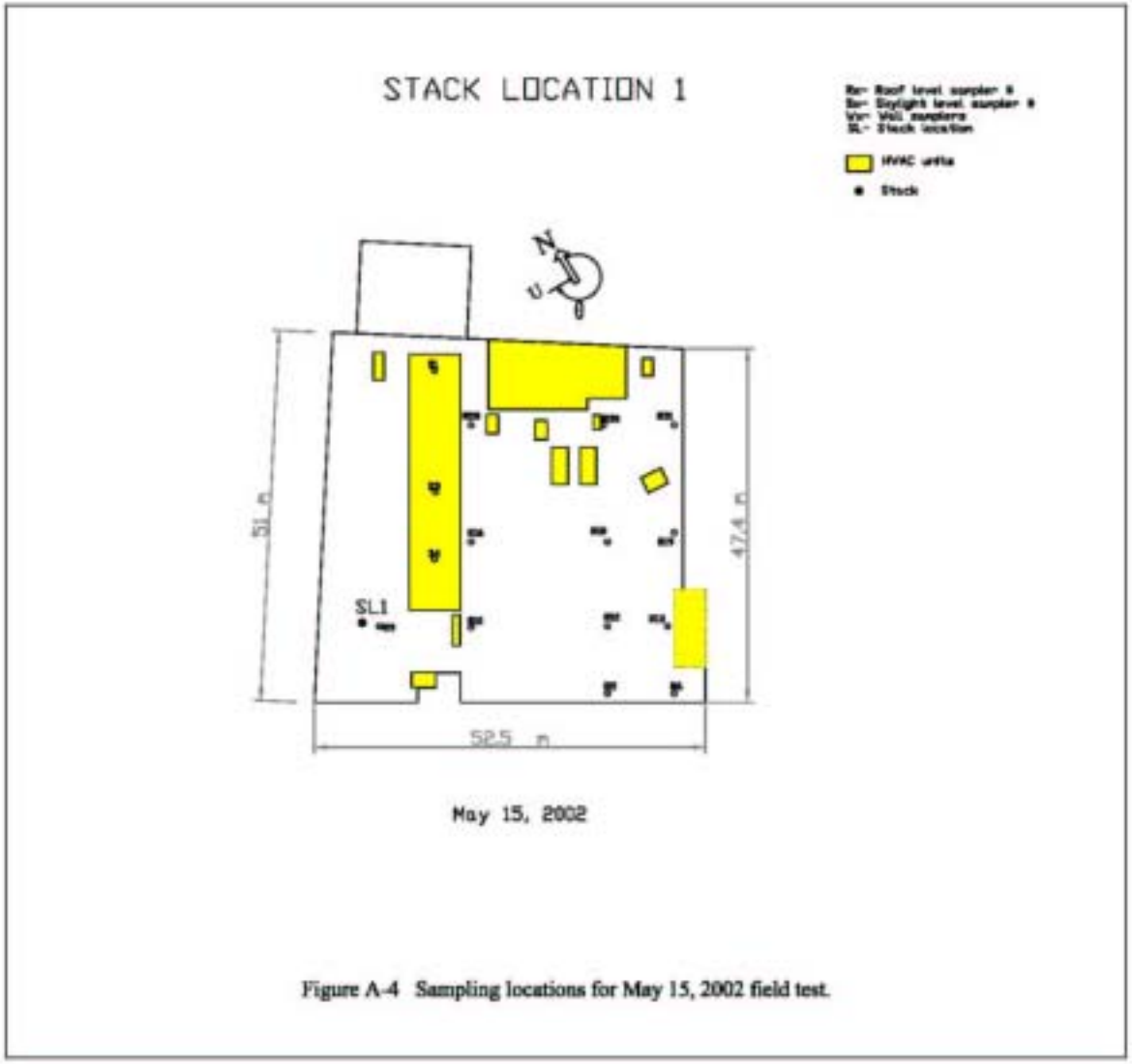

Figure A-4 Sampling locations for May 15, 2002 field test.

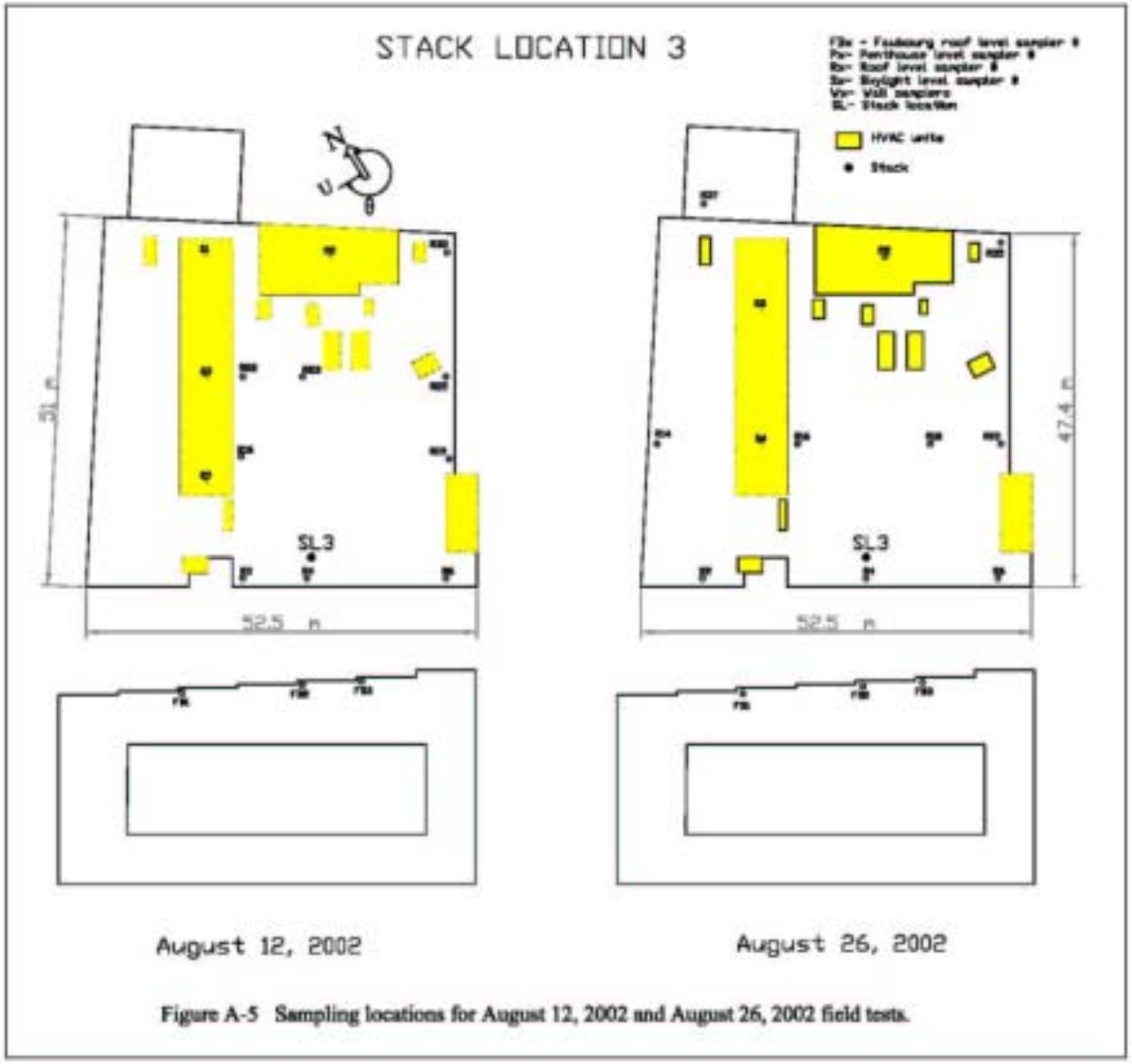

Figure A-5 Sampling locations for August 12, 2002 and August 26, 2002 field tests.

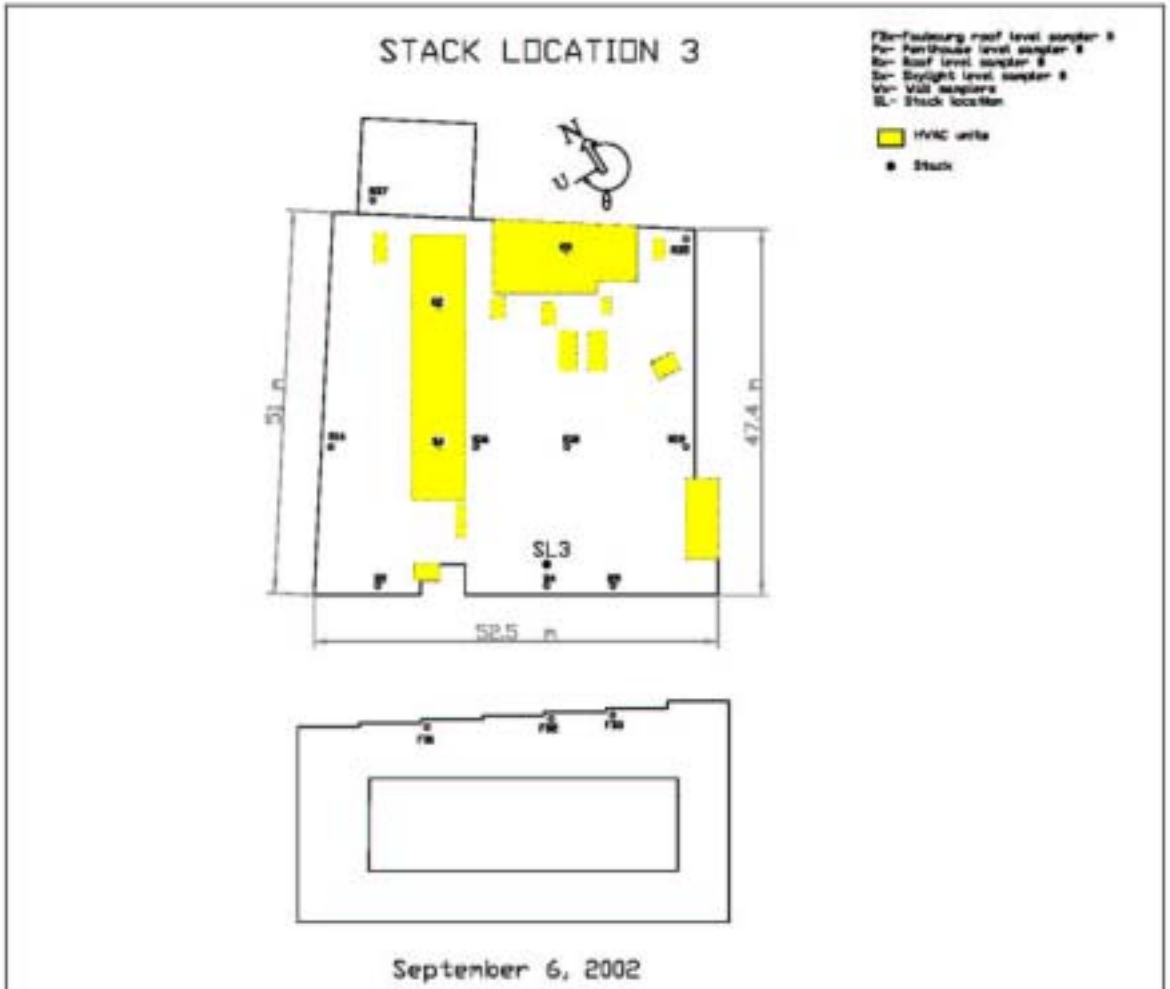

Figure A-6 Sampling locations for September 6, 2002 field test.

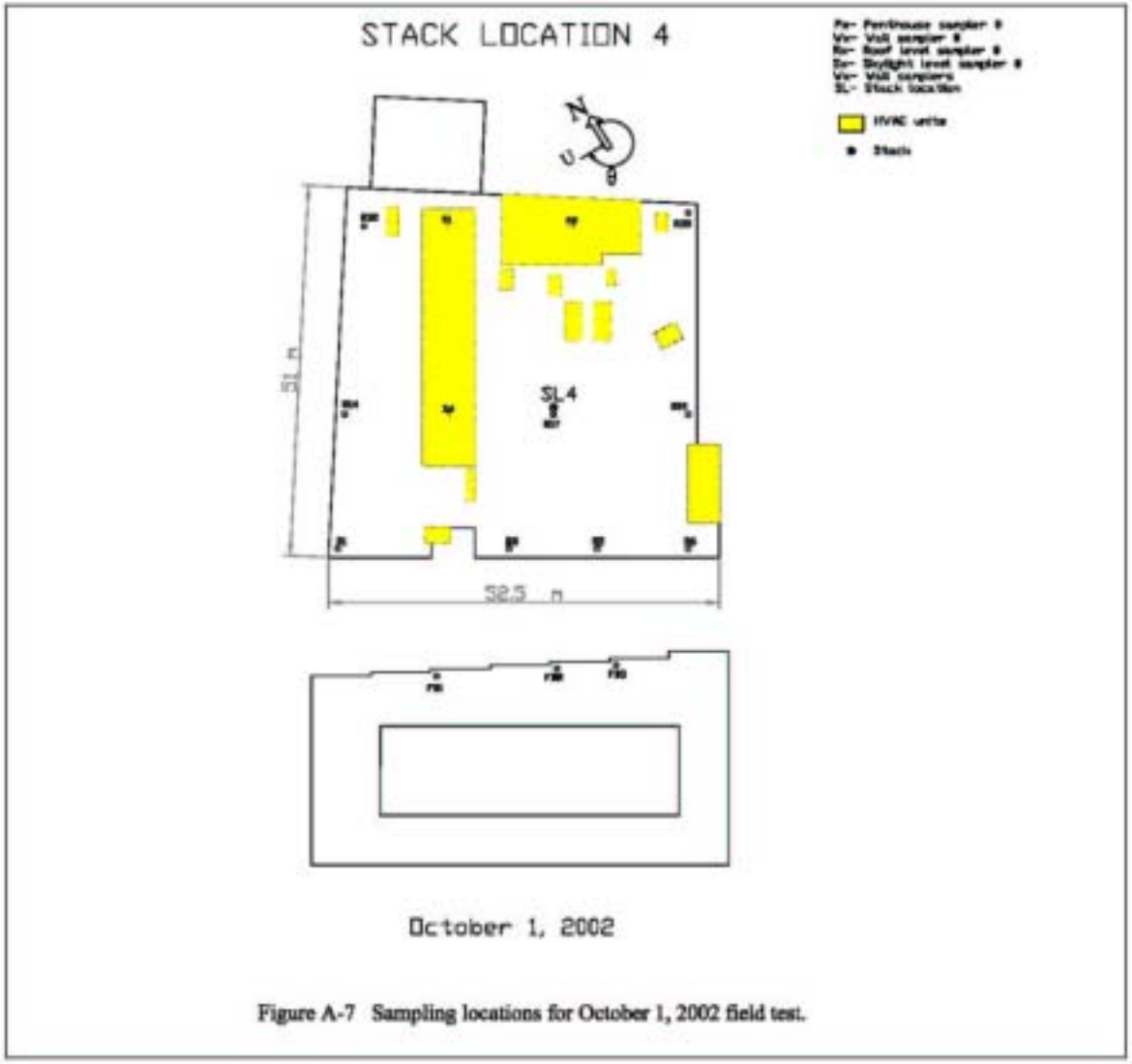

Figure A-7 Sampling locations for October 1, 2002 field test.

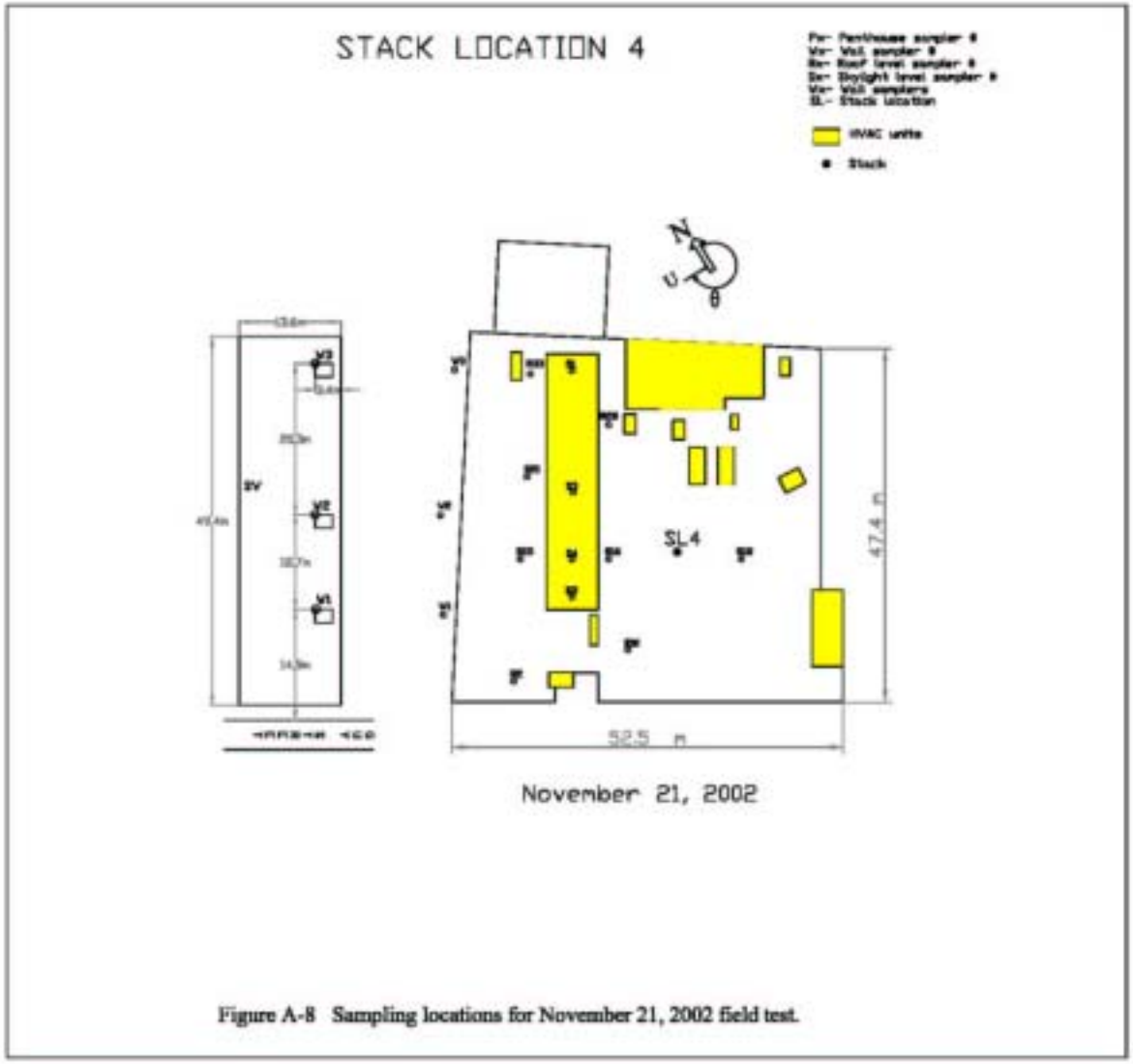

Figure A-8 Sampling locations for November 21, 2002 field test.

APPENDIX B

Comparisons of wind tunnel and field data

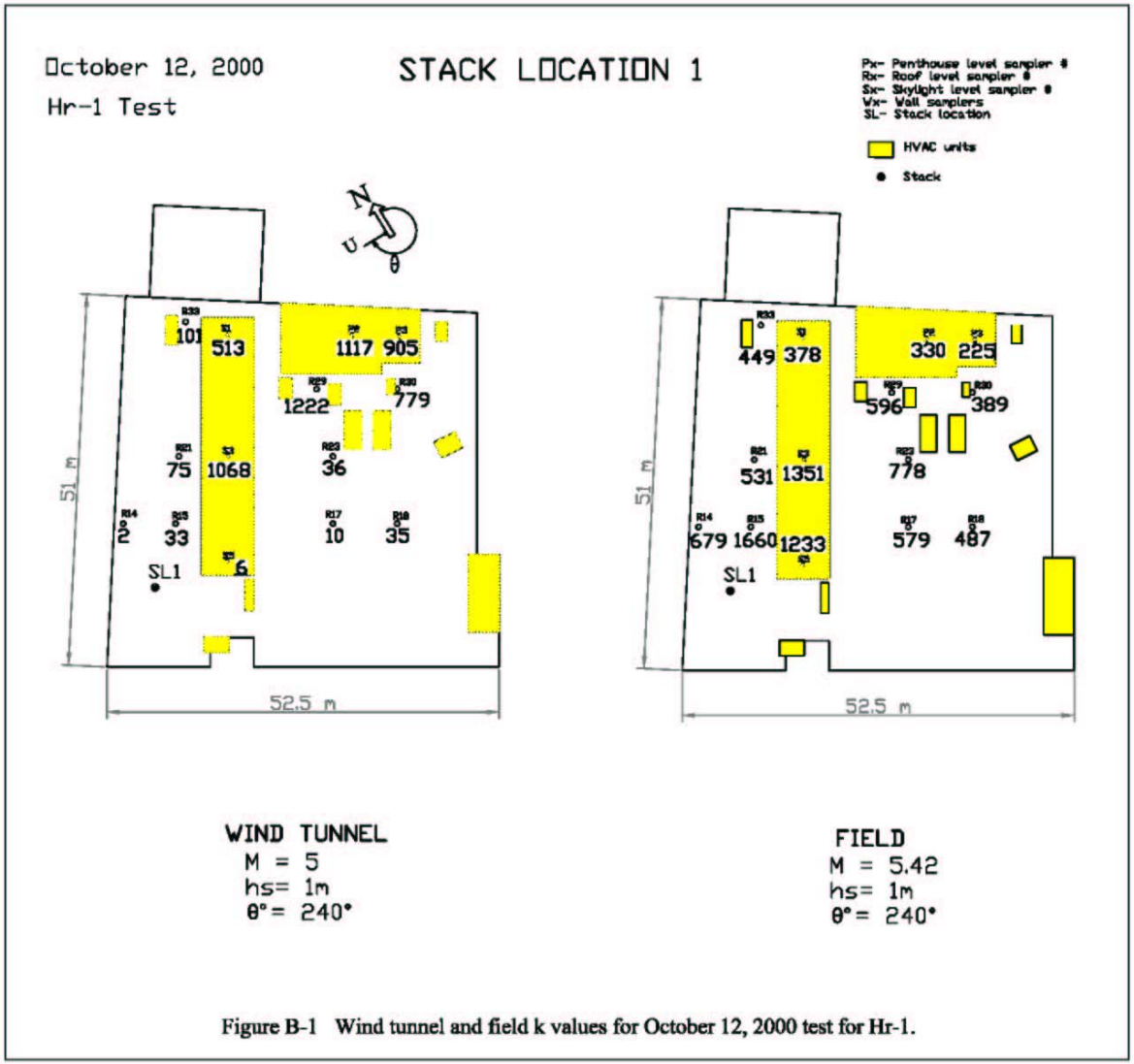

Figure B-1 Wind tunnel and field k values for October 12, 2000 test for Hr-1.

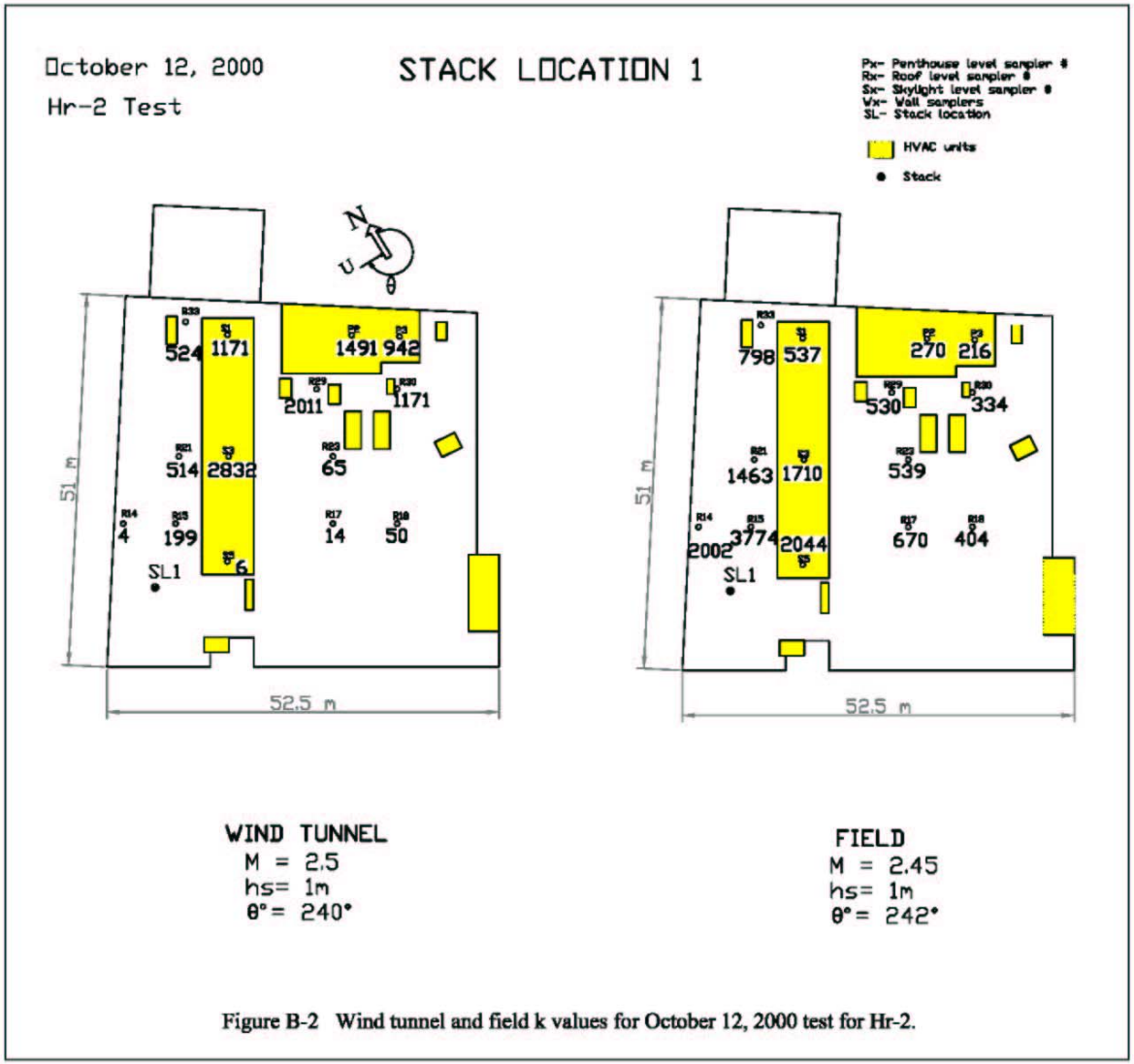

Figure B-2 Wind tunnel and field k values for October 12, 2000 test for Hr-2.

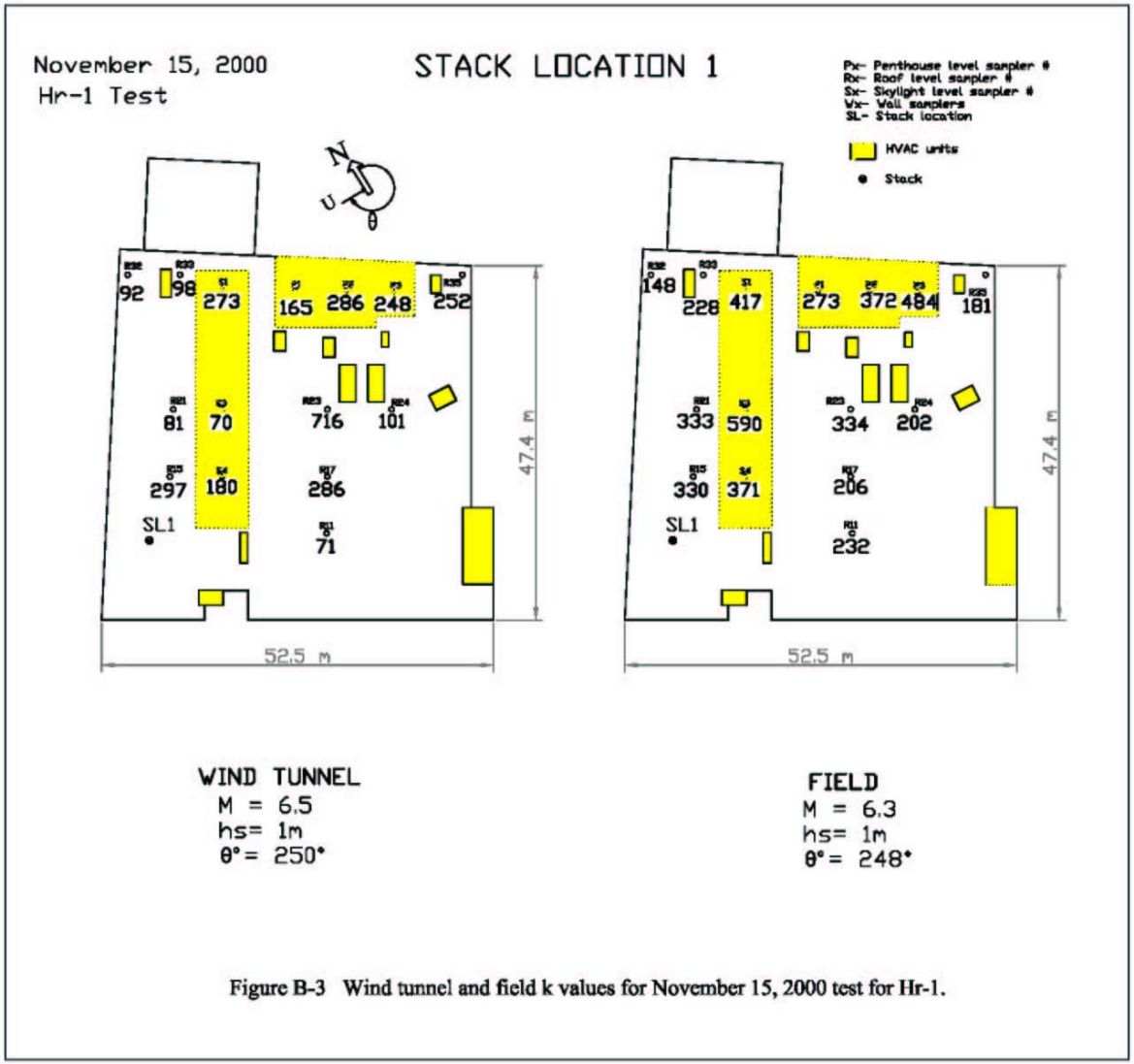

Figure B-3 Wind tunnel and field k values for November 15, 2000 test for Hr-1.

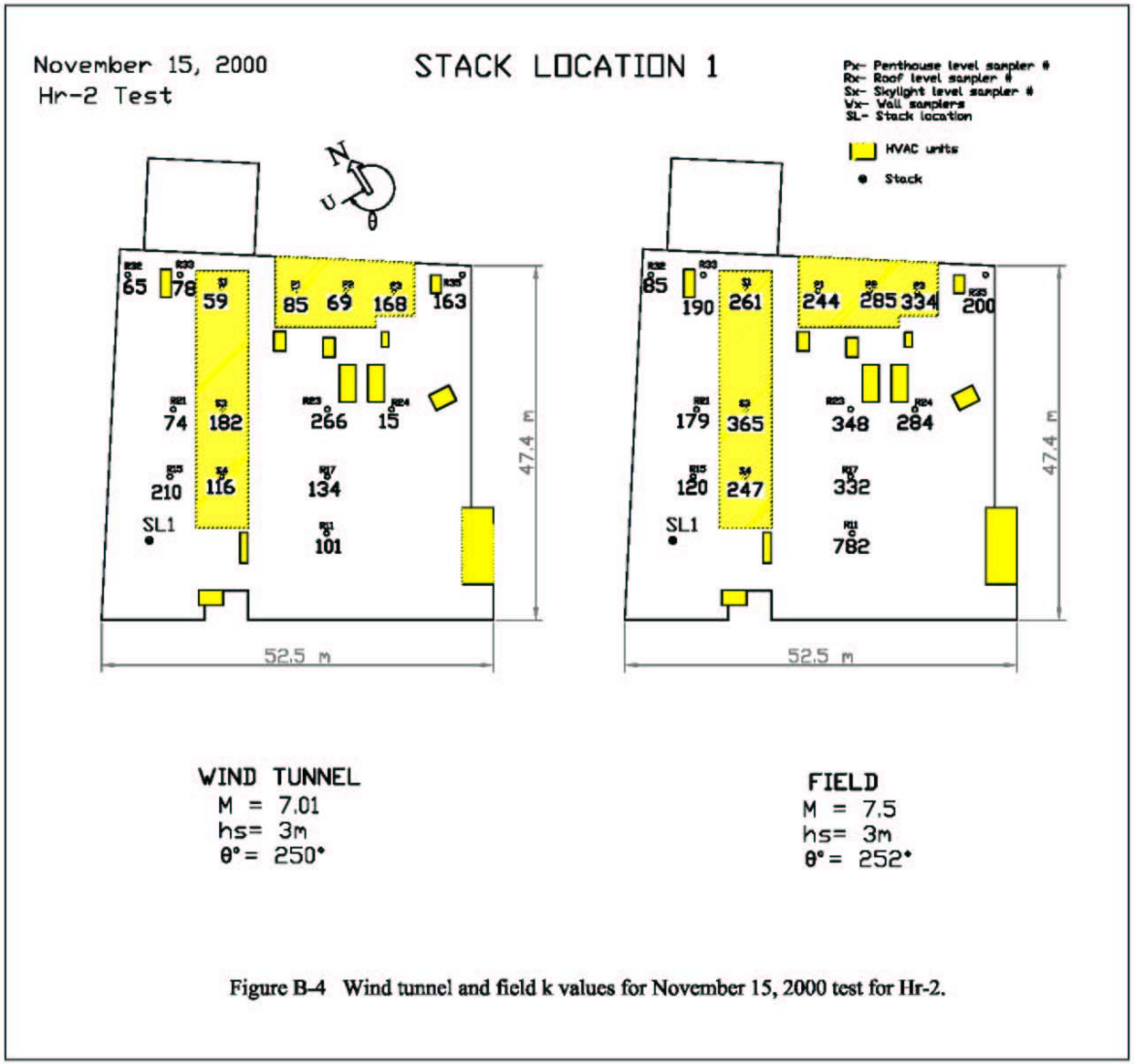

Figure B-4 Wind tunnel and field k values for November 15, 2000 test for Hr-2.

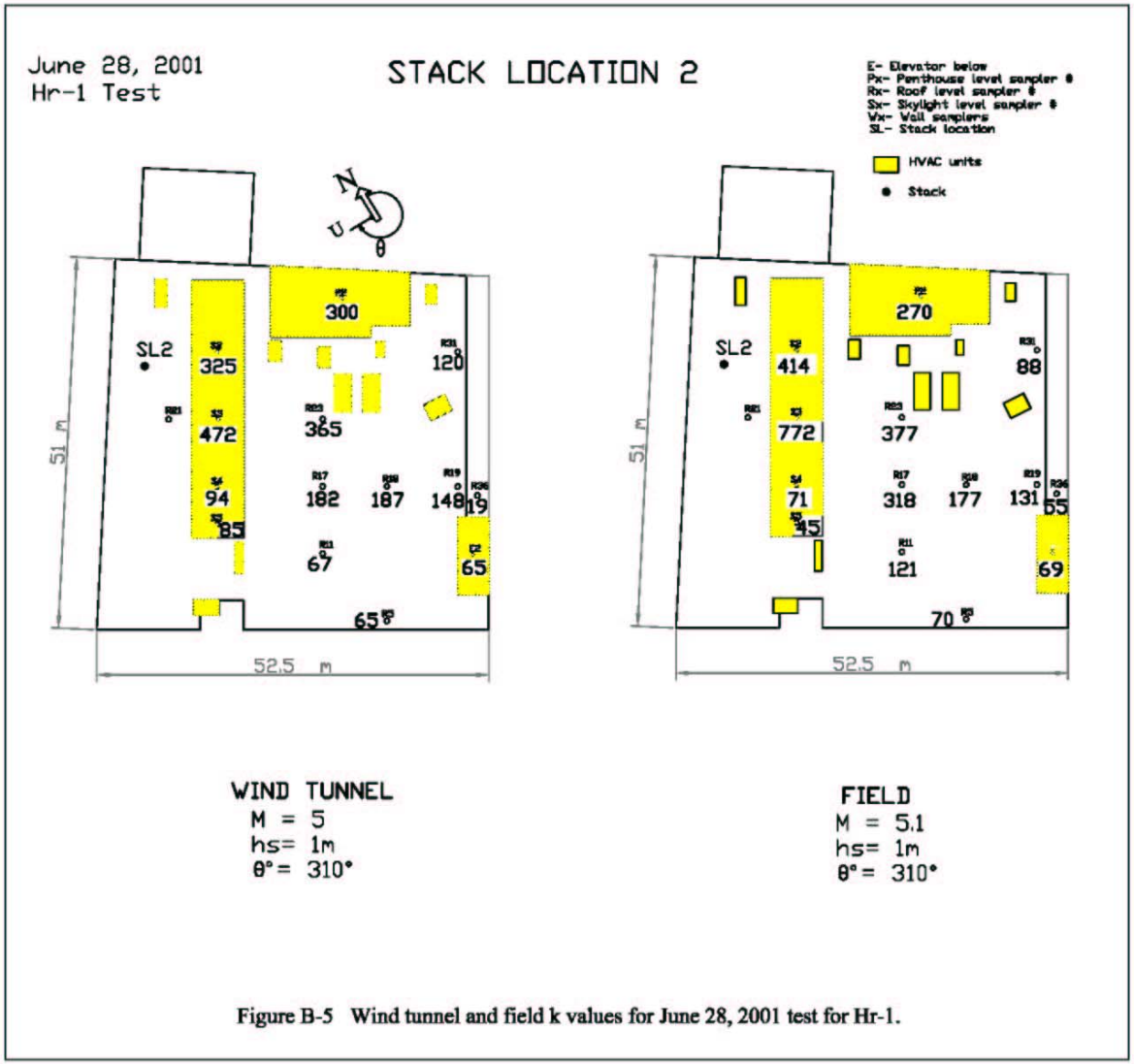

Figure B-5 Wind tunnel and field k values for June 28, 2001 test for Hr-1.

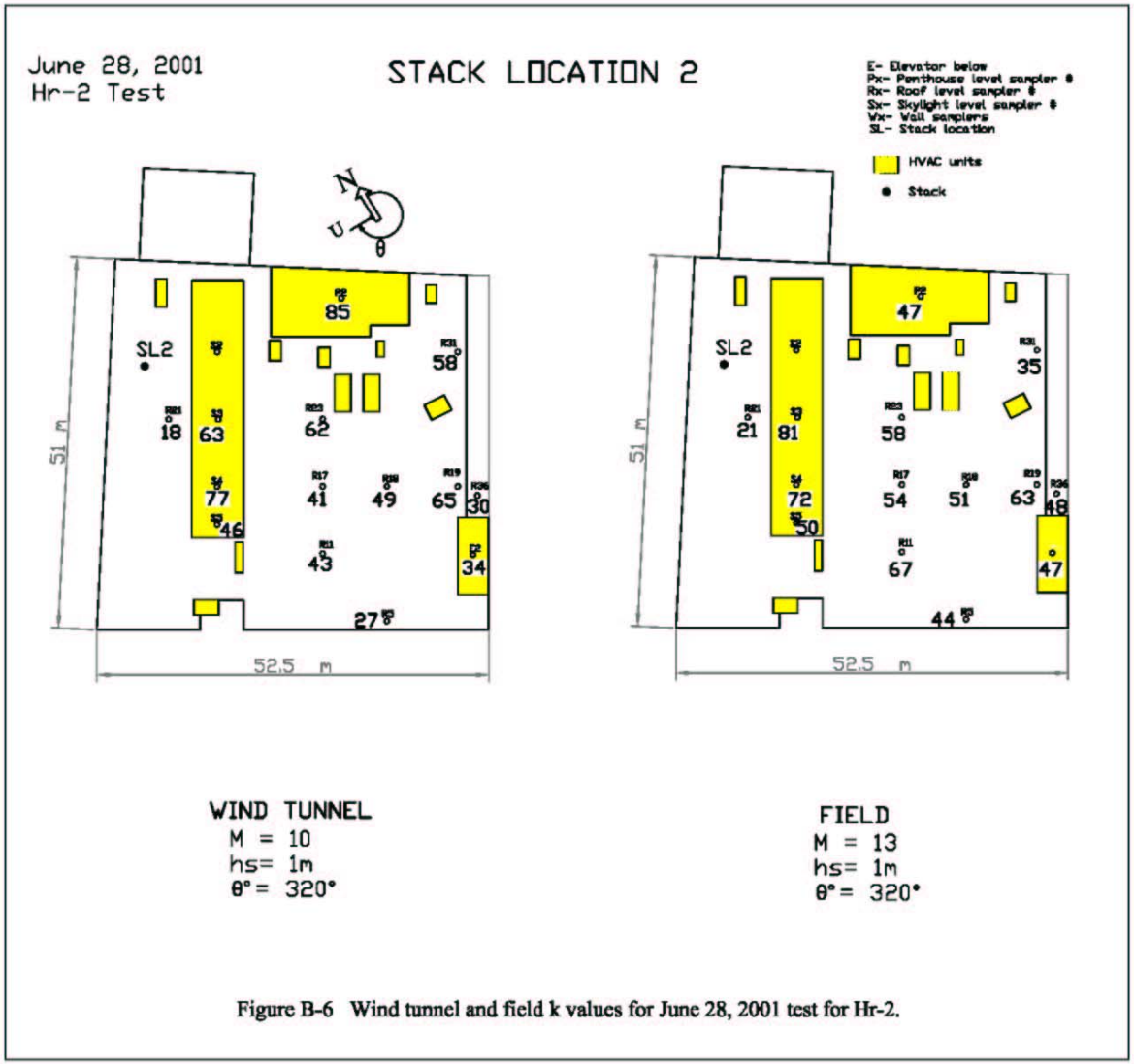

Figure B-6 Wind tunnel and field k values for June 28, 2001 test for Hr-2.

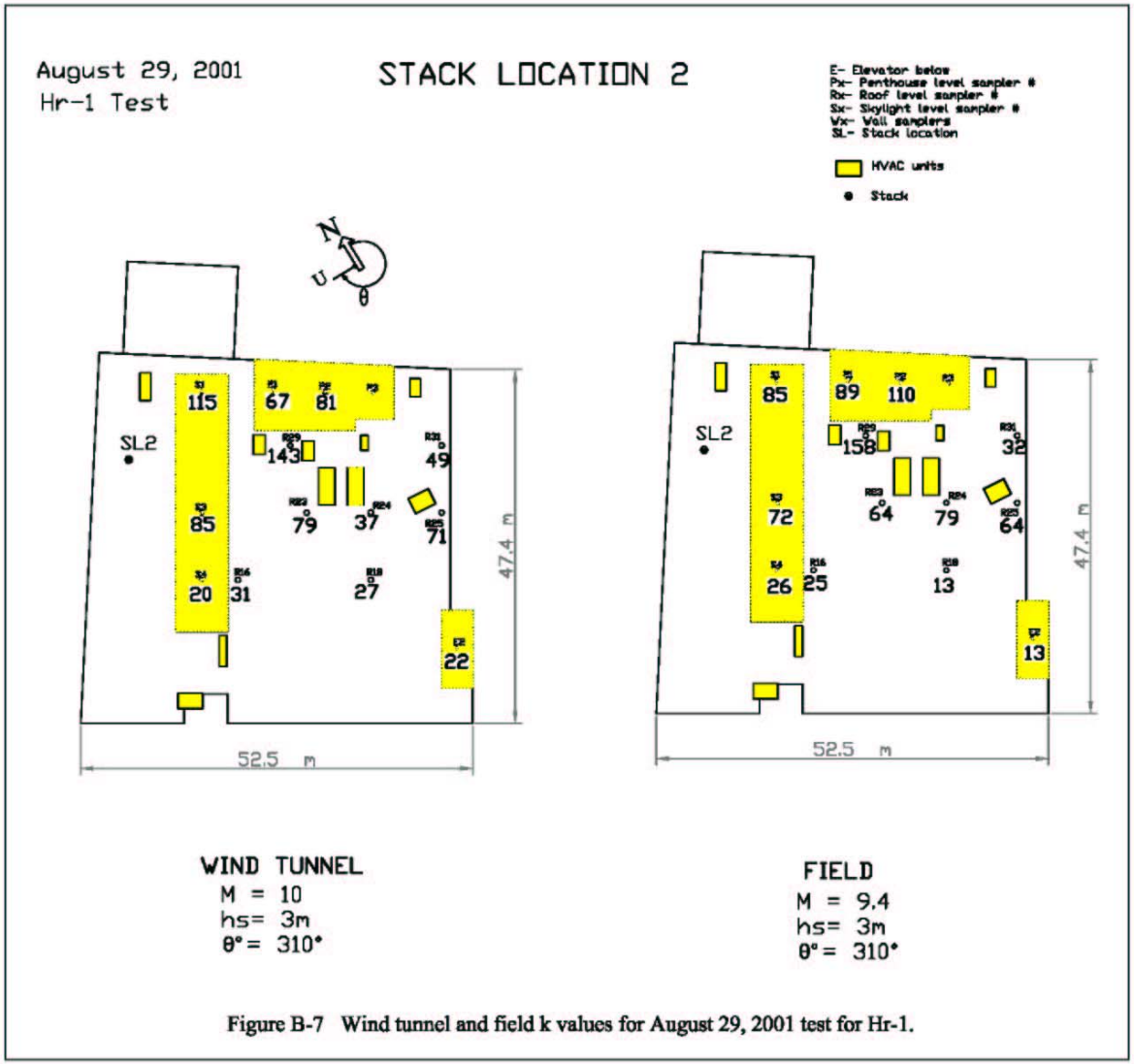

Figure B-7 Wind tunnel and field k values for August 29, 2001 test for Hr-1.

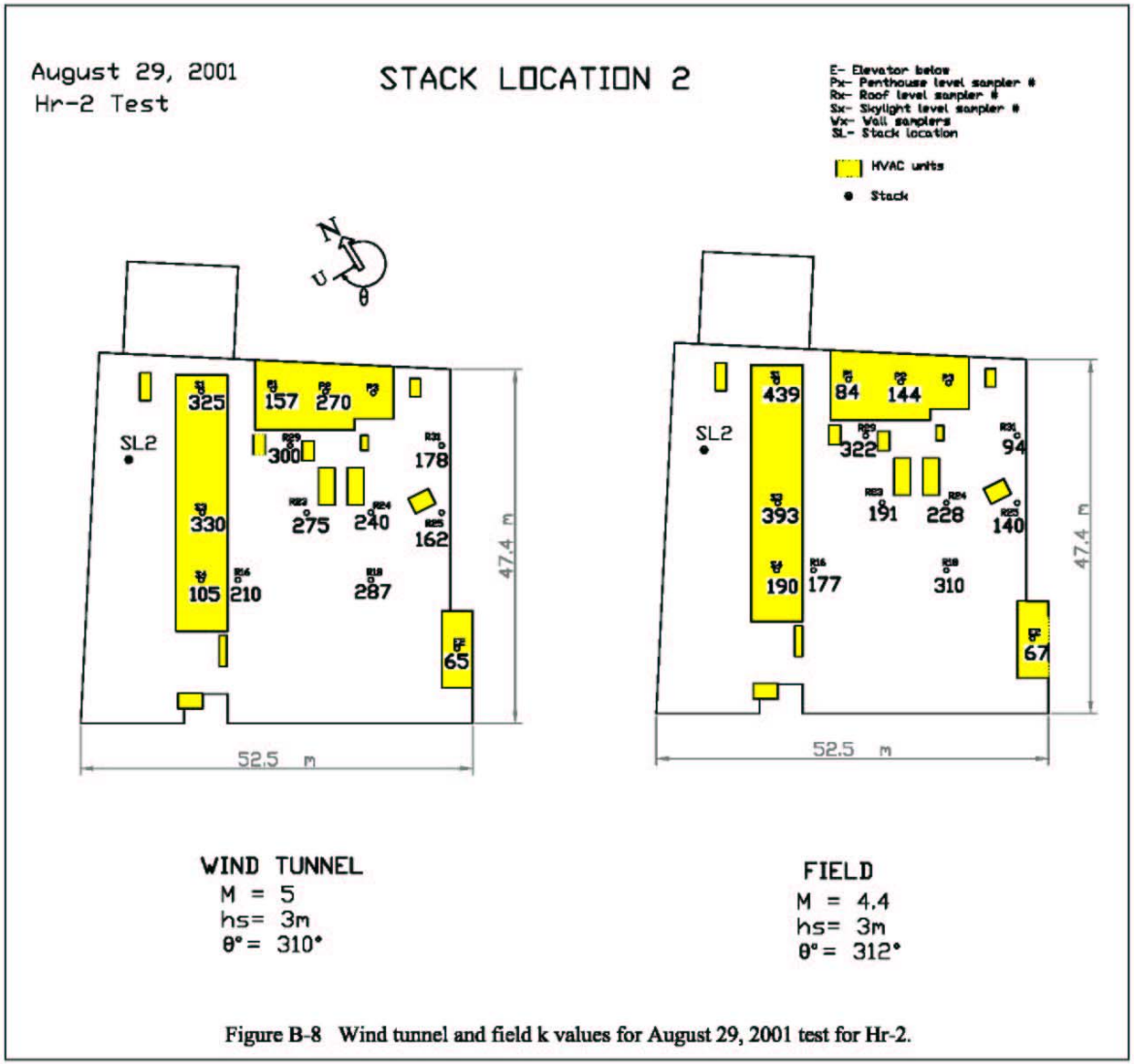

Figure B-8 Wind tunnel and field k values for August 29, 2001 test for Hr-2.

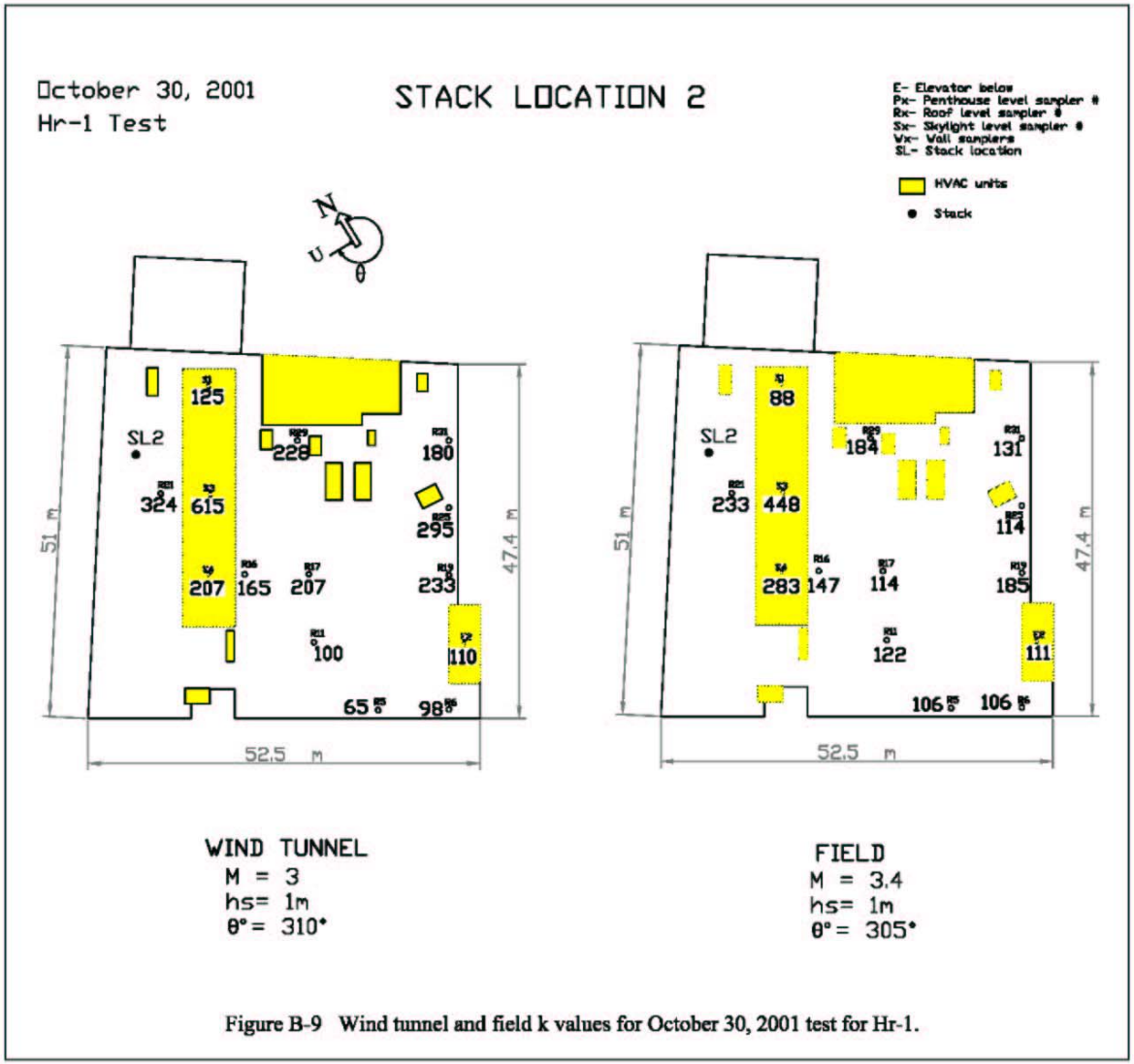

Figure B-9 Wind tunnel and field k values for October 30, 2001 test for Hr-1.

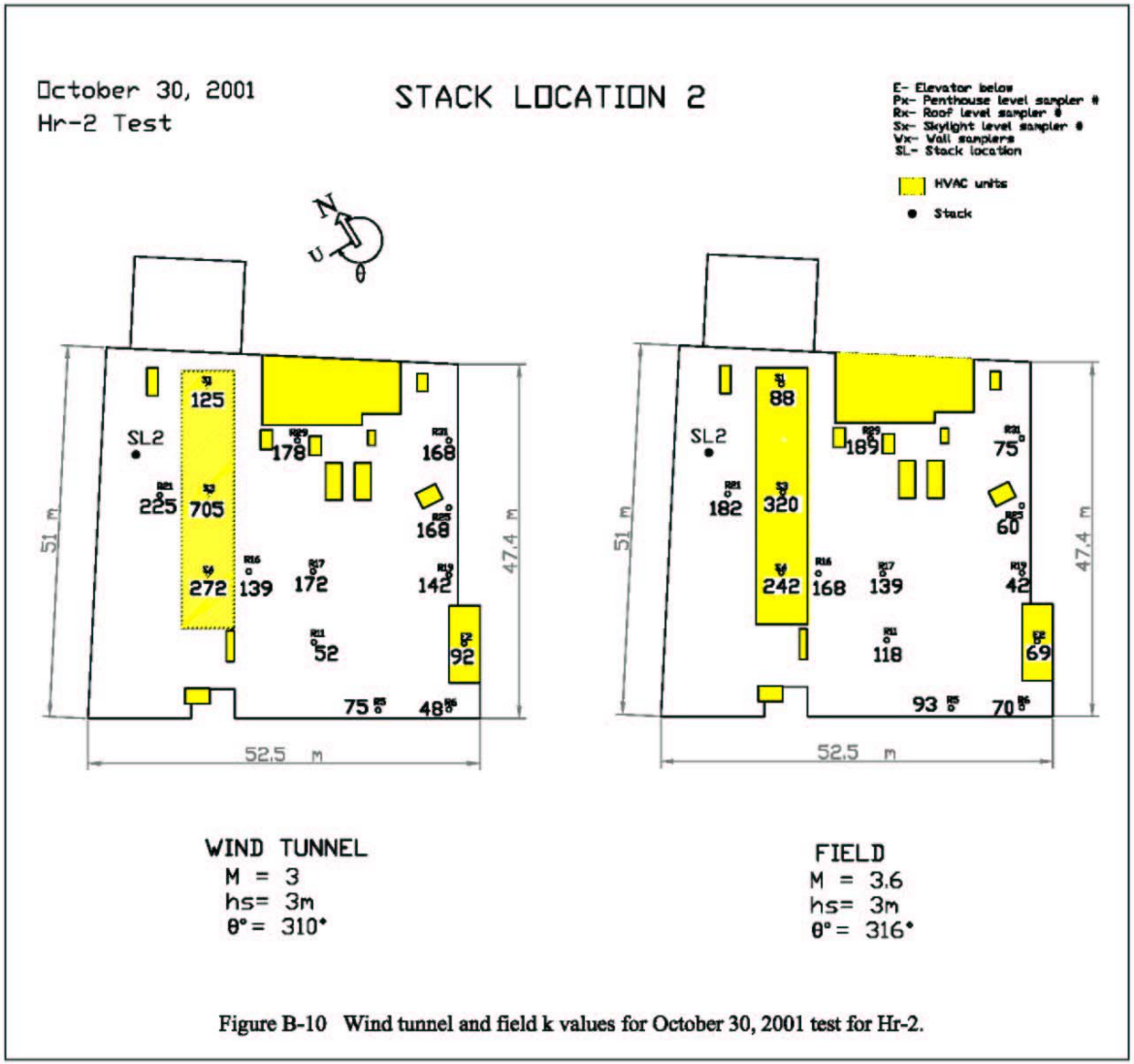

Figure B-10 Wind tunnel and field k values for October 30, 2001 test for Hr-2.

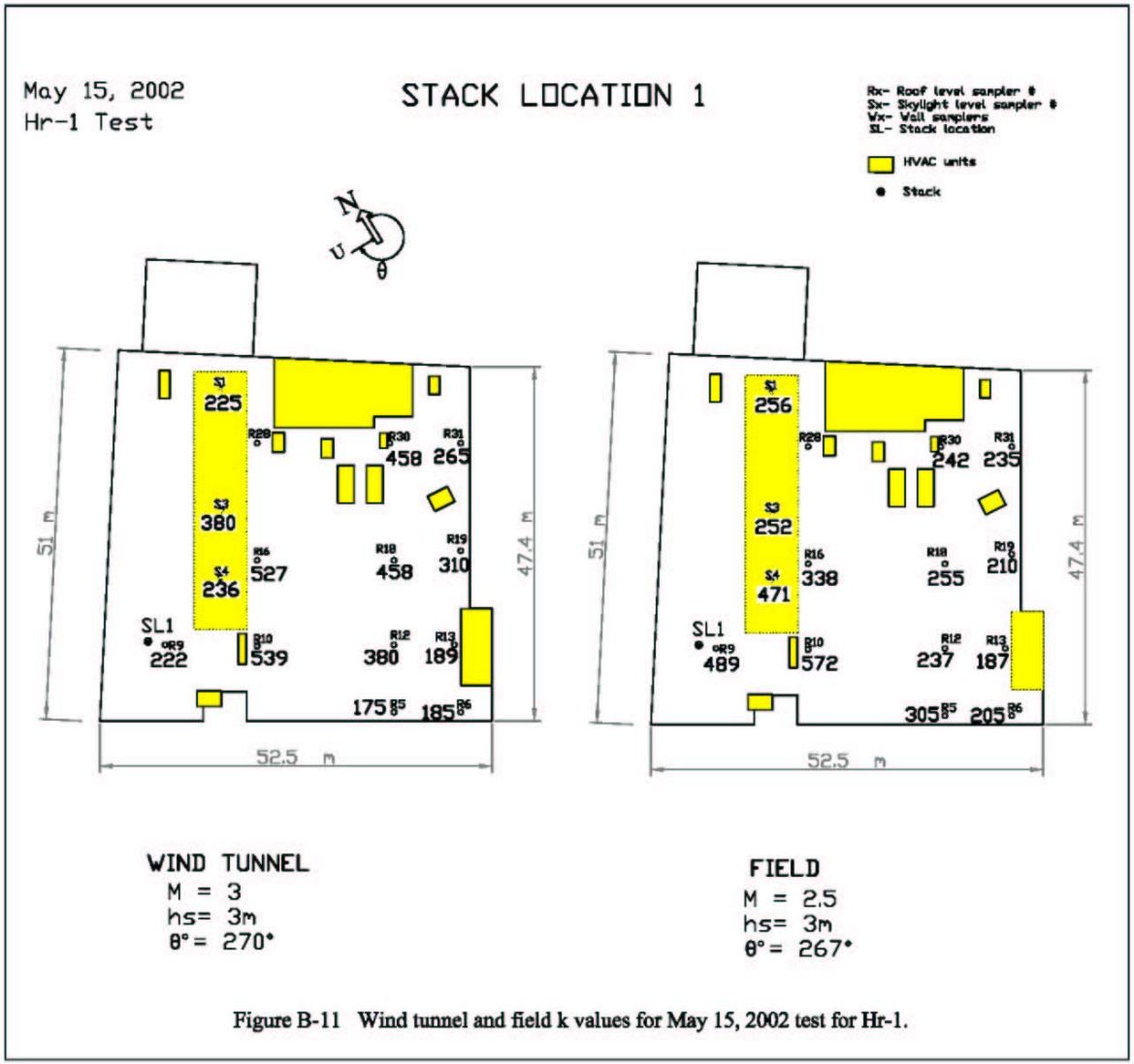

Figure B-11 Wind tunnel and field k values for May 15, 2002 test for Hr-1.

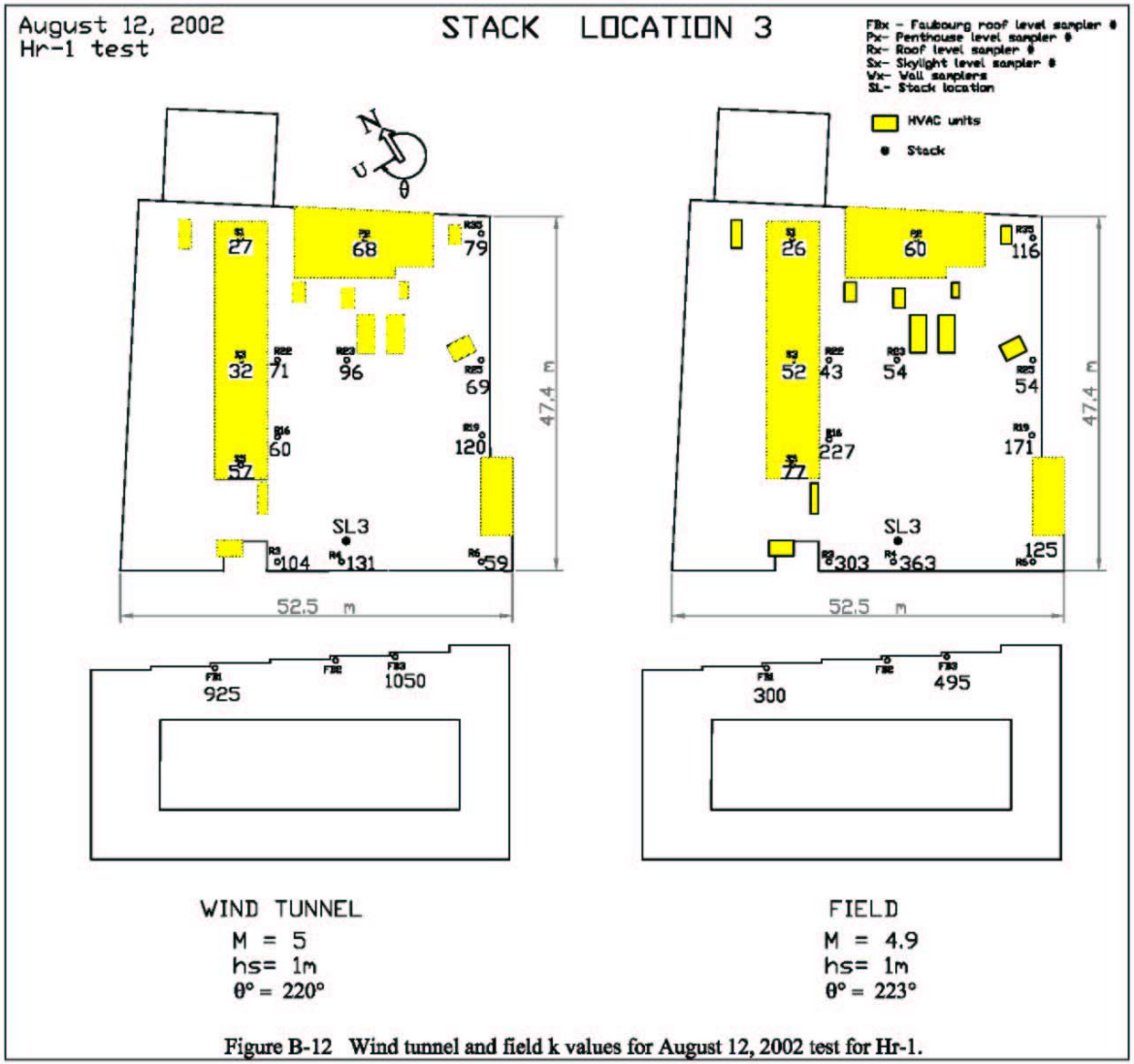

Figure B-12 Wind tunnel and field k values for August 12, 2002 test for Hr-1.

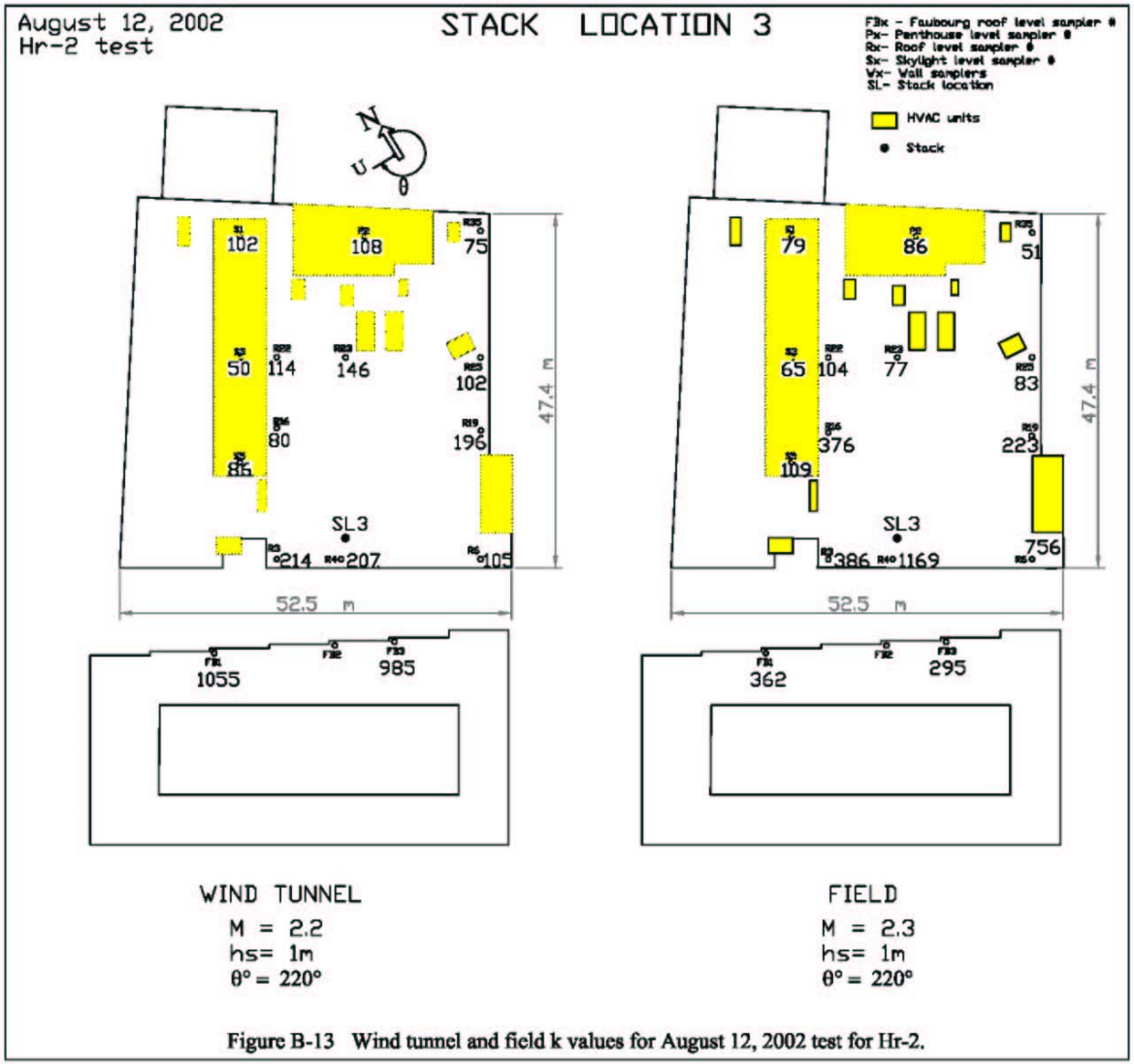

Figure B-13 Wind tunnel and field k values for August 12, 2002 test for Hr-2.

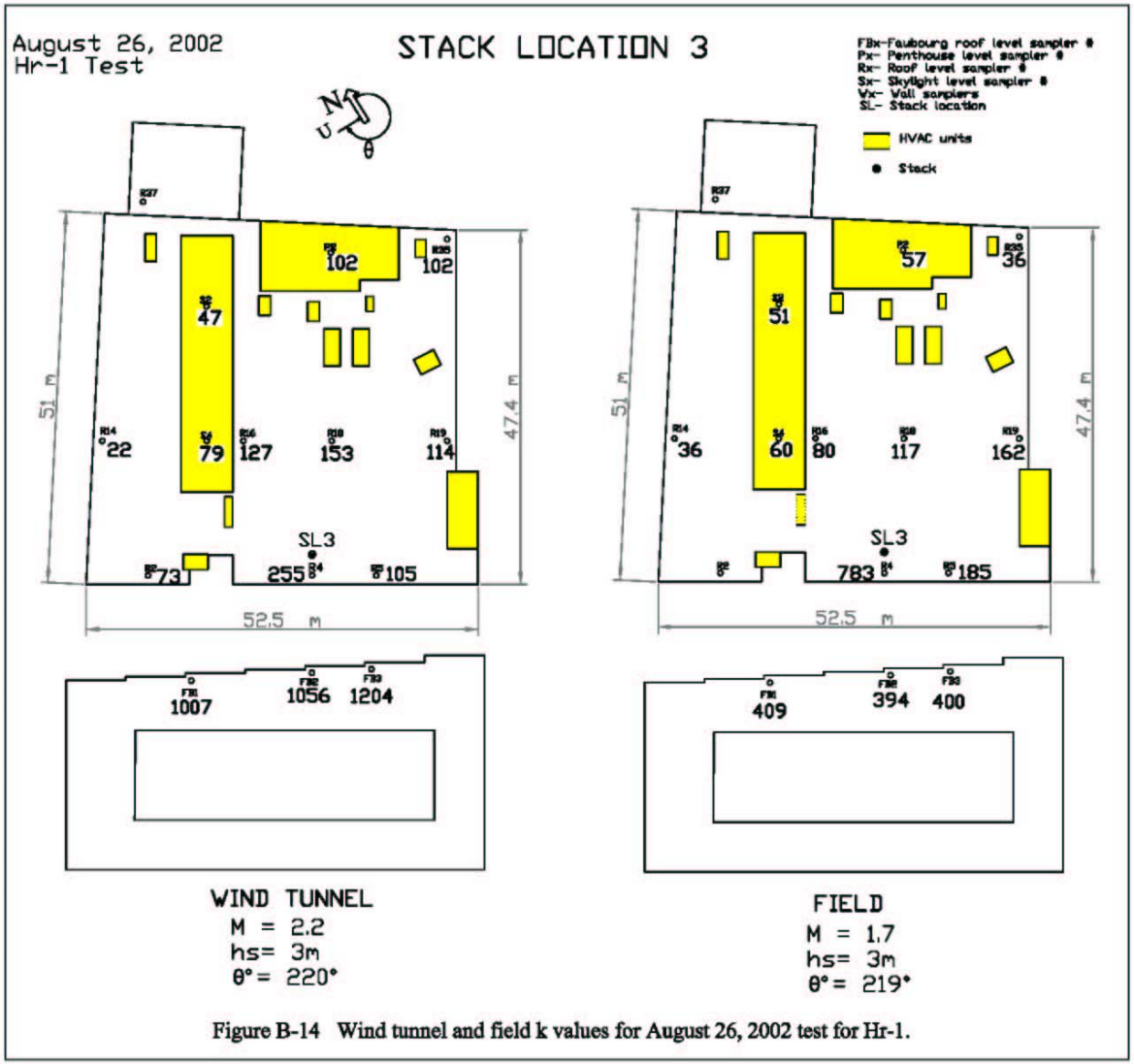

Figure B-14 Wind tunnel and field k values for August 26, 2002 test for Hr-1.

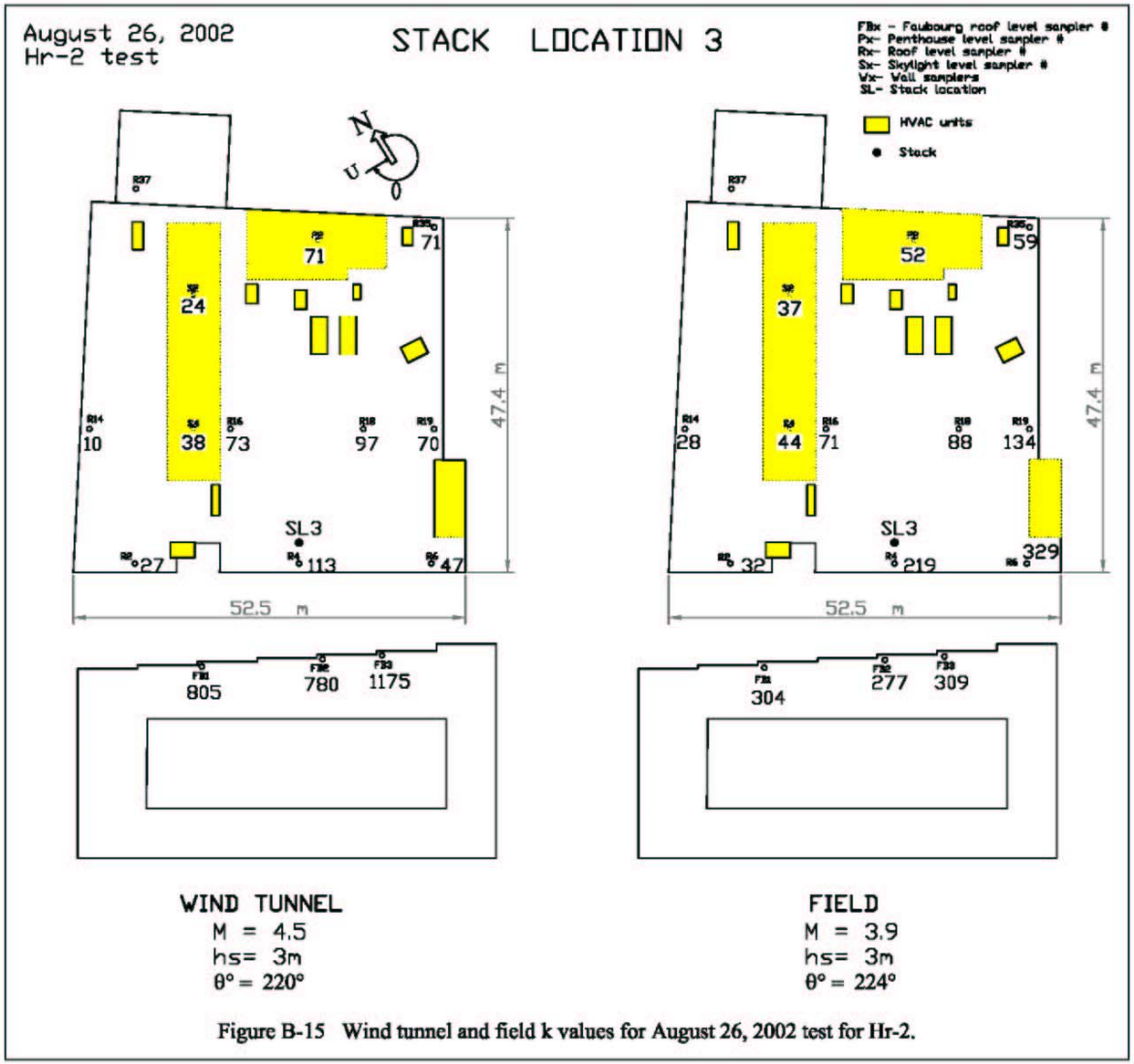

Figure B-15 Wind tunnel and field k values for August 26, 2002 test for Hr-2.

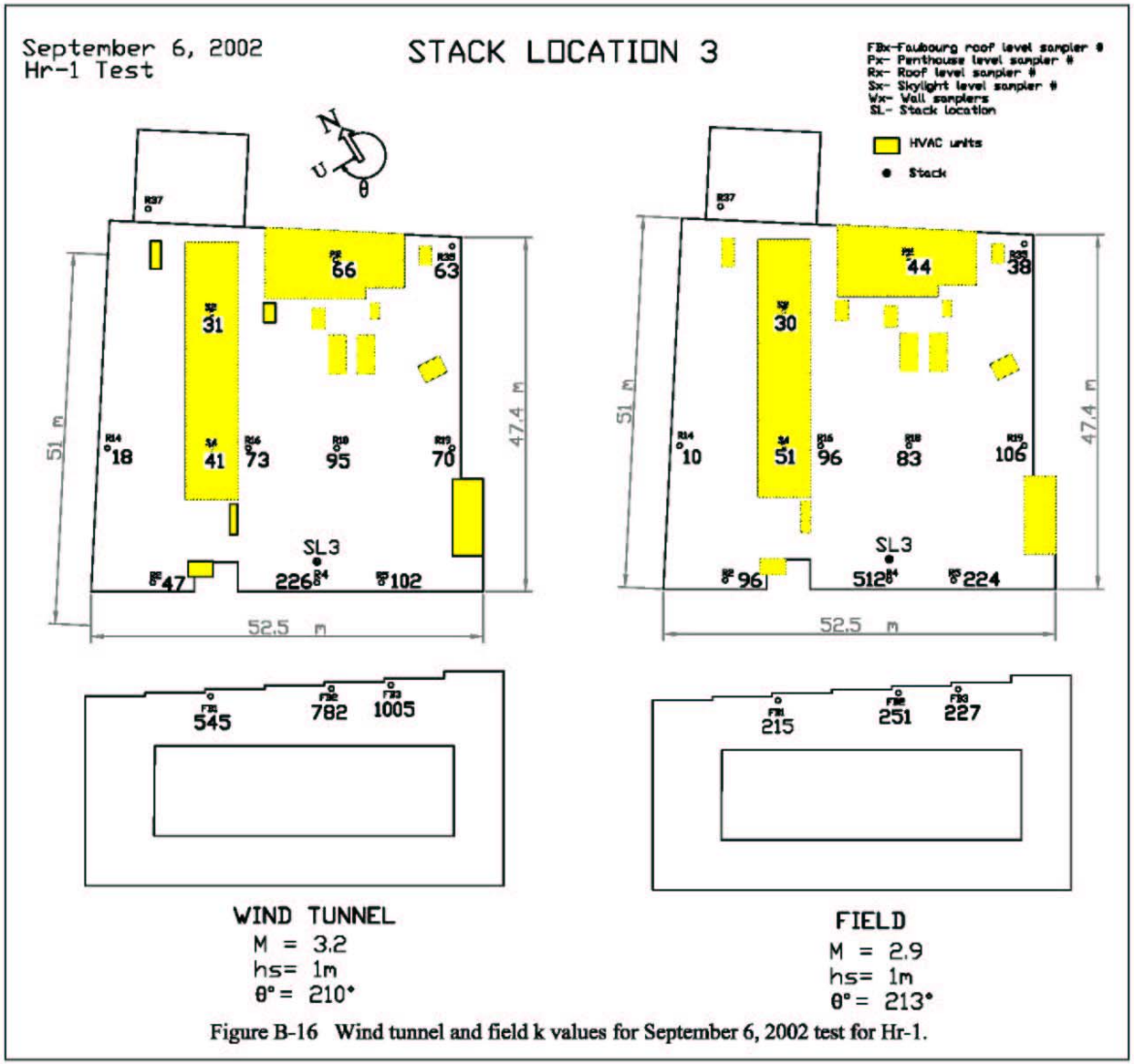

Figure B-16 Wind tunnel and field k values for September 6, 2002 test for Hr-1.

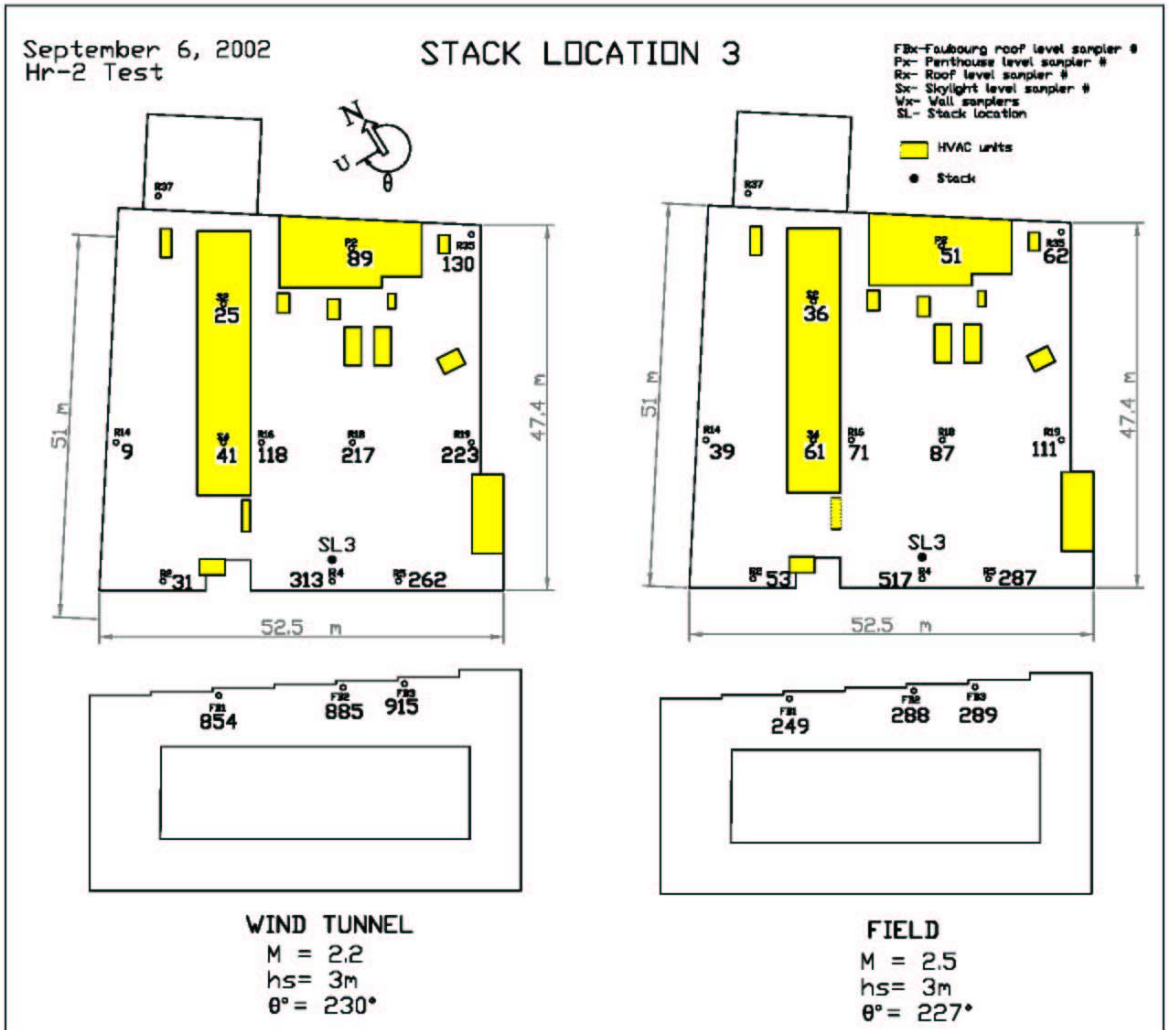

Figure B-17 Wind tunnel and field k values for September 6, 2002 test for Hr-2.

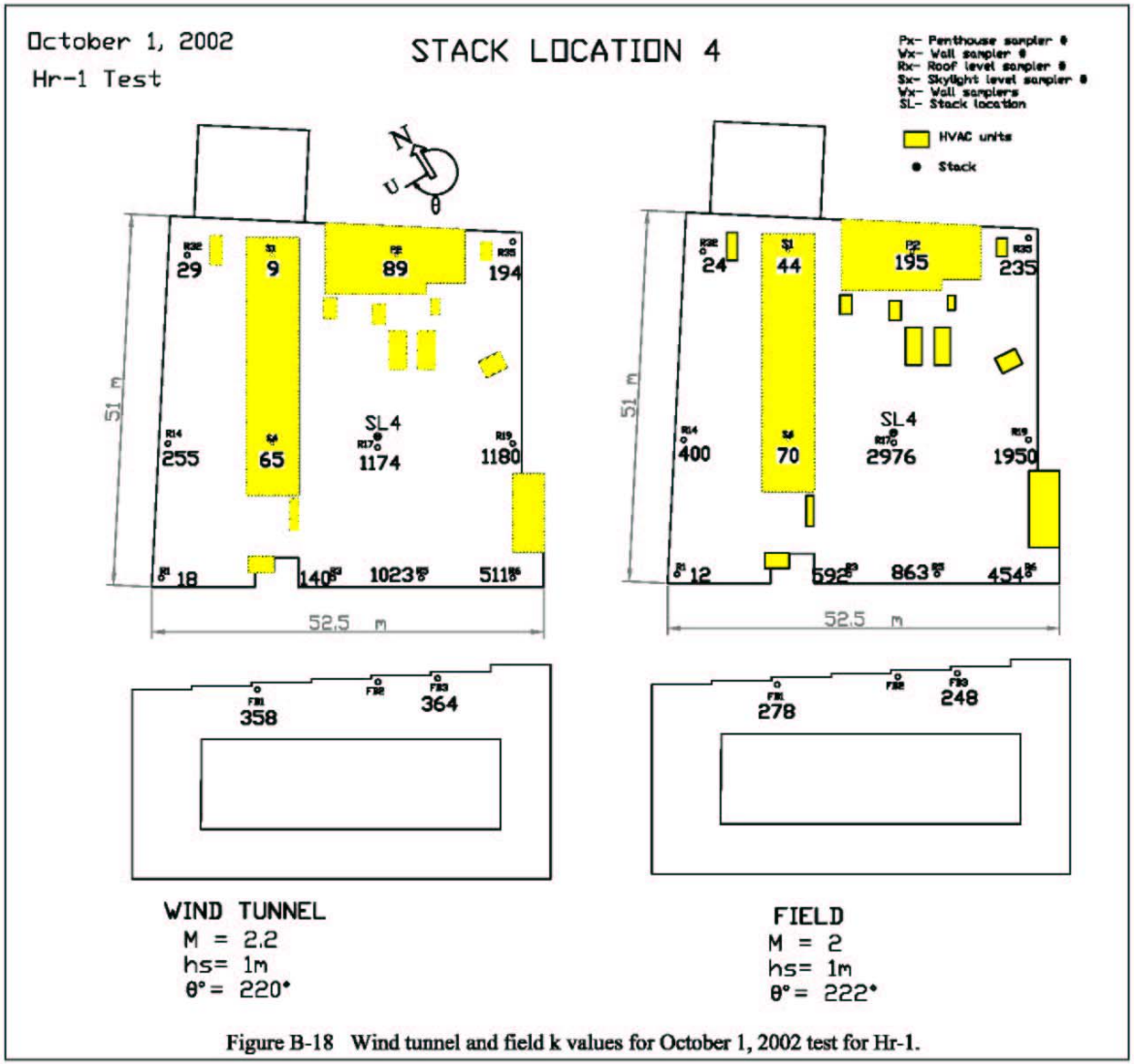

Figure B-18 Wind tunnel and field k values for October 1, 2002 test for Hr-1.

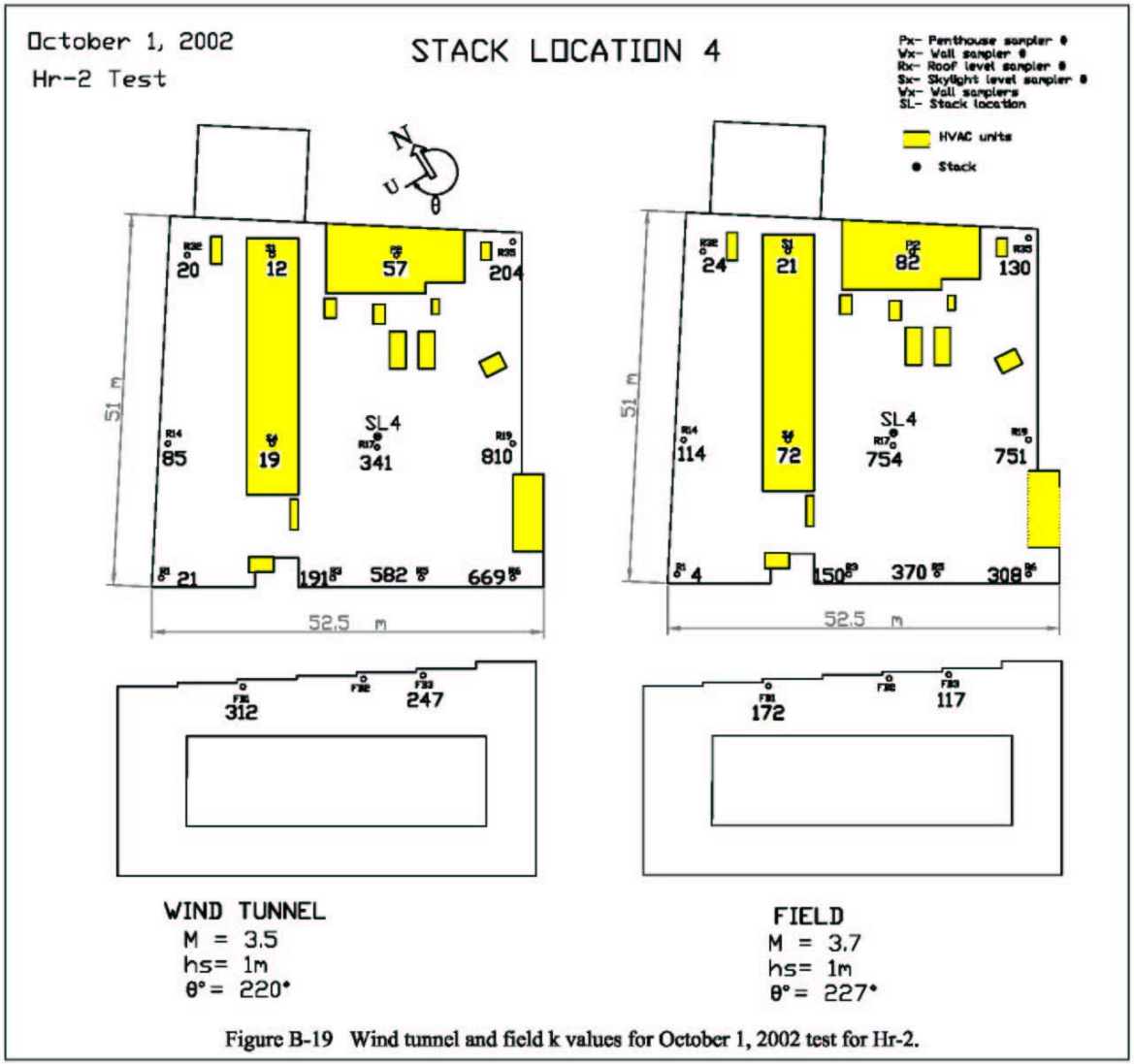

Figure B-19 Wind tunnel and field k values for October 1, 2002 test for Hr-2.

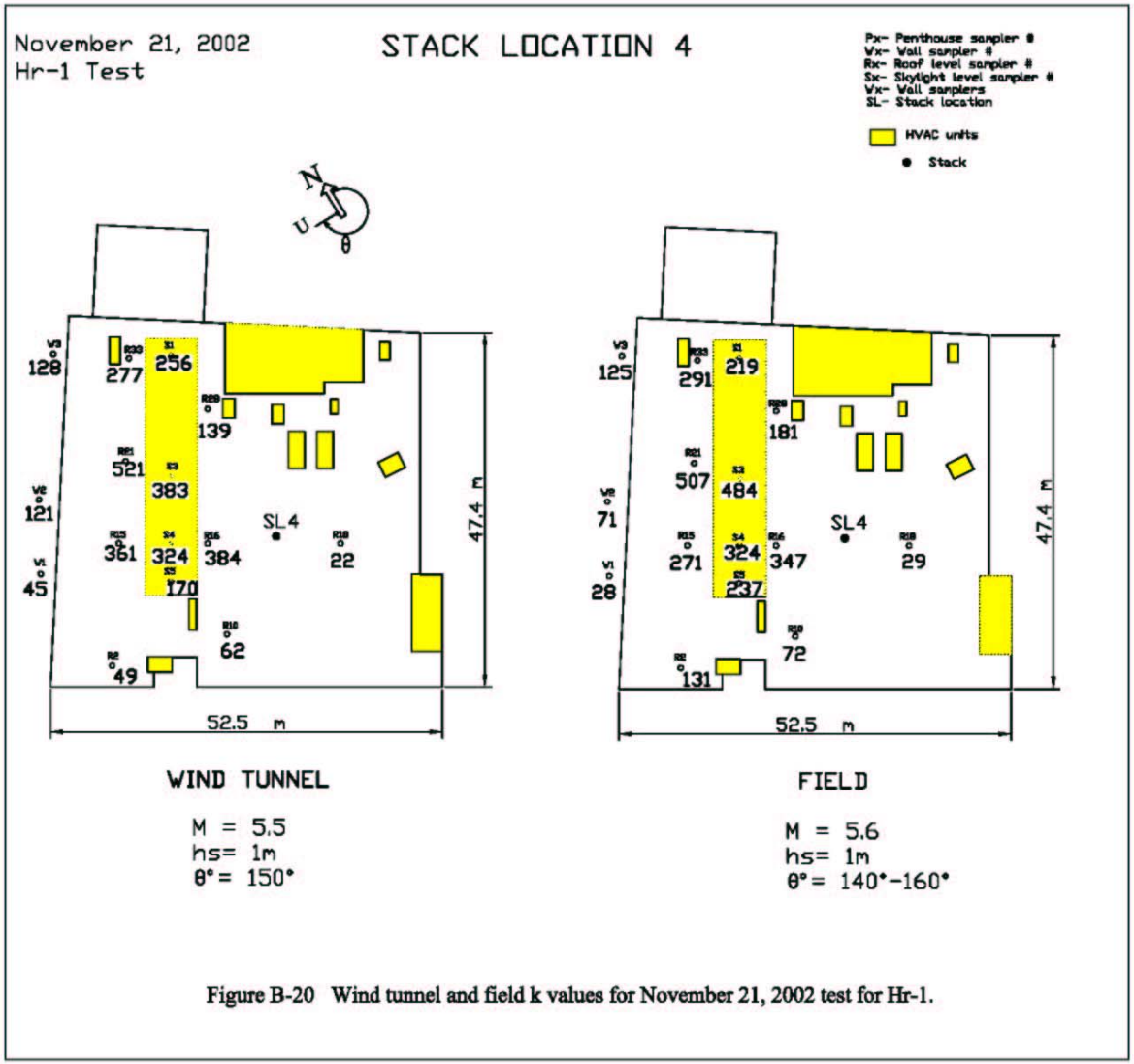

Figure B-20 Wind tunnel and field k values for November 21, 2002 test for Hr-1.

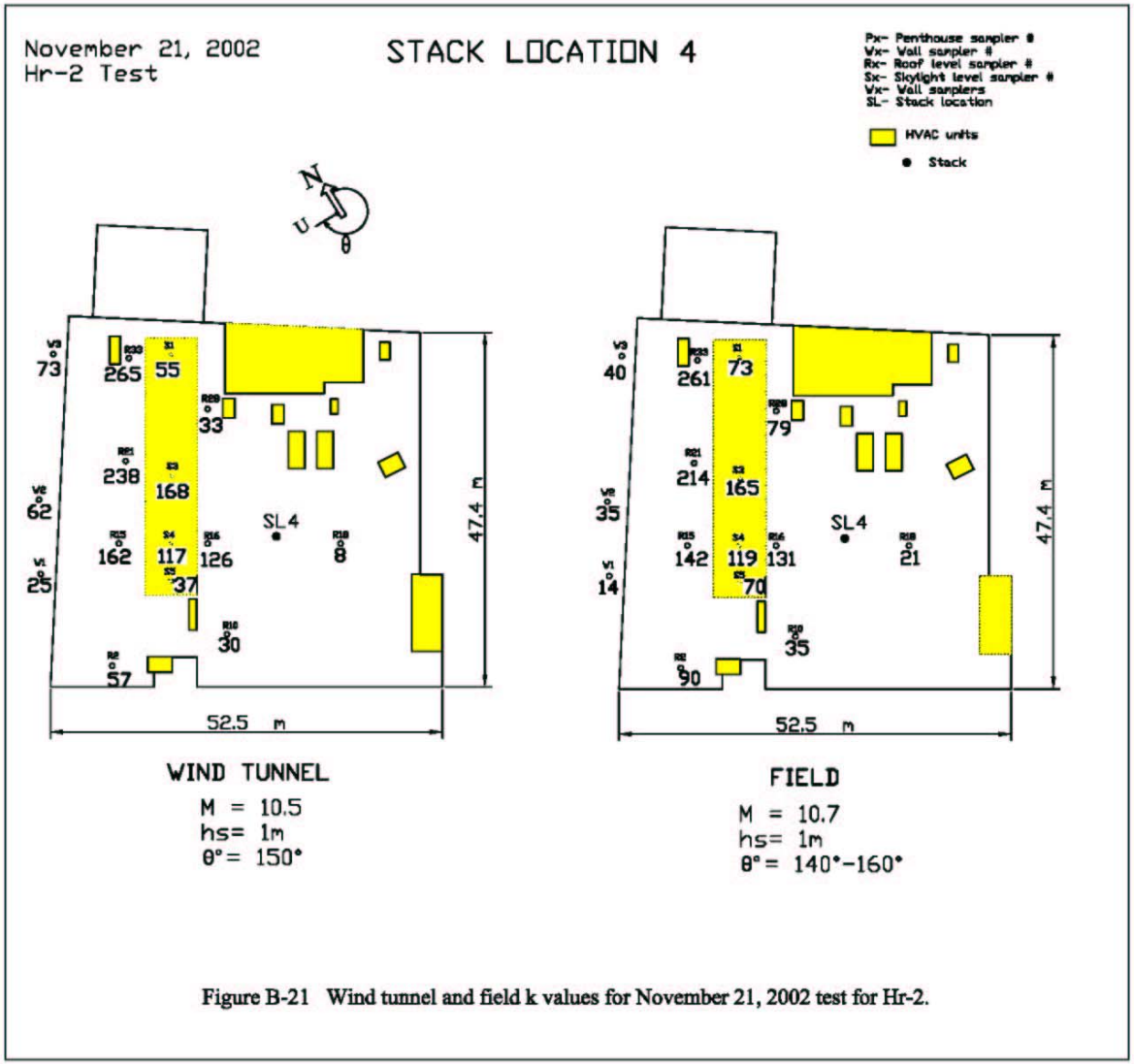

Figure B-21 Wind tunnel and field k values for November 21, 2002 test for Hr-2.

APPENDIX C

Instrumentation

Anemometers

1. A Gill ultrasonic anemometer was used to measure wind data for field tests carried out for stack locations 1 and 2. Wind data were sampled at a rate of 4 hz and and the averaging time was 1 minute. The following wind parameters were measured:

Three components of mean velocity u, v, w (m/s)
Three components of standard deviation of velocity σ_{ux}, σ_{uy}, σ_{uz} (m/s)
Three components wind direction $\sigma_{\theta x}$, $\sigma_{\theta y}$, $\sigma_{\theta z}$ (degrees)
Peak gust (m/s)

2. A Young propeller anemometer was used to measure wind data for field tests carried out for stack locations 3 and 4 (except Nov. 21, 02). Data were collected at a rate of 4 hz using a Campbell Scientific CR10(X) datalogger; an averaging time of 5 minutes was used. The following wind parameters were measured:

Mean velocity (m/s)
Standard deviation for mean velocity (m/s)
Wind direction (degrees)
Standard deviation for wind direction (degrees)

3. For the Nov. 21st-02 field test (stack location 4), a Texas Electronics 3-cup anemometer was used to measure wind speed. The data was collected using an Analogic Data 6100B waveform analyzer.

Parameter measured:
Mean velocity (v)

$y = 4.7552x + 0.3307$
$R^2 = 0.9987$

x – Voltage in volts
y – Velocity in m/s

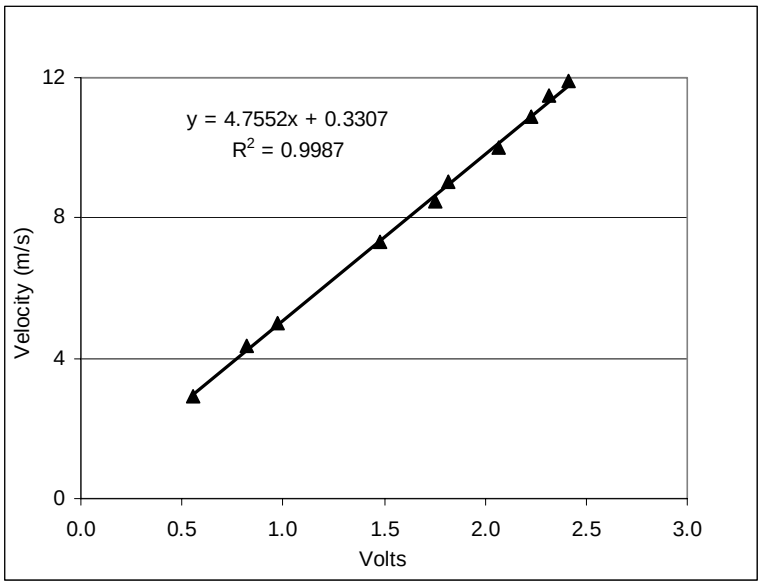

GC Calibration

A VARIAN (Model 3400) gas chromatograph in the Building Aerodynamics Lab at Concordia University was used to measure SF_6 concentrations of approximately half of the field test samples and all of the wind tunnel samples.

For GC values lying between 0 and 1.5

$y = 5.4509x + 0.0551$
$R^2 = 0.9977$

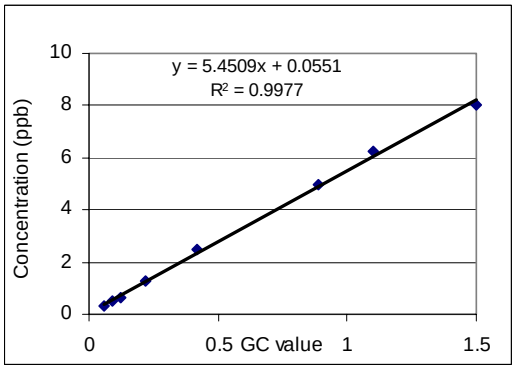

For GC values lying between 1.5 and 4.6

$y = 2.9075x^3 - 20.048x^2 + 50.308x - 32.66$
$R^2 = 0.9957$

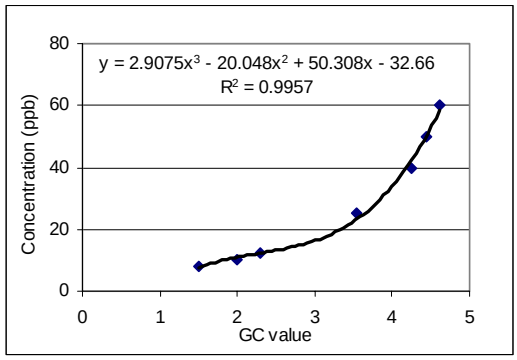

For GC values lying between 4.6 and 6.0

$y = 26.252x^2 - 157.93x + 228.9$
$R^2 = 0.9999$

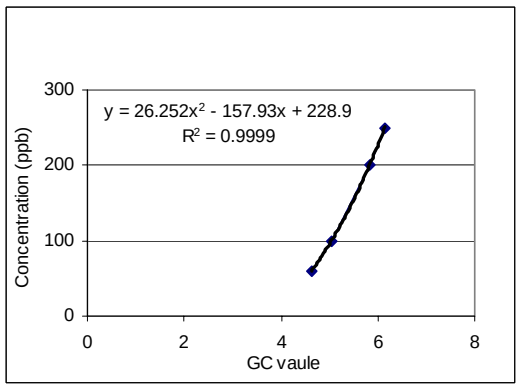

For GC values lying between 6.0 and 8.0

$y = 1513x^2 - 19667x + 64198$
$R^2 = 0.9999$

y - Concentration in ppb
x - GC values

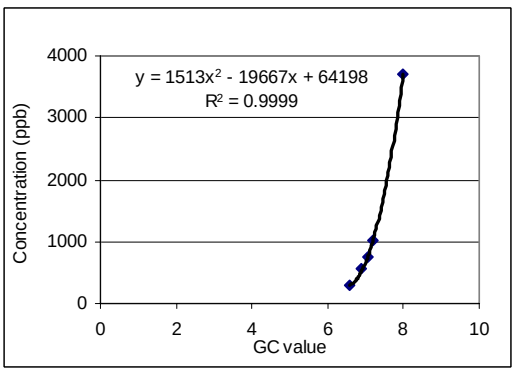

GC Calibration

Company: Lagus
Model: Autotrac

A LAGUS Autotrac GC, located at the IRSST ventilation laboratory, was used to measure SF_6 concentrations of half of the field test samples. The linear dynamic range of the instrument is 0.2 ppb to 40 ppb with a rated precision of ± 3%. The instrument is equipped with an automatic calibration system with an internal source of calibration gas that enables periodic verifications.

Mass flow meter (Concordia University)

Company: Matheson

Model: 8270
Range: 0-10 LPM

$y = 0.998x - 0.2337$
$R^2 = 1$

y – corrected inflow rate in LPM
x – outflow rate in LPM